National Library
of Canada

Acquisitions and
Bibliographic Services Branch

395 Wellington Street
Ottawa, Ontario
K1A 0N4

Bibliothèque nationale
du Canada

Direction des acquisitions et
des services bibliographiques

395, rue Wellington
Ottawa (Ontario)
K1A 0N4

Your file Votre référence

Our file Notre référence

NOTICE

The quality of this microform is heavily dependent upon the quality of the original thesis submitted for microfilming. Every effort has been made to ensure the highest quality of reproduction possible.

If pages are missing, contact the university which granted the degree.

Some pages may have indistinct print especially if the original pages were typed with a poor typewriter ribbon or if the university sent us an inferior photocopy.

AVIS

La qualité de cette microforme dépend grandement de la qualité de la thèse soumise au microfilmage. Nous avons tout fait pour assurer une qualité supérieure de reproduction.

S'il manque des pages, veuillez communiquer avec l'université qui a conféré le grade.

La qualité d'impression de certaines pages peut laisser à désirer, surtout si les pages originales ont été dactylographiées à l'aide d'un ruban usé ou si l'université nous a fait parvenir une photocopie de qualité inférieure.

Canada

Three Dimensional Multilayer Composite Finite Element Method For Stress Analysis of Composite Laminates

Jianhua Han

A Thesis

in

The Department

of

Mechanical Engineering

Presented in Partial Fulfillment of the Requirements
for the Degree of Doctor of Philosophy at
Concordia University
Montreal, Quebec, Canada

June 1994

ISBN 0-612-01283-2

Abstract

Three Dimensional Multilayer Composite Finite Element Method
for Stress Analysis of Composite Laminates

Jianhua Han, Ph.D.
Concordia University, 1994

This thesis covers four subjects. These are the *formulation of the hybrid variational functional of partial stress finite elements* for the stress analysis of laminated composite structures, *development of the iso-function method* to set up the assumed stress field which is free of spurious kinematic modes in the hybrid finite elements, *development of the method of formulating multilayer composite finite element* for three dimensional stress analysis of composite laminates and the *applications of multilayer composite finite elements* for interlaminar stress analysis of several examples.

In order to satisfy the continuous and natural discontinuous conditions in laminated composite structures, the three transverse stresses and the three in-plane strains are taken as basic variables. The basic equations based on the basic variables for stress analysis are given. The variational functional is derived by satisfying these basic equations with the application of the weighted residual method. The iso-function method is developed to set up the partial stress field which is required to form the finite element based on above variational functional. This method gives an easy

way to form a stress field and ensures that the stress field is free from zero energy modes. Three 3-D composite elements are formulated based on the variational functional and by incorporating the iso-function technique. To enforce the satisfaction of the continuity condition at interlaminar surfaces and traction free condition at the upper/lower faces of a laminate, the composite elements are multilayered to formulate a super finite element which is named as multilayer composite element. The continuity of the three transverse stresses across the laminate thickness is assured a priori by introducing a partial stress field vector associated to the lower and upper surfaces of a lamina.

By means of multilayer composite element, stresses in a beam and in a rectangular laminated plate under transverse loading are calculated. Results are compared with Exact elastic theory solutions, classical lamination theory solutions, hybrid finite element solutions and high order shear deformation theory solution. The analysis of straight edge effect problem demonstrates that the stress distributions predicted by the present multilayer composite finite element also satisfy traction free edge condition. The present finite element has clear advantage over displacement formulated finite element and computationally more efficient than the conventional hybrid elements.

Acknowledgements

I would like to gratefully express my thanks and appreciation to my thesis supervisor Dr. S.V. Hoa, for his invaluable support and assistance through this study. I am also grateful to him for careful reading and minute criticism of this thesis.

In particular, I would like to express my gratitude to Dr. Ha and Dr. Q. Huang for their valuable comments and suggestions.

Also, I would like to thank Dr. Xinran Xiao, Mrs. Lan Li, Mr. Young-Soo Kim and Sanjay Mazumdar for their friendship and help.

Finally, I wish to express my gratitude to my wife Qing Chang and my daughter Meng Han for their moral support and understanding.

Contents

List of Figures

List of Tables

List of Symbols

$\mathbf{a}$	$\mathbf{a} = [a_1, a_2, \cdots, a_n]^T$ is displacement field parameter
$\overline{\mathbf{B}}_c$	is a compatibility relation
$\mathbf{B}_c$	Matrix of compatibility relation for partial stress field
$\overline{\mathbf{B}}_g$	Partial strain-displacement relation
$\mathbf{B}_g$	transformation matrix of partial strain-displacement relation
$\mathbf{C}$	Stiffness matrix of material
$\mathbf{C}_{1,2,3}$	3 by 3 submatrix as $\mathbf{C} = \begin{bmatrix} \mathbf{C}_1 & \mathbf{C}_2 \\ \mathbf{C}_2^T & \mathbf{C}_3 \end{bmatrix}$
$\mathbf{f}$	Equivalent finite element nodal force
$\overline{\mathbf{F}}$	Prescribed body force
$\mathbf{G}$	Mapping matrix for stiffness in stress parameter space to nodal displacement space
$\mathbf{H}$	Compliance matrix in stress parameter space
$\mathbf{K}_c$	Stiffness matrix of composite finite element

$\mathbf{K}_d$ Semi-displacement stiffness matrix

$\mathbf{K}_h$ Stiffness matrix of hybrid finite element

$\mathbf{K}_m$ Stiffness matrix of multilayer composite finite element

m Total number of stress field parameters

n Total number of generalized displacements

$\vec{n}$ $\vec{n} = \{n_x,\ n_y,\ n_z\}^T$, in which n_x, n_y, n_z are the direction cosines of the external normal to the boundary surface at the point under consideration

$\mathbf{N}$ Matrix of shape function for displacement interpolation

$\mathbf{p}$ Local field vector $\mathbf{p} = \{\sigma_x,\ \sigma_y,\ \sigma_{xy},\ -\epsilon_z,\ -\epsilon_{yz},\ -\epsilon_{xz}\}^T$

$\mathbf{P}$ Assumed stress field function

$\mathbf{P}_g$ Assumed partial stress field function

$\tilde{\mathbf{P}}$ Assumed partial stress field function in terms of surface vector $\mathbf{a}^t$

$\mathbf{q}$ Global field vector $\mathbf{q} = \{\epsilon_x,\ \epsilon_y,\ \epsilon_{xy},\ \sigma_z,\ \sigma_{yz},\ \sigma_{xz}\}^T$

$\mathbf{r}$ Basic vector, $\mathbf{r} = \{u,\ v,\ w,\ \sigma_z,\ \sigma_{yz},\ \sigma_{xz}\}^T$

$\mathbf{R}$ Combined constitutive matrix

$\mathbf{R}_{1,2,3,4}$ 3 by 3 submatrix as

$$\mathbf{R} = \begin{bmatrix} \mathbf{R}_1 & \mathbf{R}_2 \\ \mathbf{R}_3 & \mathbf{R}_4 \end{bmatrix}$$

$\mathbf{S}$ Compliance matrix of material

$\mathbf{S}_{1,2,3}$ 3 by 3 submatrix as

$$\mathbf{S} = \begin{bmatrix} \mathbf{S}_1 & \mathbf{S}_2 \\ \mathbf{S}_2^T & \mathbf{S}_3 \end{bmatrix}$$

$\overline{\mathbf{T}}$	Prescribed boundary surface force.
$\mathbf{u}$	Displacement vector
$\overline{\mathbf{u}}$	Prescribed boundary displacement vector
$\mathbf{U}$	Transformation matrix of stress field parameter
u, v, w	Components of displacement vector
$\overline{u}, \overline{v}, \overline{w}$	Components of prescribed boundary displacement vector
x, y, z	Cartesian coordinates
$\boldsymbol{\alpha}^i$	Stress field parameter vector at i-th interface of a lamina
$\boldsymbol{\beta}$	Assumed stress field parameter
Φ	$\Phi = [\phi_1, \ \phi_2, \ \cdots, \ \phi_n]$ is a matrix of displacement functions of an element
$\boldsymbol{\delta}$	Nodal displacement vector of a finite element
$\boldsymbol{\varphi}^i$	Partial stress field surface parameter vector of i-th lamina
$\boldsymbol{\varphi}$	Partial stress field surface parameter vector of a laminate
$\tilde{\boldsymbol{\varphi}}$	The reduced partial stress field surface parameter vector of a laminate
$\boldsymbol{\epsilon}_g$	Global strain vector $\boldsymbol{\epsilon}_g = \{\epsilon_x, \ \epsilon_y, \ \epsilon_{xy}\}^T$
$\boldsymbol{\epsilon}_L$	Local strain vector $\boldsymbol{\epsilon}_L = \{\epsilon_z, \ \epsilon_{yz}, \ \epsilon_{xz}\}^T$
$\boldsymbol{\epsilon}$	Strain, $\boldsymbol{\epsilon} = \{\epsilon_x, \ \epsilon_y, \ \epsilon_{xy}, \ \epsilon_z, \ \epsilon_{yz}, \ \epsilon_{xz}\}^T$
$\boldsymbol{\sigma}_g$	Global stress vector $\boldsymbol{\sigma}_g = \{\sigma_z, \ \sigma_{yz}, \ \sigma_{xz}\}^T$
$\boldsymbol{\sigma}_L$	Local stress vector $\boldsymbol{\sigma}_L = \{\sigma_x, \ \sigma_y, \ \sigma_{xy}\}^T$

$\boldsymbol{\sigma}$ Stress, $\boldsymbol{\sigma} = \{\sigma_x,\ \sigma_y,\ \sigma_{xy},\ \sigma_z,\ \sigma_{yz},\ \sigma_{xz}\}^T$

$\check{\boldsymbol{\sigma}}$ Linear stress tensor

$$\check{\boldsymbol{\sigma}} = \begin{bmatrix} \sigma_x & \sigma_{xy} & \sigma_{xz} \\ \sigma_{xy} & \sigma_y & \sigma_{yz} \\ \sigma_{xz} & \sigma_{yz} & \sigma_z \end{bmatrix}$$

ξ, η, ζ Natural coordinates of finite element

λ Eigenvalue of stiffness matrix

ν Poisson ratio

2-D Two dimensional

3-D Three dimensional

8-node Eight nodes finite element

16-node Sixteen nodes finite element

20-node Twenty nodes finite element

FEM Finite Element Method

CFE Composite Finite Element

MCE Multilayer Composite Element

CLT Classical Lamination Theory

Chapter 1

Introduction

The structure of composite materials has two most distinguishable properties. The first is its anisotropic relation between strain and stress. The second is it usually appears as a lamination in structure.

Because of these properties, the main difficulty for the stress analysis of composite structures is the so called continuous and discontinuous problem or conjunction condition. Based on equilibrium and compatibility at the interlayer surfaces, the three in-plane strains and three transverse stresses must be continuous. The other three in-plane stresses and three transverse strains may be described by a finite discontinuity which is caused by the abrupt change of material property or orientation of different laminae[1].

Normal analysis techniques such as the classical lamination theory (CLT)[2, 3, 4, 5] and displacement formulated finite element method[6] have difficulties satisfying the above conditions. The classical lamination theory, which does not include transverse shear effects, can provide reasonable predictions (excluding transverse shear stresses and strains) only for relatively thin plates. As transverse shear effects come to play a

more important role in laminated composite plates with low span-to-thickness ratios, CLT leads to a very poor description of laminate response. In displacement formulated finite element method, where the stresses are obtained from the derivatives of displacement, it is difficult to enforce the continuity of three transverse stresses. Numerical analysis also showed that the results using displacement formulated finite element method are not satisfactory[7]. It is possible to employ the three dimensional anisotropic elasticity theory[1] to obtain exact solution of composite laminates as long as every lamina is treated separately and bound with other laminae with boundary conditions at interlayer surfaces. Pagano[8] presented an example on how to apply this technique. However, because of the difficulties in setting up differential formulations for complicated boundary conditions and the difficulties in obtaining solution for these differential formulations, the direct application of three dimensional anisotropic elasticity theory is limited to problems with simple loading and boundary conditions.

Since 1960's, many works have been done for the prediction of interlaminar stresses in laminates of composite materials. These previous studies can be classified as follows

(a) Finite Difference Method: Works in this area include Pipes and Pagano [9, 10, 11], and Altus et al [12]. All these works involved displacement formulation.

(b) Finite Element Method: Works with application of displacement formulation include Heppler et al [13], Engblom et al [14], Pandya et al [15] (using a displacement formulated high order plate element); and Yeh et al [16], Natarajan, Lucking and Hoa [17, 18], Chaudhuri et al [19] (using a three dimensional displacement formulated element), and Reddy [20, 21, 22] (layerwise theory). With application of stress formulation, there is Rybicki [23]. With application of hybrid formulation, there are Mau et al [24], Nishioka and Atluri [25], Wang et al [26, 27], Khalil et al.[28], Spilker [29], Liou and Sun [30, 31], Liao et al.[32, 33, 34]. With application of mixed formulation, there are Moriya

[35], Kwon and Akin [36].

(c) Perturbation Method Works include Hsu et al [37] by using displacement formulation, Tang and Levy [38](boundary-layer matching method) by using stress formulation, and Ye and Yang [39](boundary layer theory), Bar-Yoseph and Pian et al [40, 41, 42](matched asymptotic expansion method) by using stress formulation.

(d) Variational Method: Pagano [43](Rayleigh-Ritz Method, mixed formulation), Wang and Dickson [44](Garlerkin Method, mixed formulation), Vong [45] and Chatterjee, Ramnath [46](Mixed Variational Principle), Lagace [47, 48](complementary energy principle).

(e) Experimental Method: Whitney et al [49], Berhaus et al [50], Herakovich et al [51].

For theoretical and numerical methods, the above works can also be simply classified as follows

(a) Displacement Formulation, in which only a displacement field is assumed.

(b) Stress Formulation, which only assumes a stress field.

(c) Mixed Formulation, in which both stress field and displacement field are assumed.

(d) Hybrid Formulation, which assumes both the stress field and displacement field, but the assumed field at boundary surface is different from that in the interior.

During the last few years, the Finite Element Method of analysis has rapidly become a very popular technique for the computer solution of complex problem in engineering. The displacement formulated finite element and the stress formulated finite

element both have difficulty to satisfy the continuous condition of three transverse stresses and three in-plane strains and allow the remaining three transverse strains and three in-plane stresses to be discontinuous.

Many techniques have been proposed to satisfy the conjunction conditions at the interlayer surfaces, which have been mainly on the mixed or hybrid formulated finite elements. Spilker[52], and Pian[40], emphasized the continuity of transverse stresses σ_z, σ_{yz}, σ_{xz}, in their stress formulations. Reissner[53], based on potential energy principle, presented a mixed variational theorem, which requires a semi-potential energy density through partial Legendre transformation. Later[54], Reissner based his work on a generalized potential energy principle, which requires a semi-complementary energy density through partial Legendre transformation to arrive at the same results as in[53]. Reissner gave a few examples, however, he did not give the general form of the semi energy density. Moriya[35] developed an 8-node mixed plate finite element based on the modified Hu-Washizu principle. Both Reissner and Moriya took in-plane strains ϵ_x, ϵ_y, ϵ_{xy}, and transverse stresses σ_z, σ_{yz}, σ_{xz}, as independent variables for analysis of laminated structures. Huang [55, 56] presented a new type of elastic energy in terms of in-plane strains ϵ_x, ϵ_y, ϵ_{xy}, and transverse stresses σ_z, σ_{yz}, σ_{xz}. On this basis, Huang developed a laminate functional and established a corresponding variational principle.

Since the hybrid finite element has the reputation of high accuracy in stress calculations and it is easy for a hybrid element with an assumed stress field to satisfy the condition of transverse stresses continuity, many works have been done in the application of hybrid finite element in analysis of composite laminates. Mau et al.[24](1972) developed a laminated thick plate element by using hybrid method. However, in the assumption for the stress field, transverse normal stress was not included. Constant transverse displacement through the laminate thickness was also assumed. These assumptions did not agree well with the actual mechanism of deformation of laminated plates in bending. Spilker[57](1982) developed an eight-node

isoparametric multilayer plate element for the analysis of thin to thick composite plates. This model has the generality of describing laminate response but the assumption of constant transverse displacement through laminate thickness still remains. In 1987, hybrid elements[31] with linear transverse displacement have been developed for analysis of composite laminates. Usually, those hybrid elements have an assumed stress field of six stress components. Later, Liao et al.[32, 33, 34] proposed a hybrid element with partial stress field of transverse shear stresses σ_{yz}, σ_{xz}. In 1992, Han and Hoa [7] developed a composite finite element with linear transverse displacement and with a partial stress field of three transverse stresses σ_z, σ_{yz}, σ_{xz}, since these three stresses are required to be continuous through the thickness of a laminate. The assumption of the partial stress field of three transverse stresses reduces the size of the mapping matrix and compliance matrix needed for the formulation of the element stiffness matrix and makes it possible to enforce the continuity and natural discontinuity conditions exactly in advance.

It can be seen from the works of previous researchers that by taking the six globally continuous components of stress and strain(three transverse stresses, three in-plane strains) as basic variables and by treating the interlaminar surfaces as boundaries with six continuity conditions between every two adjacent layers, the formulated variational principle satisfies the three transverse stresses and three in-plane strains continuity conditions and permit possible discontinuities of three in-plane stresses and three transverse strains.

However, in order to derive finite elements based on the above mentioned variational principle, it is necessary to assume partial stress fields a priori. Finite element formulations involving an assumed stress field are cursed with zero-energy modes. These zero-energy modes have plagued the hybrid finite element method since the beginning. Previous researchers have proposed many techniques to overcome the zero-energy modes. Pian and Tong[58] proposed that the number m of the undetermined coefficients in the stress field should satisfy the relation $m \geq n - r$, where

n is the total degrees of freedom and r is the degrees of rigid body mode. Atluri et.al[59, 60], using a symmetric group theory, identified the different possible modes that exist for a certain type of element. In 1989, Huang [56] proposed a modal analysis technique to obtain the stress modes from the deformation modes of an assumed displacement field. In 1992, Han [7] proposed an iso-function method for formulating the assumed stress field. The method gives an easy way to form a stress field, which is free from spurious zero energy modes.

Thus, to develop a finite element method for stress analysis of composite laminates, a technique of taking three transverse stresses and three in-plane strains as basic variables has to be used; to form the new finite element based on the technique, a procedure to construct the partial stress field has to be developed to ensure no zero energy modes exist in the element.

This thesis covers four subjects. These are (1) the formulation of the hybrid variational functional of partial stress model finite elements for the stress analysis of laminated structures, (2) development of the iso-function method to set up the assumed stress field which is free of spurious kinematic modes in the hybrid finite elements, (3) the formulation of multilayer composite finite elements for three dimensional stress analysis of composite laminates and (4) the application of these multilayer composite finite elements for interlaminar stress analysis in several examples. The present finite element model has clear advantage over displacement formulated finite element and computationally much more efficient than the conventional hybrid elements.

Chapter 2 of this thesis discusses the continuity and discontinuity in laminated structures of composite material. It introduces the global continuity variable and a corresponding basic vector for finite element analysis. Thus the discontinuity of the three transverse strains and three in-plane stresses are allowed to occur naturally while the continuity of the three transverse stresses and three in-plane strains is enforced a priori. Basic equations for elastic stress analysis are derived based on

the basic vector instead of the usual three displacement variables. The weighted residual method is applied on those basic equations and a variational functional is derived.

In Chapter 3, the iso-function method is developed to set up the partial stress field which is required to form the finite element based on above variational functional. This method gives an easy way to form the stress field and the partial stress field and ensures the stress field is free from zero-energy modes. Partial stress fields for a three dimensional eight nodes element, a three dimensional sixteen nodes element and a three dimensional twenty nodes element are proposed with the iso function method. Numerical results prove that the finite elements with those three partial stress field are free of zero-energy mode.

Chapter 4 formulates three dimensional composite elements with 8 nodes, 16 nodes and 20 nodes based on the previously proposed variational functional with incorporation of the iso-function technique to determine the partial stress fields. For verification, stresses in a beam under sinusoidally distributed transverse loading was calculated with composite element. Results are compared with those from elastic theory and from twenty-node displacement finite element.

In Chapter 5, to enforce the satisfaction of the continuity condition of three transverse stresses and three in-plane strains at interlaminar surfaces and traction free conditions at the upper and lower faces of a composite laminate, a super finite element consisting of many layers is formulated. This element is named as multilayer composite finite element. The continuity of the three in-plane strains ϵ_x, ϵ_y, ϵ_{xy} is satisfied automatically because of the continuity of the in-plane displacements through the interfaces of composite elements. The continuity of the three transverse stresses σ_z, σ_{yz}, σ_{xz} across the laminate thickness is assured a priori by introducing a partial stress field parameter vector which is associated to the lower and upper surfaces of a lamina in a laminate. A three dimensional four node multilayer composite finite element and a three dimensional eight node multilayer composite finite

element are formulated based on the three dimensional eight-node composite finite element and sixteen node composite element respectively.

Chapter 6 applies the multilayer composite element for the stress analysis of three composite laminates. Stresses in a laminated beam under sinusoidally distributed transverse loading was re-calculated with multilayer composite element. Compared with results using the composite element, the results from the multilayer composite element are almost the same inside the beam, but is traction free at boundary. Results are also compared with those based on elasticity theory, classical lamination theory, and those by using hybrid finite element method. Numerical analysis shows that the results based on classical lamination theory, which is independent of the span-to-thickness ratio, can provide reasonable predictions only for the thin plate (i.e. span-to-thickness ratio larger than 50). Excellent agreement with exact elasticity solution is obtained for both the multilayer hybrid element of full stress model and the multilayer composite element of partial stress model. The second application is the analysis of bending of a simply supported rectangular laminated plate. Results also are compared with Exact elastic theory solution, classical lamination theory solution, hybrid finite element solution and the high order shear deformation theory solution. High accuracy of the multilayer composite finite element is observed.

The analysis of straight edge effect problem demonstrates that the stress distributions predicted by the present multilayer composite finite element also satisfy traction-free edge condition.

Chapter 2

Basic Equations and Variational Functional

The continuity and discontinuity in composite laminates or so called conjunction condition are discussed. The six globally continuous variables are defined as basic variables. In order to apply the Finite Element Method, the three displacement components are taken instead of the three in-plane strains. A basic vector is composed and equations of elastic analysis of composite laminates based on this basic vector are given. A variational functional is introduced. By defining a displacement and a partial stress field, the composite finite element equations are derived from this variational functional. The six continuous conditions are satisfied across the element.

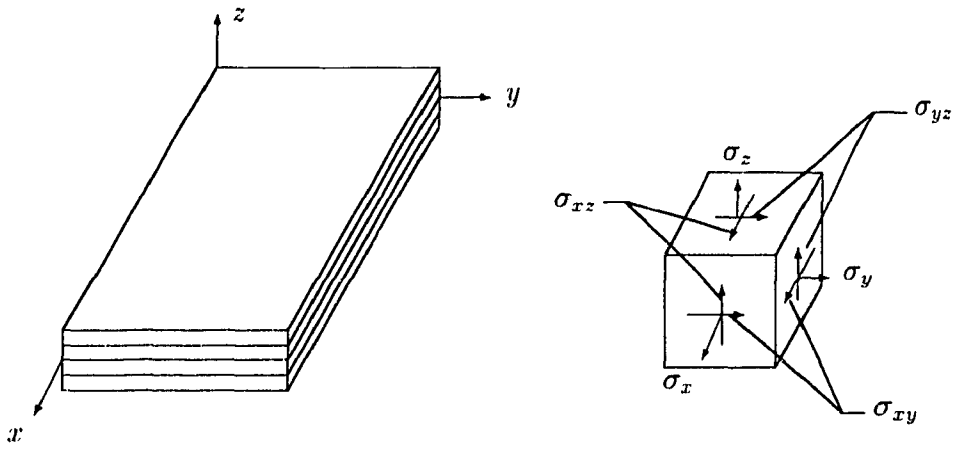

Figure 2.1: Laminate structure, coordinate system and stress convention.

2.1 Continuity and discontinuity in composite laminate

In composite laminates there are discontinuities due to variation in material property or the orientation of fibers. On the other hand, for perfectly bonded laminates, the displacements are continuous and so are the reaction forces at interlaminar surfaces.

In this thesis, the lamina plane is denoted by cartesian coordinates x, y, and in the through-thickness direction by z as shown in fig.2.1.

Within each lamina, all components of displacement, strain and stress are continuous.

At interlaminar surfaces in perfect bonding, the displacements are continuous. Their in-plane derivatives, ϵ_x, ϵ_y, ϵ_{xy} are therefore continuous. That is

$$\begin{aligned} \epsilon_x{}^i &= \epsilon_x{}^{i+1} \\ \epsilon_y{}^i &= \epsilon_y{}^{i+1} \\ \epsilon_{xy}{}^i &= \epsilon_{xy}{}^{i+1} \end{aligned} \tag{2.1}$$

From equilibrium consideration, the transverse stresses are also continuous,

$$\begin{aligned} \sigma_z{}^i &= \sigma_z{}^{i+1} \\ \sigma_{yz}{}^i &= \sigma_{yz}{}^{i+1} \\ \sigma_{xz}{}^i &= \sigma_{xz}{}^{i+1} \end{aligned} \tag{2.2}$$

where i means the i-th interface between i-th and (i+1)-th layer. However, because of changes in material properties or fiber orientation, the corresponding in-plane stresses may not be continuous across the interlaminar surfaces. For the same reasons, the corresponding transverse strains ϵ_z, ϵ_{yz}, ϵ_{xz} may not be continuous.

This means the in-plane strains and transverse stresses are globally continuous across the laminate, and the other components of strain and stress are locally continuous within each lamina but may or may not be continuous across the interlaminar surfaces. Thus all components of stress and strain can be grouped as

$$\boldsymbol{\epsilon}_g = \{\epsilon_x, \epsilon_y, \epsilon_{xy}\}^T \tag{2.3}$$

$$\boldsymbol{\epsilon}_L = \{\epsilon_z, \epsilon_{yz}, \epsilon_{xz}\}^T \tag{2.4}$$

$$\boldsymbol{\sigma}_g = \{\sigma_z, \sigma_{yz}, \sigma_{xz}\}^T \tag{2.5}$$

$$\boldsymbol{\sigma}_L = \{\sigma_x, \sigma_y, \sigma_{xy}\}^T \tag{2.6}$$

where $\boldsymbol{\epsilon}_g$, $\boldsymbol{\sigma}_g$ denotes globally continuous strain and stress vectors, $\boldsymbol{\epsilon}_L$, $\boldsymbol{\sigma}_L$ are locally continuous strain and stress vectors.

With above notation, the continuous condition can be expressed as

$$\begin{aligned} \boldsymbol{\sigma}_g{}^i|_{\text{interface}} &= \boldsymbol{\sigma}_g{}^{i+1}|_{\text{interface}} \\ \boldsymbol{\epsilon}_g{}^i|_{\text{interface}} &= \boldsymbol{\epsilon}_g{}^{i+1}|_{\text{interface}} \end{aligned} \tag{2.7}$$

2.2 Basic variables

As described in above section, a composite laminate exhibits discontinuities. From consideration of equilibrium and compatibility, the three transverse stresses σ_z, σ_{yz}, σ_{xz} and three in-plane strains ϵ_x, ϵ_y, ϵ_{xy} must exhibit global continuity. As such neither displacement formulation method nor stress formulation method can satisfy the six continuity conditions a priori.

It is obvious that if the six globally continuous variables are taken as basic variables, the six continuous conditions at the interfaces will be satisfied easily. Let the six globally continuous variables of strain and stress constitute a global field vector,

$$\mathbf{q} = \begin{Bmatrix} \boldsymbol{\epsilon}_g \\ \boldsymbol{\sigma}_g \end{Bmatrix} = \{\epsilon_x, \epsilon_y, \epsilon_{xy}, \sigma_z, \sigma_{yz}, \sigma_{xz}\}^T \tag{2.8}$$

which is continuous across the interfaces of the laminate. Let the other six variables constitute a local field vector,

$$\mathbf{p} = \begin{Bmatrix} \boldsymbol{\sigma}_L \\ -\boldsymbol{\epsilon}_L \end{Bmatrix} = \{\sigma_x, \sigma_y, \sigma_{xy}, -\epsilon_z, -\epsilon_{yz}, -\epsilon_{xz}\}^T \tag{2.9}$$

which is only continuous within the lamina. The negative sign before $\boldsymbol{\epsilon}_L$ is introduced to ensure symmetry of the combined constitutive relation.

The global field vector $\mathbf{q}$ and the local field vector $\mathbf{p}$ are related by

$$\mathbf{p} = \mathbf{R}\mathbf{q} \tag{2.10}$$

where $\mathbf{R}$ is called the combined constitutive matrix, written as

$$\begin{Bmatrix} \boldsymbol{\sigma}_L \\ -\boldsymbol{\epsilon}_L \end{Bmatrix} = \begin{bmatrix} \mathbf{R}_1 & \mathbf{R}_2 \\ \mathbf{R}_3 & \mathbf{R}_4 \end{bmatrix} \begin{Bmatrix} \boldsymbol{\epsilon}_g \\ \boldsymbol{\sigma}_g \end{Bmatrix} \tag{2.11}$$

From Hooke's law, we have

$$\boldsymbol{\sigma} = \mathbf{C}\boldsymbol{\epsilon}$$

$$\boldsymbol{\epsilon} = \mathbf{S}\boldsymbol{\sigma}$$

where

$\mathbf{C}$ — stiffness matrix of material

$\mathbf{S}$ — compliance matrix of material

and

$$\boldsymbol{\sigma} = \begin{Bmatrix} \boldsymbol{\sigma}_L \\ \boldsymbol{\sigma}_g \end{Bmatrix} = \{\sigma_x, \sigma_y, \sigma_{xy}, \sigma_z, \sigma_{yz}, \sigma_{xz}\}^T \tag{2.12}$$

$$\boldsymbol{\epsilon} = \begin{Bmatrix} \boldsymbol{\epsilon}_g \\ \boldsymbol{\epsilon}_L \end{Bmatrix} = \{\epsilon_x, \epsilon_y, \epsilon_{xy}, \epsilon_z, \epsilon_{yz}, \epsilon_{xz}\}^T . \tag{2.13}$$

This relation of strain and stress can be rewritten as

$$\begin{Bmatrix} \boldsymbol{\sigma}_L \\ \boldsymbol{\sigma}_g \end{Bmatrix} = \begin{bmatrix} \mathbf{C}_1 & \mathbf{C}_2 \\ \mathbf{C}_2^T & \mathbf{C}_3 \end{bmatrix} \begin{Bmatrix} \boldsymbol{\epsilon}_g \\ \boldsymbol{\epsilon}_L \end{Bmatrix} \tag{2.14}$$

and

$$\begin{Bmatrix} \boldsymbol{\epsilon}_g \\ \boldsymbol{\epsilon}_L \end{Bmatrix} = \begin{bmatrix} \mathbf{S}_1 & \mathbf{S}_2 \\ \mathbf{S}_2^T & \mathbf{S}_3 \end{bmatrix} \begin{Bmatrix} \boldsymbol{\sigma}_L \\ \boldsymbol{\sigma}_g \end{Bmatrix} . \tag{2.15}$$

Then we have

$$\begin{bmatrix} \mathbf{R}_1 & \mathbf{R}_2 \\ \mathbf{R}_3 & \mathbf{R}_4 \end{bmatrix} = \begin{bmatrix} \mathbf{C}_1 - \mathbf{C}_2\mathbf{C}_3^{-1}\mathbf{C}_2^T & \mathbf{C}_2\mathbf{C}_3^{-1} \\ \mathbf{C}_3^{-1}\mathbf{C}_2^T & -\mathbf{C}_3^{-1} \end{bmatrix} \tag{2.16}$$

or

$$\begin{bmatrix} \mathbf{R}_1 & \mathbf{R}_2 \\ \mathbf{R}_3 & \mathbf{R}_4 \end{bmatrix} = \begin{bmatrix} \mathbf{S}_1^{-1} & -\mathbf{S}_1^{-1}\mathbf{S}_2 \\ -\mathbf{S}_2^T\mathbf{S}_1^{-1} & \mathbf{S}_2^T\mathbf{S}_1^{-1}\mathbf{S}_2 - \mathbf{S}_3 \end{bmatrix} \tag{2.17}$$

Because **S** and **C** are symmetric matrices, it can be shown that,

$$\mathbf{R}^T = \begin{bmatrix} \mathbf{R}_1 & \mathbf{R}_2 \\ \mathbf{R}_3 & \mathbf{R}_4 \end{bmatrix}^T = \begin{bmatrix} \mathbf{R}_1^T & \mathbf{R}_3^T \\ \mathbf{R}_2^T & \mathbf{R}_4^T \end{bmatrix}. \tag{2.18}$$

Since,

$$\mathbf{R}_1^T = \mathbf{C}_1^T - \mathbf{C}_2\mathbf{C}_3^{-1T}\mathbf{C}_2^T = \mathbf{C}_1 - \mathbf{C}_2\mathbf{C}_3^{-1}\mathbf{C}_2^T = \mathbf{R}_1 \tag{2.19}$$

$$\mathbf{R}_2^T = \mathbf{C}_3^{-1T}\mathbf{C}_2^T = \mathbf{C}_3^{-1}\mathbf{C}_2^T = \mathbf{R}_3 \tag{2.20}$$

$$\mathbf{R}_3^T = \mathbf{C}_2\mathbf{C}_3^{-1T} = \mathbf{C}_2\mathbf{C}_3^{-1} = \mathbf{R}_2 \tag{2.21}$$

$$\mathbf{R}_4^T = -\mathbf{C}_3^{-1T} = -\mathbf{C}_3^{-1} = \mathbf{R}_4, \tag{2.22}$$

we have

$$\mathbf{R} = \mathbf{R}^T \tag{2.23}$$

Thus it is proved that the combined constitutive matrix is a symmetric matrix just as the stiffness matrix and the compliance matrix.

At the interlaminar surface, the global field vector **q** is the same for two adjoining laminae, but the combined constitutive matrix **R** may be different (caused by variation in material properties or fiber orientations). Generally, the local field vector at the interface is

$$\begin{aligned} \mathbf{p}_{interface}^{(i)} &= \mathbf{R}^{(i)}\mathbf{q}_{interface} \\ \mathbf{p}_{interface}^{(i+1)} &= \mathbf{R}^{(i+1)}\mathbf{q}_{interface} \end{aligned} \tag{2.24}$$

where i refers to lamina i. Discontinuity occurs naturally.

The continuous requirement of three in-plane strains ϵ_x, ϵ_y, ϵ_{xy} is equivalent to the requirement of continuity of the displacement u, v. Thus, for the convenience of applying finite element method, the following six globally continuous variables are taken as basic variables and they constitute a basic vector

$$\mathbf{r} = \begin{bmatrix} u & v & w & \sigma_z & \sigma_{yz} & \sigma_{xz} \end{bmatrix}^T \tag{2.25}$$

2.3 Basic Equations and the Variational Functional

With the definition of the above basic vector, a variational functional can be derived. Different formulation methods are available for this particular variational functional. It can be derived from the general Hellinger-Reissner Principle as Reissner suggested in his work [53, 54] and later used by Pian and Li [61], or from the Hu-Washizu Principle as did by Moriya [54]. Huang also derived the functional by means of Weighted Residual Method [56].

In this thesis, the Weighted Residual Method is used to form a variational functional for interlaminar stress analysis of composite laminates as proposed by Huang [56]. Differences between this variational functional and others will be discussed in next section.

2.3.1 Basic Equations

For applying weighted residual scheme, basic equations to be satisfied for interlaminar stress analysis of composite laminates will be derived first. These basic equations include equilibrium equation, constitutive equation, strain-displacement equation, compatibility equation and boundary condition.

Equilibrium Equation

In linear theory of elasticity, the equilibrium equations of a three dimensional elastic solid are

$$\begin{aligned} \frac{\partial \sigma_x}{\partial x} + \frac{\partial \sigma_{xy}}{\partial y} + \frac{\partial \sigma_{xz}}{\partial z} + F_x = 0 \\ \frac{\partial \sigma_{xy}}{\partial x} + \frac{\partial \sigma_y}{\partial y} + \frac{\partial \sigma_{yz}}{\partial z} + F_y = 0 \end{aligned} \tag{2.26}$$

$$\frac{\partial \sigma_{xz}}{\partial x} + \frac{\partial \sigma_{yz}}{\partial y} + \frac{\partial \sigma_z}{\partial z} + F_z = 0$$

which can be written as

$$\mathbf{A}(\boldsymbol{\sigma}) + \overline{\mathbf{F}} = 0 \tag{2.27}$$

where $\mathbf{A}$ is a corresponding operator, $\overline{\mathbf{F}}$ is prescribed body force.

Combined Constitutive Equation

Instead of the usual constitutive equations of

$$\boldsymbol{\sigma} = \mathbf{C}\boldsymbol{\epsilon} \tag{2.28}$$

or

$$\boldsymbol{\epsilon} = \mathbf{S}\boldsymbol{\sigma}, \tag{2.29}$$

for laminates, we use the combined constitutive equations:

$$\mathbf{p} = \mathbf{R}\mathbf{q} \tag{2.30}$$

Partial Strain-Displacement Equations

The partial strain-displacement relations are

$$\begin{aligned} \epsilon_x &= \frac{\partial u}{\partial x} \\ \epsilon_y &= \frac{\partial v}{\partial y} \\ \epsilon_{xy} &= \frac{\partial v}{\partial x} + \frac{\partial u}{\partial y} \end{aligned} \tag{2.31}$$

or expressed in matrix form as

$$\boldsymbol{\epsilon}_g = \overline{\mathbf{B}}_g \mathbf{u}, \tag{2.32}$$

where

$$\overline{\mathbf{B}}_g = \begin{bmatrix} \frac{\partial}{\partial x} & 0 & 0 \\ 0 & \frac{\partial}{\partial y} & 0 \\ \frac{\partial}{\partial y} & \frac{\partial}{\partial x} & 0 \end{bmatrix}, \tag{2.33}$$

$$\mathbf{u} = \begin{Bmatrix} u \\ v \\ w \end{Bmatrix}. \tag{2.34}$$

in which $\mathbf{u}$ is displacement vector, u, v and w are components of displacement vector in x, y and z directions respectively.

Compatibility Equations

Compatibility equations are

$$\begin{aligned} \epsilon_z &= \frac{\partial w}{\partial z} \\ \epsilon_{yz} &= \frac{\partial w}{\partial y} + \frac{\partial v}{\partial z} \\ \epsilon_{xz} &= \frac{\partial w}{\partial x} + \frac{\partial u}{\partial z} \end{aligned} \tag{2.35}$$

which can be expressed as

$$\boldsymbol{\epsilon}_L = \overline{\mathbf{B}}_c \mathbf{u} \tag{2.36}$$

where

$$\overline{\mathbf{B}}_c = \begin{bmatrix} 0 & 0 & \frac{\partial}{\partial z} \\ 0 & \frac{\partial}{\partial z} & \frac{\partial}{\partial y} \\ \frac{\partial}{\partial z} & 0 & \frac{\partial}{\partial x} \end{bmatrix} \tag{2.37}$$

Boundary Conditions

The geometric boundary conditions are

$$\begin{aligned} u &= \overline{u} \\ v &= \overline{v} \end{aligned} \tag{2.38}$$

$$w = \overline{w}$$

In matrix form, it is

$$\mathbf{u} = \overline{\mathbf{u}} \tag{2.39}$$

where

$$\overline{\mathbf{u}} = \begin{Bmatrix} \overline{u} \\ \overline{v} \\ \overline{w} \end{Bmatrix} \tag{2.40}$$

in which $\overline{\mathbf{u}}$ is prescribed boundary displacement vector, $\overline{u}$, $\overline{v}$ and $\overline{w}$ are components of the prescribed boundary displacement vector in x, y and z directions respectively.

The force boundary conditions are

$$\begin{aligned} \sigma_x n_x + \sigma_{xy} n_y + \sigma_{xz} n_z &= \overline{T}_x \\ \sigma_{xy} n_x + \sigma_y n_y + \sigma_{yz} n_z &= \overline{T}_y \\ \sigma_{xz} n_x + \sigma_{yz} n_y + \sigma_z n_z &= \overline{T}_z \end{aligned} \tag{2.41}$$

which can be written as

$$\breve{\boldsymbol{\sigma}} \vec{n} = \overline{\mathbf{T}}. \tag{2.42}$$

where, $\breve{\boldsymbol{\sigma}}$ is the linear stress tensor

$$\breve{\boldsymbol{\sigma}} = \begin{bmatrix} \sigma_x & \sigma_{xy} & \sigma_{xz} \\ \sigma_{xy} & \sigma_y & \sigma_{yz} \\ \sigma_{xz} & \sigma_{yz} & \sigma_z \end{bmatrix} \tag{2.43}$$

$$\vec{n} = \begin{Bmatrix} n_x \\ n_y \\ n_z \end{Bmatrix} \tag{2.44}$$

in which, n_x, n_y, n_z are the direction cosines of the external normal to the boundary surface at the point under consideration.

2.3.2 Variational Functional

By taking the six continuous variables as basic variables, the prescribed geometry boundary conditions(eq.2.38) are satisfied in advance, so are the partial strain-displacement relations(eq.2.31) and the combined constitutive equation(eq.2.30). To satisfy the rest of the basic equations (equilibrium equation, compatibility equation and forced boundary condition), we introduce these relations into the weighted residual integral, which is expressed as

$$\mathbf{I} = \sum_j \left\{ \int_{v_j} \left[\left(\mathbf{A}(\boldsymbol{\sigma}) + \overline{\mathbf{F}} \right) \mathbf{w}_1 + \left(\boldsymbol{\epsilon}_L - \overline{\mathbf{B}}_c \mathbf{u} \right) \mathbf{w}_2 \right] dv_j + \int_{s_{j\sigma}} \left(\breve{\boldsymbol{\sigma}} \vec{n} - \overline{\mathbf{T}} \right) \mathbf{w}_3 ds_j \right\} = 0 \tag{2.45}$$

where $\mathbf{w}_1, \mathbf{w}_2, \mathbf{w}_3$ are vectors of arbitrary weight functions.
Without loss of generality, these arbitrary functions can be defined as,

$$\mathbf{w}_1 = -\delta \mathbf{u} \tag{2.46}$$

$$\mathbf{w}_2 = -\delta \boldsymbol{\sigma}_g \tag{2.47}$$

$$\mathbf{w}_3 = \delta \mathbf{u} \tag{2.48}$$

$$\begin{aligned} \mathbf{I} = \sum_j \Bigg\{ - \int_{v_j} \Bigg[& \left(\frac{\partial \sigma_x}{\partial x} + \frac{\partial \sigma_{xy}}{\partial y} + \frac{\partial \sigma_{xz}}{\partial z} + F_x \right) \delta u \\ & + \left(\frac{\partial \sigma_{xy}}{\partial x} + \frac{\partial \sigma_y}{\partial y} + \frac{\partial \sigma_{yz}}{\partial z} + F_y \right) \delta v \\ & + \left(\frac{\partial \sigma_{xz}}{\partial x} + \frac{\partial \sigma_{yz}}{\partial y} + \frac{\partial \sigma_z}{\partial z} + F_z \right) \delta w \\ & - \left(\epsilon_z - \frac{\partial w}{\partial z} \right) \delta \sigma_z - \left(\epsilon_{yz} - \frac{\partial w}{\partial y} - \frac{\partial v}{\partial z} \right) \delta \sigma_{yz} \\ & - \left(\epsilon_{xz} - \frac{\partial w}{\partial x} - \frac{\partial u}{\partial z} \right) \delta \sigma_{xz} \Bigg] dv_j \end{aligned}$$

$$
\begin{aligned}
&+\int_{js_\sigma}\Big[\left(\sigma_x n_x+\sigma_{xy}n_y+\sigma_{xz}n_z-\overline{T}_x\right)\delta u\\
&+\left(\sigma_{xy}n_x+\sigma_y n_y+\sigma_{yz}n_z-\overline{T}_y\right)\delta v\\
&+\left(\sigma_{xz}n_x+\sigma_{yz}n_y+\sigma_z n_z-\overline{T}_z\right)\delta w\Big]\,ds_j\Big\}\\
&=0
\end{aligned}
\tag{2.49}
$$

Applying the technique of integrating by parts, we have the equation

$$
\begin{aligned}
&\int_{v_j}\left(\frac{\partial\sigma_x}{\partial x}+\frac{\partial\sigma_{xy}}{\partial y}+\frac{\partial\sigma_{xz}}{\partial z}\right)\delta u\,dv_j=\\
&\quad-\int_{v_j}\left(\sigma_x\frac{\partial}{\partial x}\delta u+\sigma_{xy}\frac{\partial}{\partial y}\delta u+\sigma_{xz}\frac{\partial}{\partial z}\delta u\right)dv_j\\
&\quad+\int_{s_{j\sigma}}\left(\sigma_x n_x+\sigma_{xy}n_y+\sigma_{xz}n_z\right)\delta u\,ds_j
\end{aligned}
\tag{2.50}
$$

Thus

$$
\begin{aligned}
\mathbf{I}\;=\;&\sum_j\Big\{\int_{v_j}\Big[\left(\sigma_x\frac{\partial}{\partial x}\delta u+\sigma_{xy}\frac{\partial}{\partial y}\delta u+\sigma_{xz}\frac{\partial}{\partial z}\delta u\right)\\
&+\left(\sigma_{xy}\frac{\partial}{\partial x}\delta v+\sigma_y\frac{\partial}{\partial y}\delta v+\sigma_{yz}\frac{\partial}{\partial z}\delta v\right)\\
&+\left(\sigma_{xz}\frac{\partial}{\partial x}\delta w+\sigma_{yz}\frac{\partial}{\partial y}\delta w+\sigma_z\frac{\partial}{\partial z}\delta w\right)\\
&-\delta\left(F_x u+F_y v+F_z w\right)-\delta\sigma_z\left(\epsilon_z-\frac{\partial w}{\partial z}\right)\\
&-\delta\sigma_{yz}\left(\epsilon_{yz}-\frac{\partial w}{\partial y}-\frac{\partial v}{\partial z}\right)-\delta\sigma_{xz}\left(\epsilon_{xz}-\frac{\partial w}{\partial x}-\frac{\partial u}{\partial z}\right)\Big]\,dv_j\\
&-\int_{s_{j\sigma}}\delta\left(T_x u+T_y v+T_z w\right)ds_j\Big\}=0.
\end{aligned}
\tag{2.51}
$$

This could be rearranged to be

$$
\begin{aligned}
\mathbf{I}\;=\;&\sum_j\Big\{\int_{v_j}\big[(\sigma_x\delta\epsilon_x+\sigma_y\delta\epsilon_y+\sigma_{xy}\delta\epsilon_{xy}\\
&-\epsilon_z\delta\sigma_z-\epsilon_{yz}\delta\sigma_{yz}-\epsilon_{xz}\delta\sigma_{xz})
\end{aligned}
$$

$$
\begin{aligned}
&+\sigma_z\delta\frac{\partial w}{\partial z}+\sigma_{yz}\delta\left(\frac{\partial w}{\partial y}+\frac{\partial v}{\partial z}\right)+\sigma_{xz}\delta\left(\frac{\partial w}{\partial x}+\frac{\partial u}{\partial z}\right)\\
&+\delta\sigma_z\frac{\partial w}{\partial z}+\delta\sigma_{yz}\left(\frac{\partial w}{\partial y}+\frac{\partial v}{\partial z}\right)+\delta\sigma_{xz}\left(\frac{\partial w}{\partial x}+\frac{\partial u}{\partial z}\right)\Big]\,dv_j\\
&-\int_{v_j}\delta\left(F_x u+F_y v+F_z w\right)dv_j\\
&-\int_{s_{j\sigma}}\delta\left(T_x u+T_y v+T_z w\right)ds_j\Big\}=0. \qquad (2.52)
\end{aligned}
$$

or

$$
\begin{aligned}
\mathbf{I} \;=\; &\sum_j\Big\{\int_{v_j}\mathbf{p}^T\delta\mathbf{q}\,dv_j+\int_{v_j}\delta\Big[\sigma_z\frac{\partial w}{\partial z}+\sigma_{yz}\left(\frac{\partial w}{\partial y}+\frac{\partial v}{\partial z}\right)\\
&+\sigma_{xz}\left(\frac{\partial w}{\partial x}+\frac{\partial u}{\partial z}\right)\Big]dv_j-\int_{v_j}\delta\left(F_x u+F_y v+F_z w\right)dv_j\\
&-\int_{s_{j\sigma}}\delta\left(T_x u+T_y v+T_z w\right)ds_j\Big\}=0. \qquad (2.53)
\end{aligned}
$$

In matrix form, it is

$$
\begin{aligned}
\mathbf{I} \;=\; &\sum_j\Big\{\int_{v_j}\delta\left(\frac{1}{2}\mathbf{q}^T\mathbf{R}\mathbf{q}\right)dv_j+\int_{v_j}\delta\left(\boldsymbol{\sigma}_q{}^T\overline{\mathbf{B}}_i\,\mathbf{u}\right)dv_j\\
&-\int_{v_j}\delta\left(\overline{\mathbf{F}}^T\mathbf{u}\right)dv_j-\int_{s_{j\sigma}}\delta\left(\overline{\mathbf{T}}^T\mathbf{u}\right)ds_j\Big\}=0 \qquad (2.54)
\end{aligned}
$$

or can be written as

$$
\begin{aligned}
\mathbf{I} \;=\; &\delta\sum_j\Big[\int_{v_j}\left(\frac{1}{2}\mathbf{q}^T\mathbf{R}\mathbf{q}+\boldsymbol{\sigma}_q{}^T\overline{\mathbf{B}}_i\,\mathbf{u}-\overline{\mathbf{F}}^T\mathbf{u}\right)dv_j\\
&-\int_{s_{j\sigma}}\overline{\mathbf{T}}^T\mathbf{u}\,ds_j\Big]=0 \qquad (2.55)
\end{aligned}
$$

It can be seen that $\mathbf{I}$ is a complete variation. Thus we rewrite the above integral as a variational functional as

$$\delta\Pi_C \;=\; 0$$

$$\Pi_C = \sum_j \left[\int_{v_j} \left(\frac{1}{2} \mathbf{q}^T \mathbf{R} \mathbf{q} + \boldsymbol{\sigma}^T \overline{\mathbf{B}}_c \mathbf{u} - \overline{\mathbf{F}}^T \mathbf{u} \right) dv_j - \int_{s_{j\sigma}} \overline{\mathbf{T}}^T \mathbf{u} ds_j \right] \quad (2.56)$$

where,

$\mathbf{q}$ is global vector,

$\mathbf{R}$ is combined constitutive matrix,

$\overline{\mathbf{B}}_c$ is a compatibility relation matrix,

$\overline{\mathbf{F}}$ is prescribed body force vector,

$\overline{\mathbf{T}}$ is prescribed boundary surface force vector.

2.4 Discussions on the Variational Functional

The variational functional developed in the last section can also be derived from the Hellinger Reissner principle [61]. The procedure is briefly expressed as follows.

The original version of the Hellinger-Reissner Principle which involves all the displacements and stresses is in the form

$$\delta \Pi_R = 0 \quad (2.57)$$

$$\Pi_R = \sum_n \int_{v_n} \left[-\frac{1}{2} \boldsymbol{\sigma}^T \mathbf{S} \boldsymbol{\sigma} + \boldsymbol{\sigma}^T (\mathbf{B}\mathbf{u}) \right] dv_n - W \quad (2.58)$$

where $\boldsymbol{\sigma}$ are the stresses, $\mathbf{S}$ is the compliance matrix, and the strains $\boldsymbol{\epsilon}$ are expressed

in terms of displacements u, by $\mathbf{Bu}$, as

$$\mathbf{Bu} = \begin{bmatrix} \frac{\partial}{\partial x} & 0 & 0 \\ 0 & \frac{\partial}{\partial y} & 0 \\ \frac{\partial}{\partial y} & \frac{\partial}{\partial x} & 0 \\ 0 & 0 & \frac{\partial}{\partial z} \\ 0 & \frac{\partial}{\partial z} & \frac{\partial}{\partial y} \\ \frac{\partial}{\partial z} & 0 & \frac{\partial}{\partial x} \end{bmatrix} \begin{Bmatrix} u \\ v \\ w \end{Bmatrix} \tag{2.59}$$

W represents the work by applied loads.

Divide the stresses $\boldsymbol{\sigma}$ and strains $\boldsymbol{\epsilon}$ into the global and local parts,

$$\begin{aligned} \boldsymbol{\epsilon}_g &= \{\epsilon_x, \epsilon_y, \epsilon_{xy}\}^T \\ \boldsymbol{\epsilon}_L &= \{\epsilon_z, \epsilon_{yz}, \epsilon_{xz}\}^T \\ \boldsymbol{\sigma}_g &= \{\sigma_z, \sigma_{yz}, \sigma_{xz}\}^T \\ \boldsymbol{\sigma}_L &= \{\sigma_x, \sigma_y, \sigma_{xy}\}^T \end{aligned} \tag{2.60}$$

The stress-strain relation becomes

$$\begin{Bmatrix} \boldsymbol{\epsilon}_g \\ \boldsymbol{\epsilon}_L \end{Bmatrix} = \begin{bmatrix} \mathbf{S}_1 & \mathbf{S}_2 \\ \mathbf{S}_2^T & \mathbf{S}_3 \end{bmatrix} \begin{Bmatrix} \boldsymbol{\sigma}_L \\ \boldsymbol{\sigma}_g \end{Bmatrix}. \tag{2.61}$$

By substituting Equation 2.60 into Equation 2.58 but eliminating the in-plane stresses $\boldsymbol{\sigma}_L$ by using Equation 2.61, with the definition of Equation 2.17, we obtain the modified Hellinger-Reissner Principle as

$$\Pi_{mR} = \sum_n \int_{v_n} \left[\frac{1}{2} \boldsymbol{\epsilon}_g{}^T \mathbf{R}_1 \boldsymbol{\epsilon}_g + \boldsymbol{\sigma}_g{}^T \mathbf{R}_3 \boldsymbol{\epsilon}_g + \frac{1}{2} \boldsymbol{\sigma}_g{}^T \mathbf{R}_4 \boldsymbol{\sigma}_g + \boldsymbol{\sigma}_g{}^T \boldsymbol{\epsilon}_L \right] dv_n - W \tag{2.62}$$

or can be written as

$$\Pi_{mR} = \sum_n \int_{v_n} \left[\frac{1}{2} \mathbf{q}^T \mathbf{R} \mathbf{q} + \boldsymbol{\sigma}_g{}^T \boldsymbol{\epsilon}_L \right] dv_n - W \tag{2.63}$$

This variational principle was first suggested by Reissner [53, 54] and was derived independently by Moriya [35] through the Hu-Washizu principle.

Comparing Equation 2.56 and 2.63, we find that the two variational functionals are the same. However the derivation procedures for equation 2.56 give a clear physical meaning, while that of Equation 2.63 does not.

Compared with Huang's procedure [56], the present derivation did not take the continuity condition (equation 2.7) as a basic equation. The continuity condition must be enforced later at interlaminar surfaces. This will be presented in more detail in Chapter 5.

Chapter 3

The Iso-Function Method for Assuming Partial Stress Field

To take the three transverse stresses as basic variables, a partial stress field has to be assumed. Finite element formulations involving assumed stress field have been cursed with spurious kinematic modes. These modes have plagued the hybrid formulation method since the beginning. Here, a new method was developed to form the partial stress field, which formulates the assumed stress field on the basis of the previously assumed displacement field. With this method, the partial stress fields for 3-D, 8-node, 16-node and 20-node isoparametric composite finite elements are obtained.

3.1 The Stress Field and Spurious Zero Energy Mode

In 1964, Pian[62] developed a technique of hybrid finite element in which the assumed stress field consists of several stress terms multiplied by corresponding stress field parameters as

$$\boldsymbol{\sigma} = \sigma_1\beta_1 + \sigma_2\beta_2 + \cdots + \sigma_m\beta_m = \mathbf{P}\boldsymbol{\beta}. \tag{3.1}$$

Based on Hellinger-Reissner principle:

$$\delta\Pi_H = 0, \tag{3.2}$$

$$\Pi_H = \int_V (-\frac{1}{2}\boldsymbol{\sigma}^T\mathbf{S}\boldsymbol{\sigma} + \boldsymbol{\sigma}^T\boldsymbol{\epsilon} - \overline{\mathbf{F}}^T\mathbf{u})dv - \int_{S_\sigma} \overline{\mathbf{T}}^T\mathbf{u}ds, \tag{3.3}$$

where $\boldsymbol{\beta}$ can be determined by the nodal displacement $\boldsymbol{\delta}$ as

$$\boldsymbol{\beta} = \mathbf{H}^{-1}\mathbf{G}\boldsymbol{\delta}, \tag{3.4}$$

in which

$$\mathbf{H} = \int_V \mathbf{P}^T\mathbf{S}\mathbf{P}dv, \tag{3.5}$$

and

$$\mathbf{G} = \int_V \mathbf{P}^T\mathbf{B}dv. \tag{3.6}$$

The element stiffness matrix is given by

$$\mathbf{K}_H = \mathbf{G}^T\mathbf{H}^{-1}\mathbf{G}, \tag{3.7}$$

and the element governing equation is

$$\mathbf{K}_H\boldsymbol{\delta} = \mathbf{f}, \tag{3.8}$$

where

$$\mathbf{f} = \int_V \mathbf{N}^T \overline{\mathbf{F}} dv + \int_{S_\sigma} \mathbf{N}^T \overline{\mathbf{T}} ds \tag{3.9}$$

in which, **N** is the matrix of shape function of the finite element.

A few questions have arisen since the formulation of the hybrid finite element method:

— how many stress field parameters should be assumed and

— what are the proper stress field terms.

An unproper stress field will yield spurious zero energy modes, which are not rigid body motion and without any energy produced by boundary forces. Thus spurious displacements exist due to an improperly chosen stress field.

A few researchers have attempted to provide answers to the above questions. Fraeijs de Veubeke[63], Pian and Tong[58] gave a necessary, but not sufficient condition to assure no zero-energy modes to occur:

$$m \geq n - r \tag{3.10}$$

where m is the total number of assumed stress field parameters, n is the total number of generalized displacements, r is the number of rigid body degrees of freedom of the element.

Ahmad and Irons[64] suggested use of an eigenvalue technique to assess a hybrid stress field and to determine the kinematic modes.

Spilker, Maskeri and Kania[65] stated that **G** controls the rank of the element stiffness matrix. Recently Huang [56] showed that **H** also has effects on the rank of stiffness matrix.

Brezzi[66], Babuska, Oden and Lee[67, 68], presented necessary and sufficient conditions for stability and convergence, which are named as the Ladyzhenskaya-Babuska-Brezzi conditions.

Spilker[69] investigated the 3-D hybrid elements and suggested using complete sets of each order of stress field terms.

Atluri etc. [59, 60] using a symmetric group theory, gave all the possible strain and stress field terms. By checking the integration of the products of the strain and stress terms in each sub-group, they gave two choices for 2-D, 4-node elements(5β), eight choices for 3-D, 8-node elements(18β), and 384 choices for 3-D, 20-node elements(54β). However numerical analysis has shown that most of these choices badly result with spurious zero energy problems[56].

In 1989, Huang [56] presented a modal analysis technique to form the stress field for hybrid element and the partial stress field for composite element. In his method, the stress field is assumed as

$$\boldsymbol{\sigma} = \mathbf{P}\boldsymbol{\beta} \tag{3.11}$$

where

$\boldsymbol{\sigma}$: stress in the element

$\mathbf{P} = [\sigma_1, \sigma_2, \cdots, \sigma_m]$ is *assumed stress mode*

$m = n - r$ is the total number of stress field modes

In this modal analysis technique, the stress mode $\mathbf{P}$ is formed from the deformation mode $\boldsymbol{\delta}$ of corresponding displacement formulated element by an iterative method.

The iterative equation is

$$\boldsymbol{\sigma}_j^{i+1} = \mathbf{P}^i \mathbf{H}^{i^{-1}} \mathbf{G}^i \boldsymbol{\delta}_j \tag{3.12}$$

where $j = 1, 2, \cdots, m$; m is total number of deformation modes of the element, $i = 1, 2, 3, \cdots$, is the iteration number.

$$\mathbf{H}^i = \int_V \mathbf{P}^{i^T} \mathbf{S} \mathbf{P}^i dv \tag{3.13}$$

$$\mathbf{G}^i = \int_V \mathbf{P}^{i^T} \mathbf{B} dv \tag{3.14}$$

Then

$$\mathbf{P}^{i+1} = [\sigma_1^{i+1}, \sigma_2^{i+1}, \cdots, \sigma_m^{i+1}] \tag{3.15}$$

With above method, Huang[56] analysed and gave the partial stress fields for a 4 node square plane element and an 8-node three dimensional brick element of isotropic material.

It is clear from equation(3.13) that $\mathbf{H}$ depends on the material properties. That means the stress mode $\mathbf{P}$ derived by Huang's iterative method depends on the material properties. This limits his modal analysis method to isotropic material. It is not reasonable to use an element developed from an isotropic material to formulate an element for anisotropic materials.

For 8-node three dimensional brick element of isotropic material, the assumed partial stress field given by Huang [56] is

$$\begin{Bmatrix} \sigma_\zeta \\ \sigma_{\eta\zeta} \\ \sigma_{\xi\zeta} \end{Bmatrix} = \begin{bmatrix} 1 & 0 & 0 & \xi & \eta & 0 & 0 & \xi\eta \\ 0 & 1 & 0 & 0 & 0 & \xi & \xi & 0 \\ 0 & 0 & 1 & 0 & 0 & \eta & -\eta & 0 \end{bmatrix} \tag{3.16}$$

it is obvious that this stress field does not include any arbitrary linear or high order terms in the transverse direction to make the continuity of transverse stresses across the elements possible. Thus this stress field could not satisfy the requirement of continuity of stress across elements.

Eigenvalue analysis of the finite element stiffness matrix formulated with the stress field given in (3.16) also shows this stress field weakens the stiffness of the elements.

3.2 The Iso-Function Stress Field Formulation Method

In this section, a new method called *iso-function* stress field formulation method is presented. The assumed displacement field is expressed as

$$\mathbf{u} = \Phi\mathbf{a} \tag{3.17}$$

where Φ and $\mathbf{a}$ are defined as:

$\Phi = [\phi_1, \phi_2, \cdots, \phi_n]$ is a vector of displacement functions of an element. Φ only depends on the number of element degrees of freedom, and have no relation with the element geometry and material properties.

$\mathbf{a} = [a_1, a_2, \cdots, a_n]^T$ is displacement field parameter.

n - total number degrees of freedom of the element.

Then, the nodal displacement of the element can be expressed as:

$$\boldsymbol{\delta} = \begin{bmatrix} \Phi_1 \\ \Phi_2 \\ \vdots \\ \Phi_n \end{bmatrix} \mathbf{a} = \Lambda\mathbf{a} \tag{3.18}$$

We have

$$\mathbf{a} = \Lambda^{-1}\boldsymbol{\delta} \tag{3.19}$$

and

$$\mathbf{u} = \Phi\Lambda^{-1}\boldsymbol{\delta} \tag{3.20}$$

Compare this equation with equation (4.30), we have

$$\mathbf{N} = \Phi\Lambda^{-1}, \tag{3.21}$$

where **N** is the shape function of the element.

Then the strain field could be expressed as:

$$\boldsymbol{\epsilon} = \Psi\mathbf{a} \tag{3.22}$$

where

Ψ is the first derivative of Φ

$$\Psi = \frac{\partial\Phi}{\partial(x, y, z)} \tag{3.23}$$

and the stress field derived from the assumed displacement field is

$$\boldsymbol{\sigma} = \mathbf{C}\Psi\mathbf{a} \tag{3.24}$$

Equation(3.24) can also be written as:

$$\sigma_i = \sum_{j=1}^{n}\sum_{k=1}^{n} \mathrm{C}_{ij}\psi_{\_}\ a_k = \sum\sum \psi_{jk}\mathrm{C}_{ij}a_k \tag{3.25}$$

Then, in matrix form, the stress field in equation(3.24) can be written as

$$\boldsymbol{\sigma} = \Theta\gamma \tag{3.26}$$

where, Θ is the stress function formulated from the assumed displacement field, which is only determined by the degree of freedom of element. γ is stress parameter,

which is formed from the products of C_{ij} and a_k and depends on the boundary conditions, shape of the element and element material properties.

Now, let's assume that the originally assumed stress field takes the form as

$$\boldsymbol{\sigma} = \mathbf{P}\boldsymbol{\beta} \tag{3.27}$$

where, $\mathbf{P}$ is the *assumed stress field function*, which is only determined by the degrees of freedom of the stress field. $\boldsymbol{\beta}$ is the *assumed stress field parameter*, which is determined by the element boundary conditions, element geometry, and element material properties.

The difference between the stress distributions given by equation(3.26) and (3.27) is: in equation(3.26), the stress is obtained from the derivation of displacement distribution, but in equation(3.27), the stress is basic variable.

If the assumed displacement field does exactly represent the real deformation of the elastic element, for example, in the case of $n \longrightarrow \infty$, and the assumed stress field does exactly represent the real stress distribution in the element, the stress field given by equation(3.26) and equation(3.27) should be same. That is

$$\Theta\gamma = \mathbf{P}\boldsymbol{\beta} \tag{3.28}$$

which yields

$$\mathbf{P} = \Theta \tag{3.29}$$

For real problems, n is a finite number. The assumed displacement field is only an approximation of the actual deformation state of the element. If the displacements are taken as basic variables, the stiffness matrix will be stiffened compared with the actual stiffness of the element. If the assumed stresses are taken as basic variables, the corresponding stiffness matrix will be weakened compared with the actual

stiffness of the element.

With above, the following conclusions for formulating assumed stress field can be arrived,

1) The number of assumed stress field parameters m should be:

$$m \geq n - r \tag{3.30}$$

and for composite element:

$$m \geq n - r - s \tag{3.31}$$

where s is the number of non-zero modes of the semi-displacement stiffness matrix $\mathbf{K}_d$ (see equation 4.16).

2) The corresponding displacement field of the element should converge to the real displacement field.

3) The assumed stress field function, Θ, should at least include some arbitrary linear or high order terms in the z direction in order to make the continuity of stress across the elements possible.

4) By taking

$$\Theta = \mathbf{P}, \tag{3.32}$$

an iso-function stress field is formulated:

$$\boldsymbol{\sigma} = \mathbf{P}\boldsymbol{\beta} \tag{3.33}$$

The third condition makes the continuity of stress variables through the laminate possible.

Based on similarity in form of the stress expressions, the *iso-function stress field formulation method* was presented. The formulated stress field may not be better than others, but the method proposes an easy way to form the partial stress stress field which is zero-energy-mode free as will be shown in the following sections.

3.3 Examples of the iso-function method

3.3.1 The Partial Stress Field for 3-D, 8-node Finite Element

With the above method, an iso-function partial stress field can be formed for 3-D, 8-node composite element as follows:

For a 3-D, 8-node isoparametric element (see Fig.3.1), the displacement field is

$$\mathbf{u} = \mathbf{N}\boldsymbol{\delta} \tag{3.34}$$

where

$$\mathbf{u} = \begin{Bmatrix} u(\xi,\eta,\zeta) \\ v(\xi,\eta,\zeta) \\ w(\xi,\eta,\zeta) \end{Bmatrix} \tag{3.35}$$

$$\mathbf{N} = \begin{bmatrix} N_1 & 0 & & N_2 & 0 & 0 & \cdots & N_8 & 0 & 0 \\ 0 & N_1 & 0 & 0 & N_2 & 0 & \cdots & 0 & N_8 & 0 \\ 0 & 0 & N_1 & 0 & 0 & N_2 & \cdots & 0 & 0 & N_8 \end{bmatrix} \tag{3.36}$$

in which

$$N_i = \frac{1}{8}(1+\xi_i\xi)(1+\eta_i\eta)(1+\zeta_i\zeta) \tag{3.37}$$

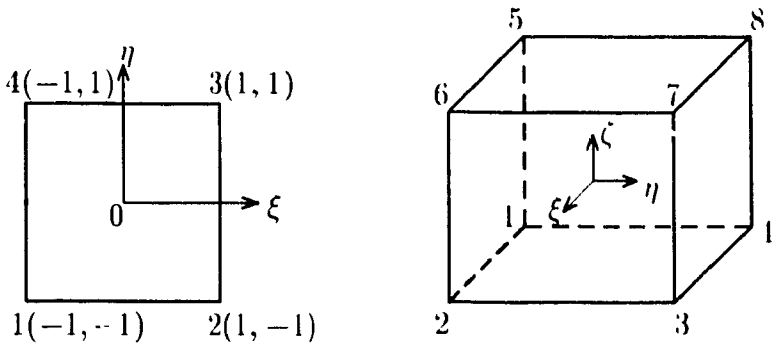

Figure 3.1: 3-D, 8-node isoparametric element

Thus we have

$$u = a_0 + a_1\xi + a_2\eta + a_3\zeta + a_4\xi\eta + a_5\xi\zeta + a_6\eta\zeta + a_7\xi\eta\zeta$$

$$v = b_0 + b_1\xi + b_2\eta + b_3\zeta + b_4\xi\eta + b_5\xi\zeta + b_6\eta\zeta + b_7\xi\eta\zeta$$

$$w = c_0 + c_1\xi + c_2\eta + c_3\zeta + c_4\xi\eta + c_5\xi\zeta + c_6\eta\zeta + c_7\xi\eta\zeta$$

or in matrix form

$$\mathbf{u} = \mathbf{\Phi a} \tag{3.38}$$

in which

$$\Phi = \begin{bmatrix} 1 & 0 & 0 & \xi & 0 & 0 & \cdots & \xi\eta\zeta & 0 & 0 \\ 0 & 1 & 0 & 0 & \xi & 0 & \cdots & 0 & \xi\eta\zeta & 0 \\ 0 & 0 & 1 & 0 & 0 & \xi & \cdots & 0 & 0 & \xi\eta\zeta \end{bmatrix} \tag{3.39}$$

$$\mathbf{a} = \left\{ \begin{array}{ccccccccccc} a_0 & b_0 & c_0 & a_1 & b_1 & c_1 & \cdots & a_7 & b_7 & c_7 \end{array} \right\}^T \tag{3.40}$$

The strains derived from the assumed displacement field are

$$\epsilon_\xi = \frac{\partial u}{\partial \xi} = a_1 + a_4\eta + a_5\zeta + a_7\eta\zeta$$

$$\epsilon_\eta = \frac{\partial v}{\partial \eta} = b_2 + b_4\xi + b_6\zeta + b_7\xi\zeta$$
$$\epsilon_\zeta = \frac{\partial w}{\partial \zeta} = c_3 + c_5\xi + c_6\eta + c_7\xi\eta$$
$$\epsilon_{\eta\zeta} = \frac{\partial w}{\partial \eta} + \frac{\partial v}{\partial \zeta} = (c_2 + b_3) + (c_4 + b_5)\xi + b_6\eta + c_6\zeta + b_7\xi\eta + c_7\xi\zeta$$
$$\epsilon_{\xi\zeta} = \frac{\partial w}{\partial \xi} + \frac{\partial u}{\partial \zeta} = (c_1 + a_3) + (c_4 + a_6)\eta + a_5\xi + c_5\zeta + a_7\xi\eta + c_7\eta\zeta$$
$$\epsilon_{\xi\eta} = \frac{\partial v}{\partial \xi} + \frac{\partial u}{\partial \eta} = (b_1 + a_2) + a_4\xi + b_4\eta + (b_5 + a_6)\zeta + b_7\eta\zeta + a_7\xi\eta$$

Then the stress field derived from the assumed displacement field is

$$\boldsymbol{\sigma} = \mathbf{C}\bar{\boldsymbol{\epsilon}} \tag{3.41}$$

in which

$$\bar{\boldsymbol{\sigma}} = \left\{ \sigma_\xi,\ \sigma_\eta,\ \sigma_\zeta,\ \sigma_{\eta\zeta},\ \sigma_{\xi\zeta},\ \sigma_{\xi\eta} \right\}^T \tag{3.42}$$
$$\bar{\boldsymbol{\epsilon}} = \left\{ \epsilon_\xi,\ \epsilon_\eta,\ \epsilon_\zeta,\ \epsilon_{\eta\zeta},\ \epsilon_{\xi\zeta},\ \epsilon_{\xi\eta} \right\}^T \tag{3.43}$$

For on-axis orthotropic material

$$\mathbf{C} = \begin{bmatrix} C_{11} & C_{12} & C_{13} & 0 & 0 & 0 \\ C_{21} & C_{22} & C_{23} & 0 & 0 & 0 \\ C_{31} & C_{32} & C_{33} & 0 & 0 & 0 \\ 0 & 0 & 0 & C_{44} & 0 & 0 \\ 0 & 0 & 0 & 0 & C_{55} & 0 \\ 0 & 0 & 0 & 0 & 0 & C_{66} \end{bmatrix} \tag{3.44}$$

Thus

$$\sigma_\zeta = C_{31}\epsilon_\xi + C_{32}\epsilon_\eta + C_{33}\epsilon_\zeta \tag{3.45}$$

$$\sigma_{\eta\zeta} = C_{44}\epsilon_{\eta\zeta} \tag{3.46}$$

$$\sigma_{\xi\zeta} = C_{55}\epsilon_{\xi\zeta} \tag{3.47}$$

or in matrix form

$$\boldsymbol{\sigma}_g = \Theta\boldsymbol{\gamma} \tag{3.48}$$

where

$$\bar{\boldsymbol{\sigma}}_g = \left[\sigma_\zeta, \sigma_{\eta\zeta}, \sigma_{\xi\zeta}\right]^T \tag{3.49}$$

$$\Theta = \begin{bmatrix} 1 & 0 & 0 & \xi & 0 & 0 & \eta & 0 & 0 & \zeta & 0 & 0 & \xi\eta & 0 & 0 & \eta\zeta & 0 & \xi\zeta & 0 \\ 0 & 1 & 0 & 0 & \xi & 0 & 0 & \eta & 0 & 0 & \zeta & 0 & 0 & \xi\eta & 0 & 0 & 0 & 0 & \xi\zeta \\ 0 & 0 & 1 & 0 & 0 & \xi & 0 & 0 & \eta & 0 & 0 & \zeta & 0 & 0 & \xi\eta & 0 & \eta\zeta & 0 & 0 \end{bmatrix} \tag{3.50}$$

$$\boldsymbol{\gamma} = [\gamma_1, \gamma_2, \gamma_3, \cdots, \gamma_{19}] \tag{3.51}$$

$$\gamma_1 = C_{31}a_1 + C_{32}b_2 + C_{33}c_3 \tag{3.52}$$

$$\gamma_2 = C_{44}(c_2 + b_3) \tag{3.53}$$

$$\gamma_3 = C_{55}(c_1 + a_3) \tag{3.54}$$

$$\gamma_4 = C_{32}b_4 + C_{33}c_5 \tag{3.55}$$

$$\gamma_5 = C_{44}(c_4 + b_5) \tag{3.56}$$

$$\gamma_6 = C_{55}a_5 \tag{3.57}$$

$$\gamma_7 = C_{31}a_4 + C_{33}c_6 \tag{3.58}$$

$$\gamma_8 = C_{44}b_6 \tag{3.59}$$

$$\gamma_9 = C_{55}(c_4 + a_6) \tag{3.60}$$

$$\gamma_{10} = C_{32}b_6 + C_{31}a_5 \tag{3.61}$$

$$\gamma_{11} = C_{44}c_6 \tag{3.62}$$

$$\gamma_{12} = C_{55}c_5 \tag{3.63}$$

$$\gamma_{13} = C_{33}c_7 \tag{3.64}$$

$$\gamma_{14} = C_{44}b_7 \tag{3.65}$$

$$\gamma_{15} = C_{55}a_7 \tag{3.66}$$

$$\gamma_{16} = C_{31}a_7 \tag{3.67}$$

$$\gamma_{17} = C_{55}c_7 \tag{3.68}$$

$$\gamma_{18} = C_{32}b_7 \tag{3.69}$$

$$\gamma_{19} = C_{44}c_7 \tag{3.70}$$

By the iso-function method, the partial stress field is

$$\boldsymbol{\sigma}_g = \mathbf{P}\boldsymbol{\beta}$$

where the partial stress field function

$$\begin{aligned}\mathbf{P} &= \Theta \\ &= \begin{bmatrix} 1 & 0 & 0 & \xi & 0 & 0 & \eta & 0 & 0 & \zeta & 0 & 0 & \xi\eta & 0 & 0 & \eta\zeta & 0 & \xi\zeta & 0 \\ 0 & 1 & 0 & 0 & \xi & 0 & 0 & \eta & 0 & 0 & \zeta & 0 & 0 & \xi\eta & 0 & 0 & 0 & 0 & \xi\zeta \\ 0 & 0 & 1 & 0 & 0 & \xi & 0 & 0 & \eta & 0 & 0 & \zeta & 0 & 0 & \xi\eta & 0 & \eta\zeta & 0 & 0 \end{bmatrix}\end{aligned} \tag{3.71}$$

Similarly, for off-axis orthotropic material with one of the symmetry planes coinciding with the ζ- or z-coordinate axis, the material stiffness matrix is

$$\mathbf{C} = \begin{bmatrix} C_{11} & C_{12} & C_{13} & 0 & 0 & C_{16} \\ C_{21} & C_{22} & C_{23} & 0 & 0 & C_{26} \\ C_{31} & C_{32} & C_{33} & 0 & 0 & C_{36} \\ 0 & 0 & 0 & C_{44} & C_{45} & 0 \\ 0 & 0 & 0 & C_{54} & C_{55} & 0 \\ C_{61} & C_{62} & C_{63} & 0 & 0 & C_{66} \end{bmatrix} \tag{3.72}$$

The transverse stresses are

$$\sigma_\zeta = C_{31}\epsilon_\xi + C_{32}\epsilon_\eta + C_{33}\epsilon_\zeta + C_{36}\epsilon_{\xi\eta} \tag{3.73}$$

$$\sigma_{\eta\zeta} = C_{44}\epsilon_{\eta\zeta} + C_{45}\epsilon_{\xi\zeta} \tag{3.74}$$

$$\sigma_{\xi\zeta} = C_{54}\epsilon_{\eta\zeta} + C_{55}\epsilon_{\xi\zeta} \tag{3.75}$$

Thus

$$\gamma = [\gamma_1, \gamma_2, \gamma_3, \cdots, \gamma_{21}] \tag{3.76}$$

in which

$$\gamma_1 = C_{31}a_1 + C_{32}b_2 + C_{33}c_3 + C_{36}(b_1 + a_2) \tag{3.77}$$

$$\gamma_2 = C_{44}(c_2 + b_3) + C_{45}(c_1 + a_3) \tag{3.78}$$

$$\gamma_3 = C_{55}(c_1 + a_3) + C_{54}(c_2 + b_3) \tag{3.79}$$

$$\gamma_4 = C_{32}b_4 + C_{33}c_5 + C_{36}a_4 \tag{3.80}$$

$$\gamma_5 = C_{44}(c_4 + b_5) + C_{45}a_5 \tag{3.81}$$

$$\gamma_6 = C_{54}(c_4 + b_5) + C_{55}a_5 \tag{3.82}$$

$$\gamma_7 = C_{31}a_4 + C_{33}c_6 + C_{36}b_4 \tag{3.83}$$

$$\gamma_8 = C_{44}b_6 + C_{45}(c_4 + a_6) \tag{3.84}$$

$$\gamma_9 = C_{54}b_6 + C_{55}(c_4 + a_6) \tag{3.85}$$

$$\gamma_{10} = C_{32}b_6 + C_{31}a_5 + C_{36}(b_5 + a_6) \tag{3.86}$$

$$\gamma_{11} = C_{44}c_6 + C_{45}c_5 \tag{3.87}$$

$$\gamma_{12} = C_{54}c_6 + C_{55}c_5 \tag{3.88}$$

$$\gamma_{13} = C_{33}c_7 + C_{36}a_7 \tag{3.89}$$

$$\gamma_{14} = C_{44}b_7 + C_{45}a_7 \tag{3.90}$$

$$\gamma_{15} = C_{54}b_7 + C_{55}a_7 \tag{3.91}$$

$$\gamma_{16} = C_{31}a_7 + C_{36}b_7 \tag{3.92}$$

$$\gamma_{17} = C_{45}c_7 \tag{3.93}$$

$$\gamma_{18} = C_{55}c_7 \tag{3.94}$$

$$\gamma_{19} = C_{32}b_7 \tag{3.95}$$

$$\gamma_{20} = C_{44}c_7 \tag{3.96}$$

$$\gamma_{21} = C_{54}c_7 \tag{3.97}$$

The corresponding partial stress field function, by the iso-function method, is

$$\mathbf{P} = \begin{bmatrix} 1 & 0 & 0 & \xi & 0 & 0 & \eta & 0 & 0 & \zeta & 0 & 0 \\ 0 & 1 & 0 & 0 & \xi & 0 & 0 & \eta & 0 & 0 & \zeta & 0 \\ 0 & 0 & 1 & 0 & 0 & \xi & 0 & 0 & \eta & 0 & 0 & \zeta \\ \xi\eta & 0 & 0 & \eta\zeta & 0 & 0 & \xi\zeta & 0 & 0 & & & \\ 0 & \xi\eta & 0 & 0 & \eta\zeta & 0 & 0 & \xi\zeta & 0 & & & \\ 0 & 0 & \xi\eta & 0 & 0 & \eta\zeta & 0 & 0 & \xi\zeta & & & \end{bmatrix} \tag{3.98}$$

.

3.3.2 The Partial Stress Field for 3-D, 16-node Finite Element

The displacement field of a 3-D,16-node isoparametric element (Fig.3.2) is

$$\mathbf{u} = \mathbf{N}\boldsymbol{\delta} \tag{3.99}$$

where

$$\mathbf{u} = \begin{Bmatrix} u(\xi,\eta,\zeta) \\ v(\xi,\eta,\zeta) \\ w(\xi,\eta,\zeta) \end{Bmatrix} \tag{3.100}$$

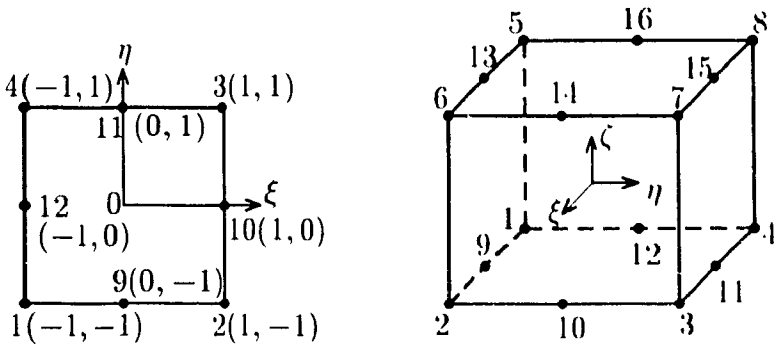

Figure 3.2: 3-D, 16-node isoparametric element

The shape function for the element is

$$\mathbf{N} = \begin{bmatrix} N_1 & 0 & & N_2 & 0 & 0 & \cdots & N_{16} & 0 & 0 \\ 0 & N_1 & 0 & 0 & N_2 & 0 & \cdots & 0 & N_{16} & 0 \\ 0 & 0 & N_1 & 0 & 0 & N_2 & \cdots & 0 & 0 & N_{16} \end{bmatrix} \tag{3.101}$$

in which, for corner nodes

$$N_i = \frac{1}{8}(1+\xi_i\xi)(1+\eta_i\eta)(1+\zeta_i\zeta)(\xi_i\xi+\eta_i\eta-1) \tag{3.102}$$

where $i = 1, 2, 3, \cdots, 8$, and for mid-side nodes

$$N_i = \frac{1}{4}(1+\xi_i\xi)(1+\eta_i\eta)(1+\zeta_i\zeta)\left[(1-\xi^2)(1-\xi_i^2)+(1-\eta^2)(1-\eta_i^2)\right] \tag{3.103}$$

where $i = 9, 10, 11, \cdots, 16$.

Equation(3.99) can be written as

$$\mathbf{u} = \mathbf{\Phi a} \tag{3.104}$$

According to equations(3.99), (3.102), and (3.103), (3.104) will be

$$\begin{aligned} u &= a_0 + a_1\xi + a_2\eta + a_3\zeta + a_4\xi\eta + a_5\xi\zeta + a_6\eta\zeta + a_7\xi\eta\zeta \\ &\quad + a_8\xi^2 + a_9\eta^2 + a_{10}\xi^2\eta + a_{11}\xi^2\zeta + a_{12}\xi\eta^2 + a_{13}\eta^2\zeta \end{aligned}$$

$$
\begin{aligned}
& + a_{14}\xi^2\eta\zeta + a_{15}\xi\eta^2\zeta \\
v &= b_0 + b_1\xi + b_2\eta + b_3\zeta + b_4\xi\eta + b_5\xi\zeta + b_6\eta\zeta + b_7\xi\eta\zeta \\
& + b_8\xi^2 + b_9\eta^2 + b_{10}\xi^2\eta + b_{11}\xi^2\zeta + b_{12}\xi\eta^2 + b_{13}\eta^2\zeta \\
& + b_{14}\xi^2\eta\zeta + b_{15}\xi\eta^2\zeta \\
w &= a_0 + c_1\xi + c_2\eta + c_3\zeta + c_4\xi\eta + c_5\xi\zeta + c_6\eta\zeta + c_7\xi\eta\zeta \\
& + c_8\xi^2 + c_9\eta^2 + c_{10}\xi^2\eta + c_{11}\xi^2\zeta + c_{12}\xi\eta^2 + c_{13}\eta^2\zeta \\
& + c_{14}\xi^2\eta\zeta + c_{15}\xi\eta^2\zeta
\end{aligned}
$$

Thus we have

$$
\Phi = \begin{bmatrix}
1 & 0 & 0 & \xi & 0 & 0 & \cdots & \xi\eta^2\zeta & 0 & 0 \\
0 & 1 & 0 & 0 & \xi & 0 & \cdots & 0 & \xi\eta^2\zeta & 0 \\
0 & 0 & 1 & 0 & 0 & \xi & \cdots & 0 & 0 & \xi\eta^2\zeta
\end{bmatrix} \tag{3.105}
$$

and

$$
\mathbf{a} = \left\{ \begin{array}{cccccccccc} a_0 & b_0 & c_0 & a_1 & b_1 & c_1 & \cdots & a_{15} & b_{15} & c_{15} \end{array} \right\}^T \tag{3.106}
$$

The strains derived from the assumed displacement field are

$$
\begin{aligned}
\epsilon_\xi = \frac{\partial u}{\partial \xi} &= a_1 + a_4\eta + a_5\zeta + a_7\eta\zeta + 2a_8\xi + 2a_{10}\xi\eta + 2a_{11}\xi\zeta \\
& + a_{12}\eta^2 + 2a_{14}\xi\eta\zeta + a_{15}\eta^2\zeta \\
\epsilon_\eta = \frac{\partial v}{\partial \eta} &= b_2 + b_4\xi + b_6\zeta + b_7\xi\zeta + 2b_9\eta + b_{10}\xi^2 + 2b_{12}\xi\eta \\
& + 2b_{13}\eta\zeta + b_{14}\xi^2\zeta + 2b_{15}\xi\eta\zeta \\
\epsilon_\zeta = \frac{\partial w}{\partial \zeta} &= c_3 + c_5\xi + c_6\eta + c_7\xi\eta + c_{11}\xi^2 + c_{13}\eta^2 + c_{14}\xi^2\eta + c_{15}\xi\eta^2 \\
\epsilon_{\eta\zeta} &= \frac{\partial w}{\partial \eta} + \frac{\partial v}{\partial \zeta} = (c_2 + b_3) + (c_4 + b_5)\xi + (2c_9 + b_6)\eta + c_6\zeta \\
& + (2c_{12} + b_7)\xi\eta + c_7\xi\zeta + 2c_{13}\eta\zeta + 2c_{15}\xi\eta\zeta \\
& + (c_{10} + b_{11})\xi^2 + b_{13}\eta^2 + b_{14}\xi^2\eta + c_{14}\xi^2\zeta + b_{15}\xi\eta^2
\end{aligned}
$$

$$
\begin{aligned}
\epsilon_{\xi\zeta} &= \frac{\partial w}{\partial \xi} + \frac{\partial u}{\partial \zeta} = (c_1 + a_3) + (2c_8 + a_5)\xi + (c_4 + a_6)\eta + c_5\zeta \\
&\quad + (2c_{10} + a_7)\xi\eta + 2c_{11}\xi\zeta + c_7\eta\zeta + 2c_{14}\xi\eta\zeta \\
&\quad + a_{11}\xi^2 + (c_{12} + a_{13})\eta^2 + a_{14}\xi^2\eta + a_{15}\xi\eta^2 + c_{15}\eta^2\zeta \\
\epsilon_{\xi\eta} &= \frac{\partial v}{\partial \xi} + \frac{\partial u}{\partial \eta} = (b_1 + a_2) + (2b_8 + a_4)\xi + (b_4 + 2a_9)\eta + (b_5 + a_6)\zeta \\
&\quad + 2(b_{10} + a_{12})\xi\eta + 2(b_{11} + a_7)\xi\zeta + (b_7 + 2a_{13})\eta\zeta + 2(b_{14} + a_{15})\xi\eta\zeta \\
&\quad + a_{10}\xi^2 + b_{12}\eta^2 + a_{14}\xi^2\eta + b_{15}\eta^2\zeta
\end{aligned}
$$

Then the stress field derived from the assumed displacement field is

$$\boldsymbol{\sigma} = \mathbf{C}\boldsymbol{\epsilon} \tag{3.107}$$

For on-axis orthotropic material, we have

$$
\begin{aligned}
\sigma_\zeta &= C_{31}\epsilon_\xi + C_{32}\epsilon_\eta + C_{33}\epsilon_\zeta \\
\sigma_{\eta\zeta} &= C_{44}\epsilon_{\eta\zeta} \\
\sigma_{\xi\zeta} &= C_{55}\epsilon_{\xi\zeta}
\end{aligned}
$$

or in matrix form

$$\boldsymbol{\sigma}_g = \Theta\boldsymbol{\gamma} \tag{3.108}$$

where

$$\boldsymbol{\sigma}_g = \begin{Bmatrix} \sigma_\zeta \\ \sigma_{\eta\zeta} \\ \sigma_{\xi\zeta} \end{Bmatrix} \tag{3.109}$$

$$\boldsymbol{\gamma} = [\gamma_1, \gamma_2, \gamma_3, \cdots, \gamma_{40}] \tag{3.110}$$

in which

$$\gamma_1 = C_{31}a_1 + C_{32}b_2 + C_{33}c_3 \tag{3.111}$$

$$\gamma_2 = C_{44}(c_2 + b_3) \tag{3.112}$$

$$\gamma_3 = C_{55}(c_1 + a_3) \tag{3.113}$$

$$\gamma_4 = 2C_{31}a_8 + C_{32}b_4 + C_{33}c_5 \tag{3.114}$$

$$\gamma_5 = C_{44}(c_4 + b_5) \tag{3.115}$$

$$\gamma_{..} = C_{55}(2c_8 + a_5) \tag{3.116}$$

$$\gamma_7 = C_{31}a_4 + 2C_{32}b_9 + C_{33}c_6 \tag{3.117}$$

$$\gamma_8 = C_{44}(2c_9 + b_6) \tag{3.118}$$

$$\gamma_9 = C_{55}(c_4 + a_6) \tag{3.119}$$

$$\gamma_{10} = C_{32}b_6 + C_{31}a_5 \tag{3.120}$$

$$\gamma_{11} = C_{44}c_6 \tag{3.121}$$

$$\gamma_{12} = C_{55}c_5 \tag{3.122}$$

$$\gamma_{13} = 2C_{31}a_{10} + 2C_{32}b_{12} + C_{33}c_7 \tag{3.123}$$

$$\gamma_{14} = C_{44}(2c_{12} + b_7) \tag{3.124}$$

$$\gamma_{15} = C_{55}(2c_{10} + a_7) \tag{3.125}$$

$$\gamma_{16} = 2C_{31}a_{11} + C_{32}b_7 \tag{3.126}$$

$$\gamma_{17} = C_{44}c_7 \tag{3.127}$$

$$\gamma_{18} = 2C_{55}c_{11} \tag{3.128}$$

$$\gamma_{19} = C_{31}a_7 + 2C_{32}b_{13} \tag{3.129}$$

$$\gamma_{20} = 2C_{44}c_{13} \tag{3.130}$$

$$\gamma_{21} = C_{55}c_7 \tag{3.131}$$

$$\gamma_{22} = 2C_{31}a_{14} + 2C_{32}b_{15} \tag{3.132}$$

$$\gamma_{23} = 2C_{44}c_{15} \tag{3.133}$$

$$\gamma_{24} = 2C_{55}c_{14} \tag{3.134}$$

$$\gamma_{25} = C_{32}b_{10} + C_{33}c_{11} \tag{3.135}$$

$$\gamma_{26} = C_{44}(c_{10} + b_{11}) \tag{3.136}$$

$$\gamma_{27} = C_{55}a_{11} \tag{3.137}$$

$$\gamma_{28} = C_{31}a_{12} + C_{33}c_{13} \tag{3.138}$$

$$\gamma_{29} = C_{44}b_{13} \tag{3.139}$$

$$\gamma_{30} = C_{55}(c_{12} + a_{13}) \tag{3.140}$$

$$\gamma_{31} = C_{33}c_{14} \tag{3.141}$$

$$\gamma_{32} = C_{44}b_{14} \tag{3.142}$$

$$\gamma_{33} = C_{55}a_{14} \tag{3.143}$$

$$\gamma_{34} = C_{32}b_{14} \tag{3.144}$$

$$\gamma_{35} = C_{44}c_{14} \tag{3.145}$$

$$\gamma_{36} = C_{33}c_{15} \tag{3.146}$$

$$\gamma_{37} = C_{44}b_{15} \tag{3.147}$$

$$\gamma_{38} = C_{55}a_{15} \tag{3.148}$$

$$\gamma_{39} = C_{31}a_{15} \tag{3.149}$$

$$\gamma_{40} = C_{55}c_{15} \tag{3.150}$$

and

$$\Theta = \begin{bmatrix} 1 & 0 & 0 & \xi & 0 & 0 & \eta & 0 & 0 & \zeta & 0 & 0 & \xi\eta & 0 & 0 & \xi\zeta & 0 & 0 \\ 0 & 1 & 0 & 0 & \xi & 0 & 0 & \eta & 0 & 0 & \zeta & 0 & 0 & \xi\eta & 0 & 0 & \xi\zeta & 0 \\ 0 & 0 & 1 & 0 & 0 & \xi & 0 & 0 & \eta & 0 & 0 & \zeta & 0 & 0 & \xi\eta & 0 & 0 & \xi\zeta \end{bmatrix}$$

$$\begin{bmatrix} \eta\zeta & 0 & 0 & \xi\eta\zeta & 0 & 0 & \xi^2 & 0 & 0 & \eta^2 & 0 & 0 & \xi^2\eta & 0 & 0 \\ 0 & \eta\zeta & 0 & 0 & \xi\eta\zeta & 0 & 0 & \xi^2 & 0 & 0 & \eta^2 & 0 & 0 & \xi^2\eta & 0 \\ 0 & 0 & \eta\zeta & 0 & 0 & \xi\eta\zeta & 0 & 0 & \xi^2 & 0 & 0 & \eta^2 & 0 & 0 & \xi^2\eta \end{bmatrix}$$

$$\begin{bmatrix} \xi^2\zeta & 0 & \xi\eta^2 & 0 & 0 & \eta^2\zeta & 0 \\ 0 & \xi^2\zeta & 0 & \xi\eta^2 & 0 & 0 & 0 \\ 0 & 0 & 0 & 0 & \xi\eta^2 & 0 & \eta^2\zeta \end{bmatrix} \tag{3.151}$$

By the iso-function method, the partial stress field is

$$\boldsymbol{\sigma}_g = \mathbf{P}\boldsymbol{\beta}.$$

Thus the partial stress field function is

$$\mathbf{P} = \Theta = \begin{bmatrix} 1 & 0 & 0 & \xi & 0 & 0 & \eta & 0 & 0 & \zeta & 0 & 0 & \xi\eta & 0 & 0 & \xi\zeta & 0 & 0 \\ 0 & 1 & 0 & 0 & \xi & 0 & 0 & \eta & 0 & 0 & \zeta & 0 & 0 & \xi\eta & 0 & 0 & \xi\zeta & 0 \\ 0 & 0 & 1 & 0 & 0 & \xi & 0 & 0 & \eta & 0 & 0 & \zeta & 0 & 0 & \xi\eta & 0 & 0 & \xi\zeta \end{bmatrix}$$

$$\begin{matrix} \eta\zeta & 0 & 0 & \xi\eta\zeta & 0 & 0 & \xi^2 & 0 & 0 & \eta^2 & 0 & 0 & \xi^2\eta & 0 & 0 \\ 0 & \eta\zeta & 0 & 0 & \xi\eta\zeta & 0 & 0 & \xi^2 & 0 & 0 & \eta^2 & 0 & 0 & \xi^2\eta & 0 \\ 0 & 0 & \eta\zeta & 0 & 0 & \xi\eta\zeta & 0 & 0 & \xi^2 & 0 & 0 & \eta^2 & 0 & 0 & \xi^2\eta \end{matrix}$$

$$\begin{matrix} \xi^2\zeta & 0 & \xi\eta^2 & 0 & 0 & \eta^2\zeta & 0 \\ 0 & \xi^2\zeta & 0 & \xi\eta^2 & 0 & 0 & 0 \\ 0 & 0 & 0 & 0 & \xi\eta^2 & 0 & \eta^2\zeta \end{matrix} \Bigg] \tag{3.152}$$

Similarly, for off-axis orthotropic material with one of the symmetry planes coincide with the ζ- or z-coordinate axis, the transverse stresses are

$$\sigma_\zeta = C_{31}\epsilon_\xi + C_{32}\epsilon_\eta + C_{33}\epsilon_\zeta + C_{36}\epsilon_{\xi\eta} \tag{3.153}$$

$$\sigma_{\eta\zeta} = C_{44}\epsilon_{\eta\zeta} + C_{45}\epsilon_{\xi\zeta} \tag{3.154}$$

$$\sigma_{\xi\zeta} = C_{54}\epsilon_{\eta\zeta} + C_{55}\epsilon_{\xi\zeta} \tag{3.155}$$

Thus

$$\gamma = [\gamma_1, \gamma_2, \gamma_3, \cdots, \gamma_{42}] \tag{3.156}$$

in which

$$\gamma_1 = C_{31}a_1 + C_{32}b_2 + C_{33}c_3 + C_{36}(b_1 + a_2) \tag{3.157}$$

$$\gamma_2 = C_{44}(c_2 + b_3) + C_{45}(c_1 + a_3) \tag{3.158}$$

$$\gamma_3 = C_{54}(c_2 + b_3) + C_{55}(c_1 + a_3) \tag{3.159}$$

$$\gamma_4 = 2C_{31}a_8 + C_{32}b_4 + C_{33}c_5 + C_{36}(2b_8 + a_4) \tag{3.160}$$

$$\gamma_5 = C_{44}(c_4 + b_5) + C_{45}(2c_8 + a_5) \tag{3.161}$$

$$\gamma_6 = C_{54}(c_4 + b_5) + C_{55}(2c_8 + a_5) \tag{3.162}$$

$$\gamma_7 = C_{31}a_4 + 2C_{32}b_9 + C_{33}c_6 + C_{36}(b_4 + 2a_9) \tag{3.163}$$

$$\gamma_8 = C_{44}(2c_9 + b_6) + C_{45}(c_4 + a_6) \tag{3.164}$$

$$\gamma_9 = C_{54}(2c_9 + b_6) + C_{55}(c_4 + a_6) \tag{3.165}$$

$$\gamma_{10} = C_{32}b_6 + C_{31}a_5 + C_{36}(b_5 + a_6) \tag{3.166}$$

$$\gamma_{11} = C_{44}c_6 + C_{45}c_5 \tag{3.167}$$

$$\gamma_{12} = C_{54}c_6 + C_{55}c_5 \tag{3.168}$$

$$\gamma_{13} = 2C_{31}a_{10} + 2C_{32}b_{12} + C_{33}c_7 + 2C_{36}(b_{10} + a_{12}) \tag{3.169}$$

$$\gamma_{14} = C_{44}(2c_{12} + b_7) + C_{45}(2c_{10} + a_7) \tag{3.170}$$

$$\gamma_{15} = C_{54}(2c_{12} + b_7) + C_{55}(2c_{10} + a_7) \tag{3.171}$$

$$\gamma_{16} = 2C_{31}a_{11} + C_{32}b_7 + 2C_{36}(b_{11} + a_7) \tag{3.172}$$

$$\gamma_{17} = C_{44}c_7 + 2C_{45}c_{11} \tag{3.173}$$

$$\gamma_{18} = C_{54}c_7 + 2C_{55}c_{11} \tag{3.174}$$

$$\gamma_{19} = C_{31}a_7 + 2C_{32}b_{13} + C_{36}(b_7 + 2a_{13}) \tag{3.175}$$

$$\gamma_{20} = 2C_{44}c_{13} + C_{45}c_7 \tag{3.176}$$

$$\gamma_{21} = 2C_{54}c_{13} + C_{55}c_7 \tag{3.177}$$

$$\gamma_{22} = 2C_{31}a_{14} + 2C_{32}b_{15} + 2C_{36}(b_{14} + a_{15}) \tag{3.178}$$

$$\gamma_{23} = 2C_{44}c_{15} + 2C_{45}c_{14} \tag{3.179}$$

$$\gamma_{24} = 2C_{54}c_{15} + 2C_{55}c_{14} \tag{3.180}$$

$$\gamma_{25} = C_{32}b_{10} + C_{33}c_{11} + C_{36}a_{10} \tag{3.181}$$

$$\gamma_{26} = C_{44}(c_{10} + b_{11}) + C_{45}a_{11} \tag{3.182}$$

$$\gamma_{27} = C_{54}(c_{10} + b_{11}) + C_{55}a_{11} \tag{3.183}$$

$$\gamma_{28} = C_{31}a_{12} + C_{33}c_{13} + C_{36}b_{12} \tag{3.184}$$

$$\gamma_{29} = C_{44}b_{13} + C_{45}(c_{12} + a_{13}) \tag{3.185}$$

$$\gamma_{30} = C_{54}b_{13} + C_{55}(c_{12} + a_{13}) \tag{3.186}$$

$$\gamma_{31} = C_{33}c_{14} + C_{36}a_{14} \tag{3.187}$$

$$\gamma_{32} = C_{44}b_{14} + C_{45}a_{14} \tag{3.188}$$

$$\gamma_{33} = C_{54}b_{14} + C_{55}a_{14} \tag{3.189}$$

$$\gamma_{34} = C_{32}b_{14} \tag{3.190}$$

$$\gamma_{35} = C_{44}c_{14} \tag{3.191}$$

$$\gamma_{36} = C_{54}c_{14} \tag{3.192}$$

$$\gamma_{37} = C_{33}c_{15} \tag{3.193}$$

$$\gamma_{38} = C_{44}b_{15} + C_{45}a_{15} \tag{3.194}$$

$$\gamma_{39} = C_{54}b_{15} + C_{55}a_{15} \tag{3.195}$$

$$\gamma_{40} = C_{31}a_{15} + C_{36}b_{15} \tag{3.196}$$

$$\gamma_{41} = C_{45}c_{15} \tag{3.197}$$

$$\gamma_{42} = C_{55}c_{15} \tag{3.198}$$

and, by the iso-function method, the partial stress field function is

$$\mathbf{P} = \begin{bmatrix} 1 & 0 & 0 & \xi & 0 & 0 & \eta & 0 & 0 & \zeta & 0 & 0 & \xi\eta & 0 & 0 & \xi\zeta & 0 & 0 \\ 0 & 1 & 0 & 0 & \xi & 0 & 0 & \eta & 0 & 0 & \zeta & 0 & 0 & \xi\eta & 0 & 0 & \xi\zeta & 0 \\ 0 & 0 & 1 & 0 & 0 & \xi & 0 & 0 & \eta & 0 & 0 & \zeta & 0 & 0 & \xi\eta & 0 & 0 & \xi\zeta \end{bmatrix}$$

$$\begin{matrix} \eta\zeta & 0 & 0 & \xi\eta\zeta & 0 & 0 & \xi^2 & 0 & 0 & \eta^2 & 0 & 0 & \xi^2\eta & 0 & 0 \\ 0 & \eta\zeta & 0 & 0 & \xi\eta\zeta & 0 & 0 & \xi^2 & 0 & 0 & \eta^2 & 0 & 0 & \xi^2\eta & 0 \\ 0 & 0 & \eta\zeta & 0 & 0 & \xi\eta\zeta & 0 & 0 & \xi^2 & 0 & 0 & \eta^2 & 0 & 0 & \xi^2\eta \end{matrix}$$

$$\begin{bmatrix} \xi^2\zeta & 0 & 0 & \xi\eta^2 & 0 & 0 & \eta^2\zeta & 0 & 0 \\ 0 & \xi^2\zeta & 0 & 0 & \xi\eta^2 & 0 & 0 & \eta^2\zeta & 0 \\ 0 & 0 & \xi^2\zeta & 0 & 0 & \xi\eta^2 & 0 & 0 & \eta^2\zeta \end{bmatrix} \tag{3.199}$$

3.3.3 The Partial Stress Field for 3-D, 20-node Finite Element

The displacement field of a 3-D, 20-node isoparametric element (Fig.3.3) is

$$\mathbf{u} = \mathbf{N}\boldsymbol{\delta} \tag{3.200}$$

where

$$\mathbf{u} = \begin{Bmatrix} u(\xi,\eta,\zeta) \\ v(\xi,\eta,\zeta) \\ w(\xi,\eta,\zeta) \end{Bmatrix} \tag{3.201}$$

$$\mathbf{N} = \begin{bmatrix} N_1 & 0 & & N_2 & 0 & 0 & \cdots & N_{20} & 0 & 0 \\ 0 & N_1 & 0 & 0 & N_2 & 0 & \cdots & 0 & N_{20} & 0 \\ 0 & 0 & N_1 & 0 & 0 & N_2 & \cdots & 0 & 0 & N_{20} \end{bmatrix} \tag{3.202}$$

in which, for corner nodes

$$N_i = \frac{1}{8}(1+\xi_i\xi)(1+\eta_i\eta)(1+\zeta_i\zeta)(\xi_i\xi+\eta_i\eta+\zeta_i\zeta-2) \tag{3.203}$$

for mid-side nodes

$$\begin{aligned} N_i &= \frac{1}{4}(1+\xi_i\xi)(1+\eta_i\eta)(1+\zeta_i\zeta)((1-\xi^2)(1-\xi_i^2) \\ &\quad +(1-\eta^2)(1-\eta_i^2)+(1-\zeta^2)(1-\zeta_i^2)) \end{aligned} \tag{3.204}$$

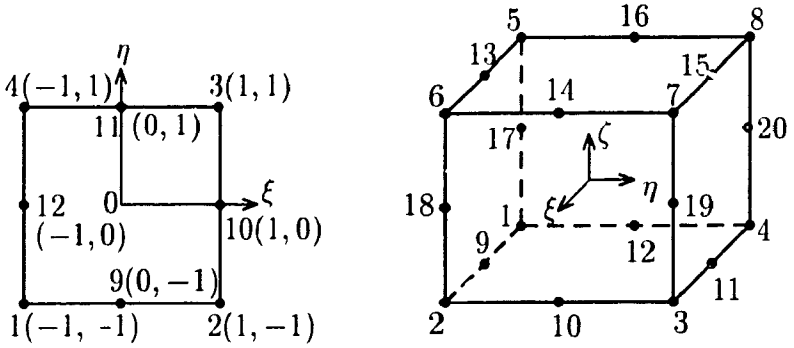

Figure 3.3: 3-D, 20-node isoparametric element

Equation(3.200) can be written as

$$\mathbf{u} = \mathbf{\Phi a} \tag{3.205}$$

According to equations(3.200) and (3.203), (3.205) will be

$$\begin{aligned}
u &= a_0 + a_1\xi + a_2\eta + a_3\zeta + a_4\xi\eta + a_5\xi\zeta + a_6\eta\zeta + a_7\xi\eta\zeta + a_8\xi^2 \\
&\quad + a_9\eta^2 + a_{10}\zeta^2 + a_{11}\xi^2\eta + a_{12}\xi^2\zeta + a_{13}\xi\eta^2 + a_{14}\eta^2\zeta + a_{15}\xi\zeta^2 \\
&\quad + a_{16}\eta\zeta^2 + a_{17}\xi^2\eta\zeta + a_{18}\xi\eta^2\zeta + a_{19}\xi\eta\zeta^2 \\
v &= b_0 + b_1\xi + b_2\eta + b_3\zeta + b_4\xi\eta + b_5\xi\zeta + b_6\eta\zeta + b_7\xi\eta\zeta + b_8\xi^2 \\
&\quad + b_9\eta^2 + b_{10}\zeta^2 + b_{11}\xi^2\eta + b_{12}\xi^2\zeta + b_{13}\xi\eta^2 + b_{14}\eta^2\zeta + b_{15}\xi\zeta^2 \\
&\quad + b_{16}\eta\zeta^2 + b_{17}\xi^2\eta\zeta + b_{18}\xi\eta^2\zeta + b_{19}\xi\eta\zeta^2 \\
w &= c_0 + c_1\xi + c_2\eta + c_3\zeta + c_4\xi\eta + c_5\xi\zeta + c_6\eta\zeta + c_7\xi\eta\zeta + c_8\xi^2 \\
&\quad + c_9\eta^2 + c_{10}\zeta^2 + c_{11}\xi^2\eta + c_{12}\xi^2\zeta + c_{13}\xi\eta^2 + c_{14}\eta^2\zeta + c_{15}\xi\zeta^2 \\
&\quad + c_{16}\eta\zeta^2 + c_{17}\xi^2\eta\zeta + c_{18}\xi\eta^2\zeta + c_{19}\xi\eta\zeta^2
\end{aligned}$$

Thus we have

$$\Phi = \begin{bmatrix} 1 & 0 & 0 & \xi & 0 & 0 & \cdots & \xi\eta\zeta^2 & 0 & 0 \\ 0 & 1 & 0 & 0 & \xi & 0 & \cdots & 0 & \xi\eta\zeta^2 & 0 \\ 0 & 0 & 1 & 0 & 0 & \xi & \cdots & 0 & 0 & \xi\eta\zeta^2 \end{bmatrix} \tag{3.206}$$

and

$$\mathbf{a} = \left\{ \begin{array}{cccccccccc} a_0 & b_0 & c_0 & a_1 & b_1 & c_1 & \cdots & a_{19} & b_{19} & c_{19} \end{array} \right\}^T \tag{3.207}$$

The strains derived from the assumed displacement field are

$$\begin{aligned}
\epsilon_\xi &= \frac{\partial u}{\partial \xi} = a_1 + a_4\eta + a_5\zeta + a_7\eta\zeta + 2a_8\xi + 2a_{11}\xi\eta + 2a_{12}\xi\zeta \\
&\quad + a_{13}\eta^2 + a_{15}\zeta^2 + 2a_{17}\xi\eta\zeta + a_{18}\eta^2\zeta + a_{19}\eta\zeta^2 \\
\epsilon_\eta &= \frac{\partial v}{\partial \eta} = b_2 + b_4\xi + b_6\zeta + b_7\xi\zeta + 2b_9\eta + b_{11}\xi^2 + 2b_{13}\xi\eta \\
&\quad + 2b_{14}\eta\zeta + b_{16}\zeta^2 + b_{17}\xi^2\zeta + 2b_{18}\xi\eta\zeta + b_{19}\xi\zeta^2 \\
\epsilon_\zeta &= \frac{\partial w}{\partial \zeta} = c_3 + c_5\xi + c_6\eta + c_7\xi\eta + 2c_{10}\zeta + c_{12}\xi^2 + c_{14}\eta^2 \\
&\quad + 2c_{15}\xi\zeta + 2c_{16}\eta\zeta + c_{17}\xi^2\eta + c_{18}\xi\eta^2 + 2c_{19}\xi\eta\zeta \\
\epsilon_{\eta\zeta} &= \frac{\partial w}{\partial \eta} + \frac{\partial v}{\partial \zeta} = (c_2 + b_3) + (c_4 + b_5)\xi + (2c_9 + b_6)\eta + (c_6 + 2b_{10})\zeta \\
&\quad + (2c_{13} + b_7)\xi\eta + (c_7 + 2b_{15})\xi\zeta + 2(c_{14} + b_{16})\eta\zeta + 2(c_{18} + b_{19})\xi\eta\zeta \\
&\quad + (c_{11} + b_{12})\xi^2 + b_{14}\eta^2 + c_{16}\zeta^2 + b_{17}\xi^2\eta + c_{17}\xi^2\zeta + b_{18}\xi\eta^2 + c_{19}\xi\zeta^2 \\
\epsilon_{\xi\zeta} &= \frac{\partial w}{\partial \xi} + \frac{\partial u}{\partial \zeta} = (c_1 + a_3) + (2c_8 + a_5)\xi + (c_4 + a_6)\eta + (c_5 + 2a_{10})\zeta \\
&\quad + (2c_{11} + a_7)\xi\eta + 2(c_{12} + a_{15})\xi\zeta + (c_7 + 2a_{16})\eta\zeta + 2(c_{17} + a_{19})\xi\eta\zeta \\
&\quad + a_{12}\xi^2 + (c_{13} + a_{14})\eta^2 + c_{15}\zeta^2 + a_{17}\xi^2\eta + a_{18}\xi\eta^2 + c_{18}\eta^2\zeta + c_{19}\eta\zeta^2 \\
\epsilon_{\xi\eta} &= \frac{\partial v}{\partial \xi} + \frac{\partial u}{\partial \eta} = (b_1 + a_2) + (2b_8 + a_4)\xi + (b_4 + 2a_9)\eta + (b_5 + a_6)\zeta \\
&\quad + 2(b_{11} + a_{13})\xi\eta + 2(b_{12} + a_7)\xi\zeta + (b_7 + 2a_{14})\eta\zeta + 2(b_{17} + a_{18})\xi\eta\zeta \\
&\quad + a_{11}\xi^2 + b_{13}\eta^2 + (b_{15} + a_{16})\zeta^2 + a_{17}\xi^2\eta + b_{18}\eta^2\zeta + a_{19}\xi\zeta^2 + b_{19}\eta\zeta^2
\end{aligned}$$

Then the stress field derived from the assumed displacement field is

$$\bar{\boldsymbol{\sigma}} = \mathbf{C}\boldsymbol{\epsilon} \tag{3.208}$$

For on-axis orthotropic material, we have

$$\begin{aligned}
\sigma_\zeta &= C_{31}\epsilon_\xi + C_{32}\epsilon_\eta + C_{33}\epsilon_\zeta \\
\sigma_{\eta\zeta} &= C_{44}\epsilon_{\eta\zeta} \\
\sigma_{\xi\zeta} &= C_{55}\epsilon_{\xi\zeta}
\end{aligned}$$

or in matrix form

$$\boldsymbol{\sigma}_g = \Theta\boldsymbol{\gamma} \tag{3.209}$$

where

$$\bar{\boldsymbol{\sigma}}_g = \begin{Bmatrix} \sigma_\zeta \\ \sigma_{\eta\zeta} \\ \sigma_{\xi\zeta} \end{Bmatrix} \tag{3.210}$$

$$\boldsymbol{\gamma} = [\gamma_1, \gamma_2, \gamma_3, \cdots, \gamma_{47}] \tag{3.211}$$

in which

$$\gamma_1 = C_{31}a_1 + C_{32}b_2 + C_{33}c_3 \tag{3.212}$$

$$\gamma_2 = C_{44}(c_2 + b_3) \tag{3.213}$$

$$\gamma_3 = C_{55}(c_1 + a_3) \tag{3.214}$$

$$\gamma_4 = 2C_{31}a_8 + C_{32}b_4 + C_{33}c_5 \tag{3.215}$$

$$\gamma_5 = C_{44}(c_4 + b_5) \tag{3.216}$$

$$\gamma_6 = C_{55}(2c_8 + a_5) \tag{3.217}$$

$$\gamma_7 = C_{31}a_4 + 2C_{32}b_9 + C_{33}c_6 \tag{3.218}$$

$$\gamma_8 = C_{44}(2c_9 + b_6) \tag{3.219}$$

$$\gamma_9 = C_{55}(c_4 + a_6) \tag{3.220}$$

$$\gamma_{10} = C_{32}b_6 + C_{31}a_5 + 2C_{33}c_{10} \tag{3.221}$$

$$\gamma_{11} = C_{44}(c_6 + 2b_{10}) \tag{3.222}$$

$$\gamma_{12} = C_{55}(c_5 + 2a_{10}) \tag{3.223}$$

$$\gamma_{13} = 2C_{31}a_{11} + 2C_{32}b_{13} + C_{33}c_7 \tag{3.224}$$

$$\gamma_{14} = C_{44}(2c_{13} + b_7) \tag{3.225}$$

$$\gamma_{15} = C_{55}(2c_{11} + a_7) \tag{3.226}$$

$$\gamma_{16} = 2C_{31}a_{12} + C_{32}b_7 + 2C_{33}c_{15} \tag{3.227}$$

$$\gamma_{17} = C_{44}(c_7 + 2b_{15}) \tag{3.228}$$

$$\gamma_{18} = 2C_{55}(c_{12} + a_{15}) \tag{3.229}$$

$$\gamma_{19} = C_{31}a_7 + 2C_{32}b_{14} + 2C_{33}c_{16} \tag{3.230}$$

$$\gamma_{20} = 2C_{44}(c_{14} + b_{16}) \tag{3.231}$$

$$\gamma_{21} = C_{55}(c_7 + 2a_{16}) \tag{3.232}$$

$$\gamma_{22} = 2C_{31}a_{17} + 2C_{32}b_{18} + 2C_{33}c_{19} \tag{3.233}$$

$$\gamma_{23} = 2C_{44}(c_{18} + b_{19}) \tag{3.234}$$

$$\gamma_{24} = 2C_{55}(c_{17} + a_{19}) \tag{3.235}$$

$$\gamma_{25} = C_{32}b_{11} + C_{33}c_{12} \tag{3.236}$$

$$\gamma_{26} = C_{44}(c_{11} + b_{12}) \tag{3.237}$$

$$\gamma_{27} = C_{55}a_{12} \tag{3.238}$$

$$\gamma_{28} = C_{31}a_{13} + C_{33}c_{14} \tag{3.239}$$

$$\gamma_{29} = C_{44}b_{14} \tag{3.240}$$

$$\gamma_{30} = C_{55}(c_{13} + a_{14}) \tag{3.241}$$

$$\gamma_{31} = C_{31}a_{15} + C_{32}b_{16} \tag{3.242}$$

$$\gamma_{32} = C_{44}c_{16} \tag{3.243}$$

$$\gamma_{33} = C_{55}a_{15} \tag{3.244}$$

$$\gamma_{34} = C_{33}c_{17} \tag{3.245}$$

$$\gamma_{35} = C_{44}b_{17} \tag{3.246}$$

$$\gamma_{36} = C_{55}a_{17} \tag{3.247}$$

$$\gamma_{37} = C_{32}b_{17} \tag{3.248}$$

$$\gamma_{38} = C_{44}c_{17} \tag{3.249}$$

$$\gamma_{39} = C_{33}c_{18} \tag{3.250}$$

$$\gamma_{40} = C_{44}b_{18} \tag{3.251}$$

$$\gamma_{41} = C_{55}a_{18} \tag{3.252}$$

$$\gamma_{42} = C_{31}a_{18} \tag{3.253}$$

$$\gamma_{43} = C_{55}c_{18} \tag{3.254}$$

$$\gamma_{44} = C_{32}b_{19} \tag{3.255}$$

$$\gamma_{45} = C_{44}c_{19} \tag{3.256}$$

$$\gamma_{46} = C_{31}a_{19} \tag{3.257}$$

$$\gamma_{47} = C_{55}c_{19} \tag{3.258}$$

By the iso-function method. the partial stress field is

$$\boldsymbol{\sigma}_g = \mathbf{P}\boldsymbol{\beta}$$

Thus the partial stress field function

$$\mathbf{P} = \Theta = \begin{bmatrix} 1 & 0 & 0 & \xi & 0 & 0 & \eta & 0 & 0 & \zeta & 0 & 0 & \xi\eta & 0 & 0 & \xi\zeta & 0 & 0 \\ 0 & 1 & 0 & 0 & \xi & 0 & 0 & \eta & 0 & 0 & \zeta & 0 & 0 & \xi\eta & 0 & 0 & \xi\zeta & 0 \\ 0 & 0 & 1 & 0 & 0 & \xi & 0 & 0 & \eta & 0 & 0 & \zeta & 0 & 0 & \xi\eta & 0 & 0 & \xi\zeta \end{bmatrix}$$

$$\begin{matrix} \eta\zeta & 0 & 0 & \xi\eta\zeta & 0 & 0 & \xi^2 & 0 & 0 & \eta^2 & 0 & 0 & \zeta^2 & 0 & 0 & \xi^2\eta & 0 \\ 0 & \eta\zeta & 0 & 0 & \xi\eta\zeta & 0 & 0 & \xi^2 & 0 & 0 & \eta^2 & 0 & 0 & \zeta^2 & 0 & 0 & \xi^2\eta \\ 0 & 0 & \eta\zeta & 0 & 0 & \xi\eta\zeta & 0 & 0 & \xi^2 & 0 & 0 & \eta^2 & 0 & 0 & \zeta^2 & 0 & 0 \end{matrix}$$

$$\begin{bmatrix} 0 & \xi^2\zeta & 0 & \xi\eta^2 & 0 & 0 & \eta^2\zeta & 0 & \xi\zeta^2 & 0 & \eta\zeta^2 & 0 \\ 0 & 0 & \xi^2\zeta & 0 & \xi\eta^2 & 0 & 0 & 0 & 0 & \xi\zeta^2 & 0 & 0 \\ \xi^2\eta & 0 & 0 & 0 & 0 & \xi\eta^2 & 0 & \eta^2\zeta & 0 & 0 & 0 & \eta\zeta^2 \end{bmatrix} \tag{3.259}$$

Similarly, for off-axis orthotropic material with one of the symmetry planes coincide with the ζ- or z-coordinate axis, the transverse stresses are

$$\sigma_\zeta = C_{31}\epsilon_\xi + C_{32}\epsilon_\eta + C_{33}\epsilon_\zeta + C_{36}\epsilon_{\xi\eta} \tag{3.260}$$

$$\sigma_{\eta\zeta} = C_{44}\epsilon_{\eta\zeta} + C_{45}\epsilon_{\xi\zeta} \tag{3.261}$$

$$\sigma_{\xi\zeta} = C_{54}\epsilon_{\eta\zeta} + C_{55}\epsilon_{\xi\zeta} \tag{3.262}$$

Thus

$$\gamma = [\gamma_1, \gamma_2, \gamma_3, \cdots, \gamma_{51}] \tag{3.263}$$

in which

$$\gamma_1 = C_{31}a_1 + C_{32}b_2 + C_{33}c_3 + C_{36}(b_1 + a_2) \tag{3.264}$$

$$\gamma_2 = C_{44}(c_2 + b_3) + C_{45}(c_1 + a_3) \tag{3.265}$$

$$\gamma_3 = C_{54}(c_2 + b_3) + C_{55}(c_1 + a_3) \tag{3.266}$$

$$\gamma_4 = 2C_{31}a_8 + C_{32}b_4 + C_{33}c_5 + C_{36}(2b_8 + a_4) \tag{3.267}$$

$$\gamma_5 = C_{44}(c_4 + b_5) + C_{45}(2c_8 + a_5) \tag{3.268}$$

$$\gamma_6 = C_{54}(c_4 + b_5) + C_{55}(2c_8 + a_5) \tag{3.269}$$

$$\gamma_7 = C_{31}a_4 + 2C_{32}b_9 + C_{33}c_6 + C_{36}(b_4 + 2a_9) \tag{3.270}$$

$$\gamma_8 = C_{44}(2c_9 + b_6) + C_{45}(c_4 + a_6) \tag{3.271}$$

$$\gamma_9 = C_{54}(2c_9 + b_6) + C_{55}(c_4 + a_6) \tag{3.272}$$

$$\gamma_{10} = C_{32}b_6 + C_{31}a_5 + 2C_{33}c_{10} + C_{36}(b_5 + a_6) \tag{3.273}$$

$$\gamma_{1.} = C_{44}(c_6 + 2b_{10}) + C_{45}(c_5 + 2a_{10}) \tag{3.274}$$

$$\gamma_{12} = C_{54}(c_6 + 2b_{10}) + C_{55}(c_5 + 2a_{10}) \tag{3.275}$$

$$\gamma_{13} = 2C_{31}a_{11} + 2C_{32}b_{13} + C_{33}c_7 + 2C_{36}(b_{11} + a_{13}) \tag{3.276}$$

$$\gamma_{14} = C_{44}(2c_{13} + b_7) + C_{45}(2c_{11} + a_7) \tag{3.277}$$

$$\gamma_{15} = C_{54}(2c_{13} + b_7) + C_{55}(2c_{11} + a_7) \tag{3.278}$$

$$\gamma_{16} = 2C_{31}a_{12} + C_{32}b_7 + 2C_{33}c_{15} + 2C_{36}(b_{12} + a_7) \tag{3.279}$$

$$\gamma_{17} = C_{44}(c_7 + 2b_{15}) + 2C_{45}(c_{12} + a_{15}) \tag{3.280}$$

$$\gamma_{18} = C_{54}(c_7 + 2b_{15}) + 2C_{55}(c_{12} + a_{15}) \tag{3.281}$$

$$\gamma_{19} = C_{31}a_7 + 2C_{32}b_{14} + 2C_{33}c_{16} + C_{36}(b_7 + 2a_{14}) \tag{3.282}$$

$$\gamma_{20} = 2C_{44}(c_{14} + b_{16}) + C_{45}(c_7 + 2a_{16}) \tag{3.283}$$

$$\gamma_{21} = 2C_{54}(c_{14} + b_{16}) + C_{55}(c_7 + 2a_{16}) \tag{3.284}$$

$$\gamma_{22} = 2C_{31}a_{17} + 2C_{32}b_{18} + 2C_{33}c_{19} + 2C_{36}(b_{17} + a_{18}) \tag{3.285}$$

$$\gamma_{23} = 2C_{44}(c_{18} + b_{19}) + 2C_{45}(c_{17} + a_{19}) \tag{3.286}$$

$$\gamma_{24} = 2C_{54}(c_{18} + b_{19}) + 2C_{55}(c_{17} + a_{19}) \tag{3.287}$$

$$\gamma_{25} = C_{32}b_{11} + C_{33}c_{12} + C_{36}a_{11} \tag{3.288}$$

$$\gamma_{26} = C_{44}(c_{11} + b_{12}) + C_{45}a_{12} \tag{3.289}$$

$$\gamma_{27} = C_{54}(c_{11} + b_{12}) + C_{55}a_{12} \tag{3.290}$$

$$\gamma_{28} = C_{31}a_{13} + C_{33}c_{14} + C_{36}b_{13} \tag{3.291}$$

$$\gamma_{29} = C_{44}b_{14} + C_{45}(c_{13} + a_{14}) \tag{3.292}$$

$$\gamma_{30} = C_{54}b_{14} + C_{55}(c_{13} + a_{14}) \tag{3.293}$$

$$\gamma_{31} = C_{31}a_{15} + C_{32}b_{16} + C_{36}(b_{15} + a_{16}) \tag{3.294}$$

$$\gamma_{32} = C_{44}c_{16} + C_{45}a_{15} \tag{3.295}$$

$$\gamma_{33} = C_{54}c_{16} + C_{55}a_{15} \tag{3.296}$$

$$\gamma_{34} = C_{33}c_{17} + C_{36}a_{17} \tag{3.297}$$

$$\gamma_{35} = C_{44}b_{17} + C_{45}a_{17} \tag{3.298}$$

$$\gamma_{36} = C_{54}b_{17} + C_{55}a_{17} \tag{3.299}$$

$$\gamma_{37} = C_{32}b_{17} \tag{3.300}$$

$$\gamma_{38} = C_{44}c_{17} \tag{3.301}$$

$$\gamma_{39} = C_{54}c_{17} \tag{3.302}$$

$$\gamma_{40} = C_{33}c_{18} \tag{3.303}$$

$$\gamma_{41} = C_{44}b_{18} + C_{45}a_{18} \tag{3.304}$$

$$\gamma_{42} = C_{54}b_{18} + C_{55}a_{18} \tag{3.305}$$

$$\gamma_{43} = C_{31}a_{18} + C_{36}b_{18} \tag{3.306}$$

$$\gamma_{44} = C_{45}c_{18} \tag{3.307}$$

$$\gamma_{45} = C_{55}c_{18} \tag{3.308}$$

$$\gamma_{46} = C_{32}b_{19} + C_{36}a_{19} \tag{3.309}$$

$$\gamma_{47} = C_{44}c_{19} \tag{3.310}$$

$$\gamma_{48} = C_{54}c_{19} \tag{3.311}$$

$$\gamma_{49} = C_{31}a_{19} + C_{36}b_{19} \tag{3.312}$$

$$\gamma_{50} = C_{45}c_{19} \tag{3.313}$$

$$\gamma_{51} = C_{55}c_{19} \tag{3.314}$$

and, by the iso-function method, the partial stress field function is

$$\mathbf{P} = \begin{bmatrix}
1 & 0 & 0 & \xi & 0 & 0 & \eta & 0 & 0 & \zeta & 0 & 0 & \xi\eta & 0 & 0 & \xi\zeta & 0 & 0 \\
0 & 1 & 0 & 0 & \xi & 0 & 0 & \eta & 0 & 0 & \zeta & 0 & 0 & \xi\eta & 0 & 0 & \xi\zeta & 0 \\
0 & 0 & 1 & 0 & 0 & \xi & 0 & 0 & \eta & 0 & 0 & \zeta & 0 & 0 & \xi\eta & 0 & 0 & \xi\zeta
\end{bmatrix}$$

$$\begin{bmatrix}
\eta\zeta & 0 & 0 & \xi\eta\zeta & 0 & 0 & \xi^2 & 0 & 0 & \eta^2 & 0 & 0 & \zeta^2 & 0 & 0 & \xi^2\eta & 0 & 0 \\
0 & \eta\zeta & 0 & 0 & \xi\eta\zeta & 0 & 0 & \xi^2 & 0 & 0 & \eta^2 & 0 & 0 & \zeta^2 & 0 & 0 & \xi^2\eta & 0 \\
0 & 0 & \eta\zeta & 0 & 0 & \xi\eta\zeta & 0 & 0 & \xi^2 & 0 & 0 & \eta^2 & 0 & 0 & \zeta^2 & 0 & 0 & \cdot
\end{bmatrix}$$

$$\begin{bmatrix}
\xi^2\zeta & 0 & 0 & \xi\eta^2 & 0 & 0 & \eta^2\zeta & 0 & 0 & \xi\zeta^2 & 0 & 0 & \eta\zeta^2 & 0 & 0 \\
0 & \xi^2\zeta & 0 & 0 & \xi\eta^2 & 0 & 0 & \eta^2\zeta & 0 & 0 & \xi\zeta^2 & 0 & 0 & \eta\zeta^2 & 0 \\
0 & 0 & \xi^2\zeta & 0 & 0 & \xi\eta^2 & 0 & 0 & \eta^2\zeta & 0 & 0 & \xi\zeta^2 & 0 & 0 & \eta\zeta^2
\end{bmatrix} \tag{3.315}$$

3.4 Eigenvalue Analysis of Elements Formulated with Different Stress Fields

This section presents the eigenvalue studies of the finite elements formulated with the partial stress field derived by the iso-function method in previous sections. Fist, the physical meanings of the eigenvalue and eigenvector in the analysis of the finite element stiffness $\mathbf{K}^e$ are explained.

3.4.1 Eigenvalues and Eigenvectors of the Finite Element

The standard eigenproblem of the finite element stiffness matrix $\mathbf{K}^e$ is

$$\mathbf{K}^e\phi = \lambda\phi \tag{3.316}$$

where $\mathbf{K}^e$ is the n by n stiffness matrix of a single finite element. If $\mathbf{K}^e$ is positive semidefinite or positive definite, there are n eigenvalues λ_i $(i = 1,2,3,\cdots,n)$ and n corresponding eigenvectors ϕ_i $(i = 1,2,3,\cdots,n)$ satisfying Equation 3.316. The i-th eigenpair is denoted as (λ_i, ϕ_i), where the eigenvalues are ordered according to their magnitudes:

$$0 \leq \lambda_1 \leq \lambda_2 \leq \cdots \leq \lambda_{n-1} \leq \lambda_n \tag{3.317}$$

If $\mathbf{K}^e$ is positive definite, $\lambda_i > 0$, $i = 1,2,\cdots,n$, and if $\mathbf{K}^e$ is positive semidefinite, $\lambda_i \geq 0$, $i = 1,2,\cdots,n$. where the number of zero eigenvalues is usually equal to the number of rigid body modes.

A poor stress field may lead to a stiffness matrix $\mathbf{K}^e$ which has more zero eigenvalues than the number of possible rigid body modes. Comparing Equation 3.316 with the

following element equilibrium equation

$$\mathbf{K}^e\boldsymbol{\delta}^e = \mathbf{f}^e \tag{3.318}$$

in which $\boldsymbol{\delta}^e$ is the element nodal displacement vector and $\mathbf{f}^e$ is the element nodal load vector, we can conclude that for a non rigid body mode, a zero eigenvalue means a deformation mode without loading or a mode of the body deformation without any energy produced by boundary forces. This kind of rigid body mode is usually named as the zero-energy mode or spurious mode. The spurious deformation exists due to the unproperly formulated element stiffness matrix.

By comparing with Equation 3.318, Equation 3.316 also shows that the physical meaning of an eigenpair (λ_i, ϕ_i) is that the ϕ_i is the deformation mode and the λ_i is the corresponding measure of the stiffness of this deformation mode.

Another frequently considered eigenproblem is the one to be solved in vibration analysis. In that case, we consider the generalized eigenproblem

$$\mathbf{K}^e\phi = \lambda\mathbf{M}^e\phi \tag{3.319}$$

where $\mathbf{K}^e$ and $\mathbf{M}^e$ are, respectively, the stiffness matrix and mass matrix of the finite element. The eigenvalues λ_i and eigenvectors ϕ_i are the free vibration frequencies (rad/sec) squared, ω_i^2, and corresponding vibration mode shape vectors, respectively. The mass matrix $\mathbf{M}^e$ may be banded or may be diagonal with $m_{ii} \geq 0$; i.e., some diagonal elements may possibly be zero. A banded mass matrix, obtained in a consistent mass analysis, is always positive definite, whereas a lumped mass matrix is positive definite only if all diagonal elements are larger than zero. In general, a diagonal mass matrix is positive semidefinite.

We note that the generalized eigenproblem in Equation 3.319 will reduce to the standard eigenproblem in Equation 3.316 if $\mathbf{M}^e$ is an identity matrix. In other

words, the eigenvalues and eigenvectors obtained from solving Equation 3.316 can also be thought of as frequencies squared and vibration mode shapes of the element when unit mass is specified at each degree of freedom. Corresponding to the possible eigenvalues in the solution of Equation 3.316, the generalized eigenproblem in Equation 3.319 has eigenvalues $\lambda_i \geq 0$, $i = 1, 2, 3, \cdots, n$, where the number of zero eigenvalues should be again equal to the number of rigid body modes in the element.

From above studies, we have following *conclusions* about the eigenvalues of the stiffness matrix of a finite element:

(1) In static studies, λ_i is the element stiffness of the i-th deformation mode and ϕ_i is the corresponding deformation mode shape of the element.

(2) In vibration studies, λ_i is the square of the i-th natural vibration frequency of the element with a unit mass matrix and ϕ_i is the corresponding natural vibration mode shape.

(3) The number of zero eigenvalues should be equal to the number of rigid body modes in the element.

(4) For an un-properly formulated finite element, if the number of zero eigenvalues exceeds the number of rigid body modes in the element, the spurious zero-energy modes are involved in the element. The exceeded number equals to the number of spurious modes involved. Generally, this element is not suitable to be applied in static analysis or vibration analysis of any systems.

3.4.2 Eigenvalue Analysis

The following tables show the results of eigenvalue analysis of elements formulated with the stress fields given by the iso-function method in previous sections and those given by other methods.

In tables 3.1 to 3.4,

$$\bar{\lambda}_i = \frac{\lambda_i}{\lambda_d}$$

where

λ_i — the i-th eigenvalue of hybrid(see equation 3.7) or composite formulated finite element with assumed stress field.

λ_d — the i-th eigenvalue of the corresponding displacement formulated finite element.

$\bar{\lambda}_i = 0$ indicates a zero-energy (deformation, or natural vibration shape) mode brought by an assumed stress field. $\lambda_i = 1$ means the i-th mode of the element formulated with an assumed stress field has the same static and dynamic performance as that of the corresponding displacement formulated element.

In the tables, field F-1 to F-8 are the eight choices given by S.N. Atluri [59, 60] by using group theory, field F-9 is given by T.H.H. Pian [70], field F-10 is the partial stress field given by Huang [56]. Field 11 is the partial stress field for 3-D, 8-node composite element formulated by the present iso-function method, and field 12 is for 3-D, 20-node one.

The results of eigenvalue analysis show the composite finite elements formulated using the iso-function stress field have the same eigenvalue property as the corresponding displacement elements. This is generaliy true because the iso-function method just equates the assumed stress function to the stress function derived from the displacement field. This property also makes the composite elements to have less obstacle to be applied in dynamic analysis of composite laminates.

Table 3.1: Eigenvalue analysis results of stress fields

Field	F-1	F-2	F-3	F-4	F-5	F-6	F-7	F-8	F-9
λ_1	0.000	0.000	0.000	0.000	0.157	0.000	0.000	0.000	0.867
λ_2	0.504	0.053	0.000	0.000	0.566	0.000	0.504	0.000	0.867
λ_3	0.473	0.086	0.029	0.000	0.309	0.029	0.473	0.086	0.473
λ_4	0.473	0.198	0.198	0.029	0.473	0.198	0.473	0.309	0.546
λ_5	0.473	0.309	0.275	0.086	0.473	0.309	0.473	0.473	0.546
λ_6	0.667	0.189	0.333	0.121	0.289	0.667	0.333	0.289	0.667
λ_7	0.667	0.333	0.333	0.189	0.333	0.667	0.333	0.289	0.667
λ_8	1.000	0.333	0.333	0.333	0.333	1.000	0.333	0.333	0.667
λ_9	0.929	0.250	0.929	0.500	0.250	0.929	0.929	0.500	0.929
λ_{10}	0.619	0.167	0.667	0.428	0.167	0.619	0.667	0.428	0.619
λ_{11}	0.667	0.167	0.702	0.502	0.167	0.667	0.702	0.502	0.619
λ_{12}	0.702	0.667	0.786	0.667	0.667	0.702	0.786	0.667	0.667
λ_{13}	1.000	1.000	1.000	1.000	1.000	1.000	1.000	1.000	1.000
λ_{14}	1.000	1.000	1.000	1.000	1.000	1.000	1.000	1.000	1.000
λ_{15}	1.000	1.000	1.000	1.000	1.000	1.000	1.000	1.000	1.000
λ_{16}	1.000	1.000	1.000	1.000	1.000	1.000	1.000	1.000	1.000
λ_{17}	1.000	1.000	1.000	1.000	1.000	1.000	1.000	1.000	1.000
λ_{18}	1.000	1.000	1.000	1.000	1.000	1.000	1.000	1.000	1.000

3.5 Conclusion

The iso-function method is developed in this Chapter. The method gives an easy way to determine that how many stress field parameters should be assumed and what are the proper stress field terms, which will ensure that no spurious zero energy modes exist in the finite element.

The method takes the same number of stress field parameters as those from a displacement field. However, the values of the stress field parameters form a displacement field are decided by the displacement solution through the displacement-strain relation and constitutive relation, while the values of the stress field parameters

Table 3.2: Eigenvalue analysis of partial stress fields, 8-node element

Field	F-10	F-11
$\bar{\lambda}_1$	1.000	1.000
λ_2	1.000	1.000
λ_3	0.636	1.000
λ_4	0.701	1.000
λ_5	0.701	1.000
λ_6	0.667	1.000
λ_7	0.806	1.000
$\bar{\lambda}_8$	0.806	1.000
λ_9	0.929	1.000
λ_{10}	0.667	1.000
λ_{11}	0.930	1.000
λ_{12}	0.930	1.000
$\bar{\lambda}_{13}$	1.000	1.000
$\vdots$	$\vdots$	$\vdots$
λ_{18}	1.000	1.000

Table 3.3: Results of eigenvalue analysis, 16-node element

Field	F-12
λ_1	1.000
λ_2	1.000
$\vdots$	$\vdots$
λ_{42}	1.000

Table 3.4: Results of eigenvalue analysis of 20-node element

Field	F-12
λ_1	1.000
λ_2	1.000
$\vdots$	$\vdots$
λ_{54}	1.000

assumed with the iso-function method are determined by solving a finite element equation directly.

The iso-function method takes the same stress field terms as those from a displacement field. This ensures that all the stress modes exist in a good displacement element will be available in a corresponding hybrid or composite element and ensures no spurious deformation modes exist in the element.

The number of stress field parameters and corresponding stress field terms, suggested by the iso-function method, are sufficient for expelling the spurious modes, but may not necessary. The hybrid or composite element composed of the stress field assumed by the iso-function method has the same stiffness and natural vibration properties as the corresponding displacement element. Reducing the stress field formed with the iso-function method will certainly weaken the finite element, but not necessary introduce in the spurious modes. Thus, the stress field provided by the iso-function method could be treated as a base field for further reduction to weaken the element and save computational efforts, or for further enlargement to include special functions for some particular applications.

Chapter 4

The Composite Finite Elements

With the iso-function method for establishing partial stress field in Chapter 3 and the variational functional described in chapter 2, three dimensional composite finite elements can be formulated based on existing displacement formulated finite element. This chapter gives a general procedure for the formulation of composite finite elements. Specifically, a 3-D, 8-node, a 3-D, 16 node and a 3-D, 20-node are formulated.

4.1 Composite Finite Element Method

4.1.1 Element Governing Equation

The composite finite element governing equation is derived from the variational functional presented in chapter 2 equation 2.56, which is repeated here

$$\begin{aligned} \delta \Pi_C &= 0 \\ \Pi_C &= \sum_j \left[\int_{v_j} \left(\frac{1}{2} \mathbf{q}^T \mathbf{R} \mathbf{q} + \boldsymbol{\sigma}_g{}^T \overline{\mathbf{B}}_c \mathbf{u} - \overline{\mathbf{F}}^T \mathbf{u} \right) dv_j - \int_{s_{j\sigma}} \overline{\mathbf{T}}^T \mathbf{u} ds_j \right] \end{aligned} \tag{4.1}$$

in which,

$$\mathbf{u} = \mathbf{N}\boldsymbol{\delta} \tag{4.2}$$

$$\mathbf{q} = \begin{Bmatrix} \boldsymbol{\epsilon}_n \\ \boldsymbol{\sigma}_g \end{Bmatrix} = \{ \epsilon_x, \epsilon_y, \epsilon_{xy}, \sigma_z, \sigma_{yz}, \sigma_{xz} \}^T \tag{4.3}$$

$$\boldsymbol{\sigma}_g = \mathbf{P}_g \boldsymbol{\beta} \tag{4.4}$$

$$\mathbf{R} = \begin{bmatrix} \mathbf{R}_1 & \mathbf{R}_2 \\ \mathbf{R}_3 & \mathbf{R}_4 \end{bmatrix} \tag{4.5}$$

$$= \begin{bmatrix} \mathbf{C}_1 - \mathbf{C}_2 \mathbf{C}_3^{-1} \mathbf{C}_2^T & \mathbf{C}_2 \mathbf{C}_3^{-1} \\ \mathbf{C}_3^{-1} \mathbf{C}_2^T & -\mathbf{C}_3^{-1} \end{bmatrix} \tag{4.6}$$

$$= \begin{bmatrix} \mathbf{S}_1^{-1} & -\mathbf{S}_1^{-1} \mathbf{S}_2 \\ -\mathbf{S}_2^T \mathbf{S}_1^{-1} & \mathbf{S}_2^T \mathbf{S}_1^{-1} \mathbf{S}_2 - \mathbf{S}_3 \end{bmatrix} \tag{4.7}$$

$$\overline{\mathbf{B}}_c = \begin{bmatrix} 0 & 0 & \frac{\partial}{\partial z} \\ 0 & \frac{\partial}{\partial z} & \frac{\partial}{\partial y} \\ \frac{\partial}{\partial z} & 0 & \frac{\partial}{\partial x} \end{bmatrix} \tag{4.8}$$

where

$\mathbf{u}$ is the displacement vector at a point in an finite element,

$\boldsymbol{\delta}$ nodal displacement vector

$\mathbf{N}$ matrix of element shape function

$\mathbf{q}$ global vector,

$\boldsymbol{\sigma}_g$ transverse stress,

$\boldsymbol{\beta}$ partial stress field parameter vector,

$\mathbf{R}$ combined constitution matrix,

$\mathbf{B}_c$ matrix of compatibility relations,

$\overline{\mathbf{F}}$ is prescribed body force,

$\overline{\mathbf{T}}$ is prescribed boundary surface force.

The basic variables are

$$\boldsymbol{\sigma}_g = \begin{Bmatrix} \sigma_z \\ \sigma_{yz} \\ \sigma_{xz} \end{Bmatrix} \tag{4.9}$$

$$\boldsymbol{\epsilon}_g = \begin{Bmatrix} \epsilon_x \\ \epsilon_y \\ \epsilon_{xy} \end{Bmatrix} = \mathbf{B}_g \boldsymbol{\delta} \tag{4.10}$$

where $\mathbf{B}_g$ is the transformation matrix of partial strain-displacement relation.

$$\mathbf{B}_g = \overline{\mathbf{B}}_g \mathbf{N} \tag{4.11}$$

in which, $\overline{\mathbf{B}}_g$ has been defined (2.33).

The three in-plane stresses and three transverse strains are the derivatives of above basic variables and can be obtained as

$$\boldsymbol{\sigma}_L = \left\{ \begin{array}{c} \sigma_x \\ \sigma_y \\ \sigma_{xy} \end{array} \right\} = \mathbf{R}_1 \boldsymbol{\epsilon}_g + \mathbf{R}_2 \boldsymbol{\sigma}_g \tag{4.12}$$

$$-\boldsymbol{\epsilon}_L = -\left\{ \begin{array}{c} \epsilon_z \\ \epsilon_{yz} \\ \epsilon_{xz} \end{array} \right\} = \mathbf{R}_3 \boldsymbol{\epsilon}_g + \mathbf{R}_4 \boldsymbol{\sigma}_g \tag{4.13}$$

Substitute the global field vector

$$\mathbf{q} = \left\{ \begin{array}{c} \boldsymbol{\epsilon}_g \\ \boldsymbol{\sigma}_g \end{array} \right\} \tag{4.14}$$

into the variational functional (4.1), we have

$$\begin{aligned} \Pi_C &= \sum_j \left[\int_{v_j} \left(\frac{1}{2} \left[\begin{array}{cc} \boldsymbol{\epsilon}_g{}^T & \boldsymbol{\sigma}_g{}^T \end{array} \right] \left[\begin{array}{cc} \mathbf{R}_1 & \mathbf{R}_2 \\ \mathbf{R}_3 & \mathbf{R}_4 \end{array} \right] \left\{ \begin{array}{c} \boldsymbol{\epsilon}_g \\ \boldsymbol{\sigma}_g \end{array} \right\} + \boldsymbol{\sigma}_g{}^T \overline{\mathbf{B}}_c \mathbf{u} \right) dv_j \right. \\ &\quad \left. - \left(\int_{v_j} \overline{\mathbf{F}}^T \mathbf{u} dv_j + \int_{s_{j\sigma}} \overline{\mathbf{T}}^T \mathbf{u} ds_j \right) \right] \\ &= \sum_j \left[\int_{v_j} \frac{1}{2} \left(\boldsymbol{\epsilon}_g{}^T \mathbf{R}_1 \boldsymbol{\epsilon}_g + \boldsymbol{\sigma}_g{}^T \mathbf{R}_3 \boldsymbol{\epsilon}_g + \boldsymbol{\epsilon}_g{}^T \mathbf{R}_2 \boldsymbol{\sigma}_g + \boldsymbol{\sigma}_g{}^T \mathbf{R}_4 \boldsymbol{\sigma}_g + 2 \boldsymbol{\sigma}_g{}^T \overline{\mathbf{B}}_c \mathbf{u} \right) dv_j \right. \\ &\quad \left. - \left(\int_{v_j} \overline{\mathbf{F}}^T \mathbf{u} dv_j + \int_{s_{j\sigma}} \overline{\mathbf{T}}^T \mathbf{u} ds_j \right) \right] \\ &= \sum_j \left[\int_{v_j} \left(\frac{1}{2} \boldsymbol{\epsilon}_g{}^T \mathbf{R}_1 \boldsymbol{\epsilon}_g + \frac{1}{2} \boldsymbol{\sigma}_g{}^T \mathbf{R}_4 \boldsymbol{\sigma}_g + \boldsymbol{\sigma}_g{}^T \mathbf{R}_3 \boldsymbol{\epsilon}_g + \boldsymbol{\sigma}_g{}^T \overline{\mathbf{B}}_c \mathbf{u} \right) dv_j \right. \\ &\quad \left. - \left(\int_{v_j} \overline{\mathbf{F}}^T \mathbf{u} dv_j + \int_{s_{j\sigma}} \overline{\mathbf{T}}^T \mathbf{u} ds_j \right) \right] \\ &= \sum_j \left[\int_{v_j} \left(\frac{1}{2} \boldsymbol{\delta}^T \mathbf{B}_g{}^T \mathbf{S}_1^{-1} \mathbf{B}_g \boldsymbol{\delta} - \frac{1}{2} \boldsymbol{\beta}^T \mathbf{P}_g{}^T \mathbf{C}_3^{-1} \mathbf{P}_g \boldsymbol{\beta} \right. \right. \end{aligned}$$

$$+\boldsymbol{\beta}^T \mathbf{P}_g{}^T \left(\overline{\mathbf{B}}_c \mathbf{N} - \mathbf{S}_2^T \mathbf{S}_1^{-1} \mathbf{B}_g\right) \boldsymbol{\delta}\Big) \, dv_j$$
$$- \left(\int_{v_j} \boldsymbol{\delta}^T \mathbf{N}^T \overline{\mathbf{F}} dv_j + \int_{s_{j\sigma}} \boldsymbol{\delta}^T \mathbf{N}^T \overline{\mathbf{T}} ds_j \right) \Bigg] \tag{4.15}$$

Define

$$\mathbf{K}_d = \int_{v_j} \mathbf{B}_g{}^T \mathbf{S}_1^{-1} \mathbf{B}_g dv_j \tag{4.16}$$

$$\mathbf{H} = \int_{v_j} \mathbf{P}_g{}^T \mathbf{C}_3^{-1} \mathbf{P}_g dv_j \tag{4.17}$$

$$\mathbf{G} = \int_{v_j} \mathbf{P}_g{}^T \left(\mathbf{B}_c - \mathbf{S}_2^T \mathbf{S}_1^{-1} \mathbf{B}_g\right) dv_j \tag{4.18}$$

$$\mathbf{f} = \int_{v_j} \mathbf{N}^T \overline{\mathbf{F}} dv + \int_{s_{j\sigma}} \mathbf{N}^T \overline{\mathbf{T}} ds_j \tag{4.19}$$

where

$$\mathbf{B}_c = \overline{\mathbf{B}}_c \mathbf{N} \tag{4.20}$$

in which, $\overline{\mathbf{B}}_c$ has been defined in (2.37).

The variational functional will take the following form:

$$\Pi_C = \sum_j \left[\frac{1}{2} \boldsymbol{\delta}^T \mathbf{K}_d \boldsymbol{\delta} - \frac{1}{2} \boldsymbol{\beta}^T \mathbf{H} \boldsymbol{\beta} + \boldsymbol{\beta}^T \mathbf{G} \boldsymbol{\delta} - \boldsymbol{\delta}^T \mathbf{f} \right] \tag{4.21}$$

From the partial stationary condition of Π_C

$$\frac{\partial \Pi_C}{\partial \boldsymbol{\beta}} = 0 \tag{4.22}$$

the partial stress field parameter can be expressed as

$$\boldsymbol{\beta} = \mathbf{H}^{-1} \mathbf{G} \boldsymbol{\delta} \tag{4.23}$$

Substitute equation(4.23) into equation(4.21), the functional takes the form:

$$\Pi_C = \sum_J \left[\frac{1}{2}\boldsymbol{\delta}^T \mathbf{K}_d \boldsymbol{\delta} + \frac{1}{2}\boldsymbol{\delta}^T \mathbf{G}^T \mathbf{H}^{-1} \mathbf{G}\boldsymbol{\delta} - \boldsymbol{\delta}^T \mathbf{f}\right] \tag{4.24}$$

Using another partial stationary condition of Π_C

$$\frac{\partial \Pi_C}{\partial \boldsymbol{\delta}} = 0 \tag{4.25}$$

We have the composite finite element equation

$$\mathbf{K}_C \boldsymbol{\delta} = \mathbf{f} \tag{4.26}$$

where

$$\mathbf{K}_C = \mathbf{K}_d + \mathbf{G}^T \mathbf{H}^{-1} \mathbf{G} \tag{4.27}$$

Equation(4.26) is called the *composite* finite element equation. The stiffness matrix of composite element is made of two parts, one semi-displacement formulated stiffness matrix $\mathbf{K}_d$ and one semi-hybrid formulated stiffness matrix $\mathbf{G}^T\mathbf{H}^{-1}\mathbf{G}$. The term composite here means a combination of displacements and hybrid formulation, and also means the element is designed for the stress analysis of composite laminates. The element itself has no relations to composite materials.

4.1.2 Formulation Procedure of Composite Finite Element

Since the three displacements and the three transverse stresses are taken as the basic variables, a displacement field and a partial stress field for the element have to be set up in order to form the composite finite element equations with above variational principle.

Partial Stress Field

There are several different assumptions of the stress field. Here, the partial stress field in a composite finite element is assumed as

$$\boldsymbol{\sigma}_g{}^e = \mathbf{P}_g \boldsymbol{\beta}^e \tag{4.28}$$

where

$\mathbf{P}_g = [\mathbf{P}_1, \mathbf{P}_2, \cdots, \mathbf{P}_m]$ is a $3 \times m$ matrix of *assumed stress field functions.*

$\boldsymbol{\beta}^e = [\beta_1, \beta_2, \cdots, \beta_m]^T$ is the *assumed stress field parameter vector* in a composite finite element.

m is the degree of freedom of the assumed stress field.

$\boldsymbol{\sigma}_g{}^e$ is the global stress vector in the element

$$\boldsymbol{\sigma}_g{}^e = \begin{Bmatrix} \sigma_x \\ \sigma_{yz} \\ \sigma_{xz} \end{Bmatrix}^e \tag{4.29}$$

Displacement Field

The displacement field in an element is assumed as

$$\mathbf{u}^e = \mathbf{N}\boldsymbol{\delta}^e \tag{4.30}$$

where

$\mathbf{u}^e$ is displacement vector at point (x, y, z) in an element

$$\mathbf{u} = \begin{Bmatrix} u(x,y,z) \\ v(x,y,z) \\ w(x,y,z) \end{Bmatrix} \tag{4.31}$$

$\mathbf{N}$ is a matrix of shape functions.

$$\mathbf{N} = [\, N_1\mathbf{I}, N_2\mathbf{I}, \cdots, N_n\mathbf{I} \,] \tag{4.32}$$

in which

$$N_i = \begin{cases} 0 & \text{at any node except i;} \\ 1 & \text{at the i-th node} \end{cases} \tag{4.33}$$

and

$$\mathbf{I} = \begin{bmatrix} 1 & 0 & 0 \\ 0 & 1 & 0 \\ 0 & 0 & 1 \end{bmatrix} \tag{4.34}$$

$\boldsymbol{\delta}^e$ is the element nodal displacement vector

$$\boldsymbol{\delta}^e = \begin{bmatrix} \mathbf{u}_1 & \mathbf{u}_2 & \cdots & \mathbf{u}_n \end{bmatrix}^T \tag{4.35}$$

in which n is the total number of nodes of the finite element and $\mathbf{u}_i = \{u_i, v_i, w_i\}, i = 1, 2, \cdots, n$ is the displacement vector of the i-th node of the element

With the displacement field, the globally continuous in-plane strains at any point in the element will be

$$\boldsymbol{\epsilon}_g{}^e = \mathbf{B}_g \boldsymbol{\delta}^e \tag{4.36}$$

where

$$\mathbf{B}_g = \overline{\mathbf{B}}_g \mathbf{N}$$

$$= \begin{bmatrix} \frac{\partial}{\partial x} & 0 & 0 \\ 0 & \frac{\partial}{\partial y} & 0 \\ \frac{\partial}{\partial y} & \frac{\partial}{\partial x} & 0 \end{bmatrix} \mathbf{N} \tag{4.37}$$

Element Stiffness Matrix

The element stiffness matrix of the composite finite element is

$$\mathbf{K}_C{}^e = \mathbf{K}_d{}^e + \mathbf{G}^{eT}\mathbf{H}^{e-1}\mathbf{G}^e \tag{4.38}$$

in which

$$\mathbf{K}_d{}^e = \int_{V_e} \mathbf{B}_g{}^T \mathbf{S}_1^{-1} \mathbf{B}_g dv_e, \tag{4.39}$$

$$\mathbf{H}^e = \int_{V_e} \mathbf{P}_g{}^T \mathbf{C}_3^{-1} \mathbf{P}_g dv_e, \tag{4.40}$$

$$\mathbf{G}^e = \int_{V_e} \mathbf{P}_g{}^T \left(\mathbf{B}_c - \mathbf{S}_2^T \mathbf{S}_1^{-1} \mathbf{B}_g \right) dv_e, \tag{4.41}$$

$$\mathbf{f}^e = \int_{V_e} \mathbf{N}^T \overline{\mathbf{F}}^e dv + \int_{S_{\sigma_e}} \mathbf{N}^T \overline{\mathbf{T}}^e ds_e, \tag{4.42}$$

where

$$\mathbf{B}_c = \overline{\mathbf{B}}_c \mathbf{N}$$

$$= \begin{bmatrix} 0 & 0 & \frac{\partial}{\partial z} \\ 0 & \frac{\partial}{\partial z} & \frac{\partial}{\partial y} \\ \frac{\partial}{\partial z} & 0 & \frac{\partial}{\partial x} \end{bmatrix} \mathbf{N} \tag{4.43}$$

Stress and Strain

After solving the governing equation, the displacement $\mathbf{u}^e$, stress $\boldsymbol{\sigma}^e$ and strain $\boldsymbol{\epsilon}^e$

are given by following relations, in terms of nodal displacement $\boldsymbol{\delta}^e$.

$$\mathbf{u}^e = \mathbf{N}\boldsymbol{\delta}^e \tag{4.44}$$

$$\boldsymbol{\beta}^e = \mathbf{H}^{e-1}\mathbf{G}^e\boldsymbol{\delta}^e \tag{4.45}$$

$$\boldsymbol{\sigma}_g{}^e = \left\{ \begin{array}{c} \sigma_z \\ \sigma_{yz} \\ \sigma_{xz} \end{array} \right\}^e = \mathbf{P}_g\boldsymbol{\beta}^e = \mathbf{P}_g\mathbf{H}^{e-1}\mathbf{G}\boldsymbol{\delta}^e \tag{4.46}$$

$$\boldsymbol{\epsilon}_g{}^e = \left\{ \begin{array}{c} \epsilon_x \\ \epsilon_y \\ \epsilon_{xy} \end{array} \right\}^e = \mathbf{B}_g\boldsymbol{\delta}^e \tag{4.47}$$

$$\begin{aligned} \boldsymbol{\sigma}_L{}^e &= \left\{ \begin{array}{c} \sigma_x \\ \sigma_y \\ \sigma_{xy} \end{array} \right\}^e = \mathbf{R}_1\boldsymbol{\epsilon}_g{}^e + \mathbf{R}_2\boldsymbol{\sigma}_g{}^e \\ &= \left[\mathbf{S}_1^{-1}\mathbf{B}_g - \mathbf{S}_1^{-1}\mathbf{S}_2^T\mathbf{P}_g\mathbf{H}^{e-1}\mathbf{G}^e\right]\boldsymbol{\delta}^e \end{aligned} \tag{4.48}$$

$$\begin{aligned} -\boldsymbol{\epsilon}_L{}^e &= -\left\{ \begin{array}{c} \epsilon_z \\ \epsilon_{yz} \\ \epsilon_{xz} \end{array} \right\}^e = \mathbf{R}_3\boldsymbol{\epsilon}_g{}^e + \mathbf{R}_4\boldsymbol{\sigma}_g{}^e \\ &= \left[-\mathbf{S}_2^T\mathbf{S}_1^{-1}\mathbf{B}_g - \mathbf{C}_3^{-1}\mathbf{P}_g\mathbf{H}^{e-1}\mathbf{G}^e\right]\boldsymbol{\delta}^e \end{aligned} \tag{4.49}$$

or

$$\boldsymbol{\sigma}^e = \begin{Bmatrix} \sigma_x \\ \sigma_y \\ \sigma_{xy} \\ \sigma_z \\ \sigma_{yz} \\ \sigma_{xz} \end{Bmatrix}^e = \begin{bmatrix} \mathbf{S}_1^{-1}\mathbf{B}_g - \mathbf{S}_1^{-1}\mathbf{S}_2^T\mathbf{P}_g\mathbf{H}^{e-1}\mathbf{G}^e \\ \mathbf{P}_g\mathbf{H}^{e-1}\mathbf{G}^e \end{bmatrix} \boldsymbol{\delta}^e \qquad (4.50)$$

$$\boldsymbol{\epsilon}^e = \begin{Bmatrix} \epsilon_x \\ \epsilon_y \\ \epsilon_{yz} \\ \epsilon_z \\ \epsilon_{yz} \\ \epsilon_{xz} \end{Bmatrix}^e = \begin{bmatrix} \mathbf{B}_g \\ \mathbf{S}_2^T\mathbf{S}_1^{-1}\mathbf{B}_g + \mathbf{C}_3^{-1}\mathbf{P}_g\mathbf{H}^{e-1}\mathbf{G}^e \end{bmatrix} \boldsymbol{\delta}^e \qquad (4.51)$$

4.2 3-D Composite Finite Elements

With the previously developed formulation procedures of composite finite element and the iso-function technique for assuming a partial stress field, three dimensional composite elements are formulated based on the existing various finite elements with a displacement shape functions. In this section, we applied the composite finite element method in three iso-parametric finite elements, and formulated a 3-D, 8-node composite element, a 3-D, 16-node composite element and a 3-D, 20-node composite element.

4.2.1 3-D, 8-node Composite Element

Figure 4.1 shows a three dimensional eight-node isoparametric finite element. The

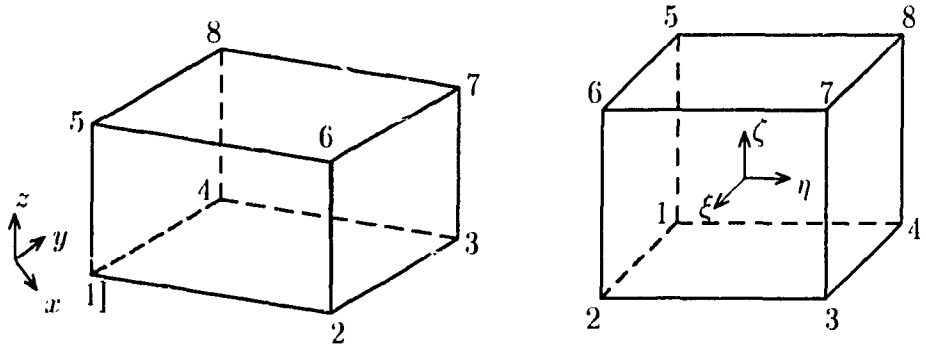

(a) in global coordinates (b) in local coordinates

Figure 4.1: 3-D, 8-node composite element

displacement field in the natural coordinates is defined as

$$\mathbf{u}^e = \mathbf{N}\boldsymbol{\delta}^e \tag{4.52}$$

in which

$$\mathbf{u}^e = \begin{Bmatrix} u(\xi,\eta,\zeta) \\ v(\xi,\eta,\zeta) \\ w(\xi,\eta,\zeta) \end{Bmatrix} \tag{4.53}$$

$$\mathbf{N} = \begin{bmatrix} N_1 & 0 & 0 & N_2 & 0 & 0 & \cdots & N_8 & 0 & 0 \\ 0 & N_1 & 0 & 0 & N_2 & 0 & \cdots & 0 & N_8 & 0 \\ 0 & 0 & N_1 & 0 & 0 & N_2 & \cdots & 0 & 0 & N_8 \end{bmatrix} \tag{4.54}$$

where $\mathbf{N}$ is the shape function of the element, in which

$$N_i = \frac{1}{8}(1+\xi_i\xi)(1+\eta_i\eta)(1+\zeta_i\zeta) \tag{4.55}$$

for $i = 1, 2, 3, \cdots, 8$.

The isoparametric finite element has the coordinate relation between the natural (local) and global coordinates, according to the shape function of the element, as

$$\begin{Bmatrix} x \\ y \\ z \end{Bmatrix} = \mathbf{N} \begin{Bmatrix} \mathbf{x}_1 \\ \mathbf{x}_2 \\ \vdots \\ \mathbf{x}_8 \end{Bmatrix} \tag{4.56}$$

in which $\mathbf{x}_i$ is element nodal global coordinates,

$$\mathbf{x}_i = \begin{Bmatrix} x_i \\ y_i \\ z_i \end{Bmatrix} \tag{4.57}$$

where $i = 1, 2, \cdots, 8$, or can be written as

$$x = \sum_{j=1}^{8} \frac{1}{8} \left(1 + \xi_j \xi\right) \left(1 + \eta_j \eta\right) \left(1 + \zeta_j \zeta\right) x_j \tag{4.58}$$

$$y = \sum_{j=1}^{8} \frac{1}{8} \left(1 + \xi_j \xi\right) \left(1 + \eta_j \eta\right) \left(1 + \zeta_j \zeta\right) y_j \tag{4.59}$$

$$z = \sum_{j=1}^{8} \frac{1}{8} \left(1 + \xi_j \xi\right) \left(1 + \eta_j \eta\right) \left(1 + \zeta_j \zeta\right) z_j \tag{4.60}$$

The partial stress field is

$$\boldsymbol{\sigma}_g{}^r = \mathbf{P}_g \boldsymbol{\beta}^r \tag{4.61}$$

in which, the stress field function matrix $\mathbf{P}_g$ has already been formed by iso function method in chapter 3. For on-axis orthotropic material, equation (3.71) repeated here

is

$$\mathbf{P}_q = \begin{bmatrix} 1 & 0 & 0 & \xi & 0 & 0 & \eta & 0 & 0 & \zeta & 0 & 0 & \xi\eta & 0 & 0 & \eta\zeta & 0 & \xi\zeta & 0 \\ 0 & 1 & 0 & 0 & \xi & 0 & 0 & \eta & 0 & 0 & \zeta & 0 & 0 & \xi\eta & 0 & 0 & 0 & 0 & \xi\zeta \\ 0 & 0 & 1 & 0 & 0 & \xi & 0 & 0 & \eta & 0 & 0 & \zeta & 0 & 0 & \xi\eta & 0 & \eta\zeta & 0 & 0 \end{bmatrix}, \tag{4.62}$$

and the corresponding element partial stress field parameter vector $\boldsymbol{\beta}^e$ is

$$\boldsymbol{\beta}^e = \begin{bmatrix} \beta_1, & \beta_2, & \cdots, & \beta_{19} \end{bmatrix}^T \tag{4.63}$$

For off-axis orthotropic material, equation (3.98) repeated here is

$$\mathbf{P} = \begin{bmatrix} 1 & 0 & 0 & \xi & 0 & 0 & \eta & 0 & 0 & \zeta & 0 & 0 \\ 0 & 1 & 0 & 0 & \zeta & 0 & 0 & \eta & 0 & 0 & \zeta & 0 \\ 0 & 0 & 1 & 0 & 0 & \xi & 0 & 0 & \eta & 0 & 0 & \zeta \end{bmatrix}$$

$$\begin{bmatrix} \xi\eta & 0 & 0 & \eta\zeta & 0 & 0 & \xi\zeta & 0 & 0 \\ 0 & \xi\eta & 0 & 0 & \eta\zeta & 0 & 0 & \xi\zeta & 0 \\ 0 & 0 & \xi\eta & 0 & 0 & \eta\zeta & 0 & 0 & \xi\zeta \end{bmatrix} \tag{4.64}$$

and the corresponding element partial stress field parameter vector $\boldsymbol{\beta}^e$ is

$$\boldsymbol{\beta}^e = \begin{bmatrix} \beta_1, & \beta_2, & \cdots, & \beta_{21} \end{bmatrix}^T \tag{4.65}$$

.

4.2.2 3-D, 16-node Composite Element

Figure 4.2 shows a three dimensional sixteen-node isoparameter finite element.

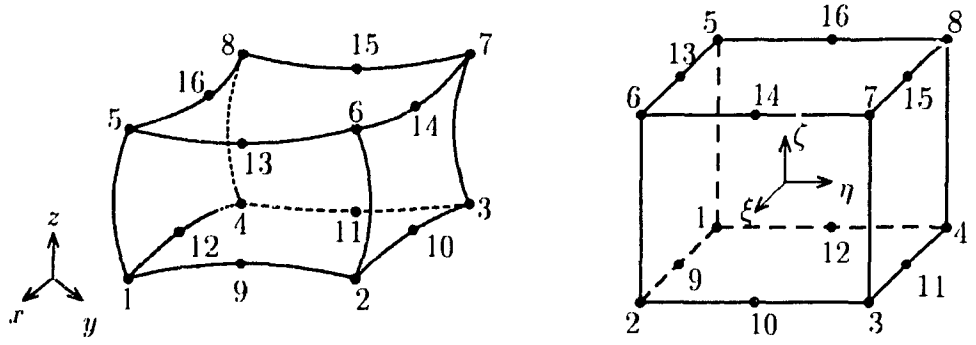

(a) in global coordinates (b) in local coordinates

Figure 4.2: 3-D, 16-node composite element

The displacement field of the element in the natural coordinates is defined as

$$\mathbf{u}^e = \mathbf{N}\boldsymbol{\delta}^e \tag{4.66}$$

where

$$\mathbf{u}^e = \begin{Bmatrix} u(\xi,\eta,\zeta) \\ v(\xi,\eta,\zeta) \\ w(\xi,\eta,\zeta) \end{Bmatrix} \tag{4.67}$$

$$\mathbf{N} = \begin{bmatrix} N_1 & 0 & 0 & N_2 & 0 & 0 & \cdots & N_{16} & 0 & 0 \\ 0 & N_1 & 0 & 0 & N_2 & 0 & \cdots & 0 & N_{16} & 0 \\ 0 & 0 & N_1 & 0 & 0 & N_2 & \cdots & 0 & 0 & N_{16} \end{bmatrix} \tag{4.68}$$

where $\mathbf{N}$ is the shape function of the element, in which, for corner nodes

$$N_i = \frac{1}{8}(1+\xi_i\xi)(1+\eta_i\eta)(1+\zeta_i\zeta)(\xi_i\xi+\eta_i\eta-1) \tag{4.69}$$

where $i = 1, 2, 3, \cdots, 8$

for mid-side nodes

$$N_i = \frac{1}{4}(1+\xi_i\xi)(1+\eta_i\eta)(1+\zeta_i\zeta)\left[(1-\xi^2)(1-\xi_i^2)+(1-\eta^2)(1-\eta_i^2)\right] \qquad (4.70)$$

where $i = 9, 10, 11, \cdots, 16$.

The coordinate relation between the natural (local) and global coordinates of an isoparametric finite element is defined according to the shape function of the element as

$$\begin{Bmatrix} x \\ y \\ z \end{Bmatrix} = \mathbf{N} \begin{Bmatrix} \mathbf{x}_1 \\ \mathbf{x}_2 \\ \vdots \\ \mathbf{x}_{16} \end{Bmatrix} \qquad (4.71)$$

in which $\mathbf{x}_i$ is element nodal global coordinates,

$$\mathbf{x}_i = \begin{Bmatrix} x_i \\ y_i \\ z_i \end{Bmatrix} \qquad (4.72)$$

where $i = 1, 2, \cdots, 16$, or can be written as

$$\begin{aligned} x = &\sum_{i=1}^{8} \frac{1}{8}(1+\xi_i\xi)(1+\eta_i\eta)(1+\zeta_i\zeta)(\xi_i\xi+\eta_i\eta-1)x_i \\ &+\sum_{i=9}^{16} \frac{1}{4}(1+\xi_i\xi)(1+\eta_i\eta)(1+\zeta_i\zeta)\left[(1-\xi^2)(1-\xi_i^2)+(1-\eta^2)(1-\eta_i^2)\right]x_i \end{aligned} \qquad (4.73)$$

$$\begin{aligned} y = &\sum_{i=1}^{8} \frac{1}{8}(1+\xi_i\xi)(1+\eta_i\eta)(1+\zeta_i\zeta)(\xi_i\xi+\eta_i\eta-1)y_i \\ &+\sum_{i=9}^{16} \frac{1}{4}(1+\xi_i\xi)(1+\eta_i\eta)(1+\zeta_i\zeta)\left[(1-\xi^2)(1-\xi_i^2)+(1-\eta^2)(1-\eta_i^2)\right]y_i \end{aligned} \qquad (4.74)$$

$$z = \sum_{i=1}^{8} \frac{1}{8}(1+\xi_i\xi)(1+\eta_i\eta)(1+\zeta_i\zeta)(\xi_i\xi+\eta_i\eta-1)z_i$$

$$+\sum_{i=9}^{16}\frac{1}{4}(1+\xi_i\xi)(1+\eta_i\eta)(1+\zeta_i\zeta)\left[(1-\xi^2)(1-\xi_i^2)+(1-\eta^2)(1-\eta_i^2)\right]z_i \tag{4.75}$$

The partial stress field is

$$\boldsymbol{\sigma}_g{}^e = \mathbf{P}_g\boldsymbol{\beta}^e \tag{4.76}$$

in which, the stress field function matrix $\mathbf{P}_g$ has already been formed by iso-function method in chapter 3. For on-axis orthotropic material, equation (3.152) repeated here is

$$\mathbf{P}_g = \begin{bmatrix}
1 & 0 & 0 & \xi & 0 & 0 & \eta & 0 & 0 & \zeta & 0 & 0 & \xi\eta & 0 & 0 & \xi\zeta & 0 & 0 \\
0 & 1 & 0 & 0 & \xi & 0 & 0 & \eta & 0 & 0 & \zeta & 0 & 0 & \xi\eta & 0 & 0 & \xi\zeta & 0 \\
0 & 0 & 1 & 0 & 0 & \xi & 0 & 0 & \eta & 0 & 0 & \zeta & 0 & 0 & \xi\eta & 0 & 0 & \xi\zeta
\end{bmatrix}$$

$$\begin{bmatrix}
\eta\zeta & 0 & 0 & \xi\eta\zeta & 0 & 0 & \xi^2 & 0 & 0 & \eta^2 & 0 & 0 & \xi^2\eta & 0 & 0 \\
0 & \eta\zeta & 0 & 0 & \xi\eta\zeta & 0 & 0 & \xi^2 & 0 & 0 & \eta^2 & 0 & 0 & \xi^2\eta & 0 \\
0 & 0 & \eta\zeta & 0 & 0 & \xi\eta\zeta & 0 & 0 & \xi^2 & 0 & 0 & \eta^2 & 0 & 0 & \xi^2\eta
\end{bmatrix}$$

$$\begin{bmatrix}
\xi^2\zeta & 0 & \xi\eta^2 & 0 & 0 & \eta^2\zeta & 0 \\
0 & \xi^2\zeta & 0 & \xi\eta^2 & 0 & 0 & 0 \\
0 & 0 & 0 & 0 & \xi\eta^2 & 0 & \eta^2\zeta
\end{bmatrix} \tag{4.77}$$

and the corresponding partial stress field parameter vector $\boldsymbol{\beta}^e$ is

$$\boldsymbol{\beta}^e = \begin{bmatrix} \beta_1, & \beta_2, & \cdots, & \beta_{40} \end{bmatrix}^T \tag{4.78}$$

For off-axis orthotropic material, equation (3.199) repeated here is

$$\mathbf{P} = \begin{bmatrix} 1 & 0 & 0 & \xi & 0 & 0 & \eta & 0 & 0 & \zeta & 0 & 0 & \xi\eta & 0 & 0 & \xi\zeta & 0 & 0 \\ 0 & 1 & 0 & 0 & \xi & 0 & 0 & \eta & 0 & 0 & \zeta & 0 & 0 & \xi\eta & 0 & 0 & \xi\zeta & 0 \\ 0 & 0 & 1 & 0 & 0 & \xi & 0 & 0 & \eta & 0 & 0 & \zeta & 0 & 0 & \xi\eta & 0 & 0 & \xi\zeta \end{bmatrix}$$

$$\begin{matrix} \eta\zeta & 0 & 0 & \xi\eta\zeta & 0 & 0 & \xi^2 & 0 & 0 & \eta^2 & 0 & 0 & \xi^2\eta & 0 & 0 \\ 0 & \eta\zeta & 0 & 0 & \xi\eta\zeta & 0 & 0 & \xi^2 & 0 & 0 & \eta^2 & 0 & 0 & \xi^2\eta & 0 \\ 0 & 0 & \eta\zeta & 0 & 0 & \xi\eta\zeta & 0 & 0 & \xi^2 & 0 & 0 & \eta^2 & 0 & 0 & \xi^2\eta \end{matrix}$$

$$\begin{matrix} \xi^2\zeta & 0 & 0 & \xi\eta^2 & 0 & 0 & \eta^2\zeta & 0 & 0 \\ 0 & \xi^2\zeta & 0 & 0 & \xi\eta^2 & 0 & 0 & \eta^2\zeta & 0 \\ 0 & 0 & \xi^2\zeta & 0 & 0 & \xi\eta^2 & 0 & 0 & \eta^2\zeta \end{matrix} \Bigg] \tag{1.79}$$

and the corresponding partial stress field parameter vector $\boldsymbol{\beta}^e$ is

$$\boldsymbol{\beta}^e = \begin{bmatrix} \beta_1, & \beta_2, & \cdots, & \beta_{42} \end{bmatrix}^T \tag{4.80}$$

.

4.2.3 3-D, 20-node Composite Element

Figure 4.3 shows a three dimensional twenty-node isoparametric finite element.

The displacement field of the element in the natural coordinates is defined as

$$\mathbf{u}^e = \mathbf{N}\boldsymbol{\delta}^e \tag{4.81}$$

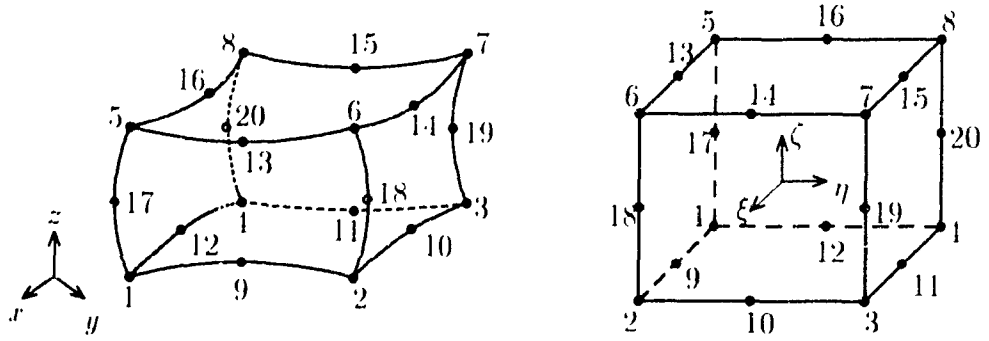

(a) in global coordinates (b) in local coordinates

Figure 1.3: 3-D, 20-node composite element

in which

$$\mathbf{u}^e = \begin{Bmatrix} u(\xi,\eta,\zeta) \\ v(\xi,\eta,\zeta) \\ w(\xi,\eta,\zeta) \end{Bmatrix} \tag{1.82}$$

$$\mathbf{N} = \begin{bmatrix} N_1 & 0 & 0 & N_2 & 0 & 0 & \cdots & N_{20} & 0 & 0 \\ 0 & N_1 & 0 & 0 & N_2 & 0 & \cdots & 0 & N_{20} & 0 \\ 0 & 0 & N_1 & 0 & 0 & N_2 & \cdots & 0 & 0 & N_{20} \end{bmatrix} \tag{1.83}$$

where $\mathbf{N}$ is the shape function of the element, in which, for corner nodes

$$N_i = \frac{1}{8}(1+\xi_i\xi)(1+\eta_i\eta)(1+\zeta_i\zeta)(\xi_i\xi+\eta_i\eta+\zeta_i\zeta-2) \tag{1.84}$$

where $i = 1,2,3,\cdots,8$

for mid-side nodes

$$\begin{aligned} N_i \;=\; & \frac{1}{4}(1+\xi_i\xi)(1+\eta_i\eta)(1+\zeta_i\zeta)\left[(1-\xi^2)(1-\xi_i^2)\right. \\ & \left.+(1-\eta^2)(1-\eta_i^2)+(1-\zeta^2)(1-\zeta_i^2)\right] \end{aligned} \tag{1.85}$$

where $i = 9,10,11,\cdots,20$.

The coordinate relation between the natural (local) and global coordinates of an isoparametric finite element is defined according to the shape function of the element as

$$\begin{Bmatrix} x \\ y \\ z \end{Bmatrix} = \mathbf{N} \begin{Bmatrix} \mathbf{x}_1 \\ \mathbf{x}_2 \\ \vdots \\ \mathbf{x}_{20} \end{Bmatrix} \tag{4.86}$$

in which $\mathbf{x}_i$ is element nodal global coordinates,

$$\mathbf{x}_i = \begin{Bmatrix} x_i \\ y_i \\ z_i \end{Bmatrix} \tag{4.87}$$

where $i = 1, 2, \cdots, 20$, or can be written as

$$\begin{aligned} x = & \sum_{i=1}^{8} \frac{1}{8}(1+\xi_i\xi)(1+\eta_i\eta)(1+\zeta_i\zeta)(\xi_i\xi+\eta_i\eta+\zeta_i\zeta-2)x_i \\ & + \sum_{i=9}^{20} \frac{1}{4}(1+\xi_i\xi)(1+\eta_i\eta)(1+\zeta_i\zeta)\left[(1-\xi^2)(1-\xi_i^2)\right. \\ & \left. +(1-\eta^2)(1-\eta_i^2)+(1-\zeta^2)(1-\zeta_i^2)\right]x_i \end{aligned} \tag{4.88}$$

$$\begin{aligned} y = & \sum_{i=1}^{8} \frac{1}{8}(1+\xi_i\xi)(1+\eta_i\eta)(1+\zeta_i\zeta)(\xi_i\xi+\eta_i\eta+\zeta_i\zeta-2)y_i \\ & + \sum_{i=9}^{20} \frac{1}{4}(1+\xi_i\xi)(1+\eta_i\eta)(1+\zeta_i\zeta)\left[(1-\xi^2)(1-\xi_i^2)\right. \\ & \left. +(1-\eta^2)(1-\eta_i^2)+(1-\zeta^2)(1-\zeta_i^2)\right]y_i \end{aligned} \tag{4.89}$$

$$\begin{aligned} z = & \sum_{i=1}^{8} \frac{1}{8}(1+\xi_i\xi)(1+\eta_i\eta)(1+\zeta_i\zeta)(\xi_i\xi+\eta_i\eta+\zeta_i\zeta-2)z_i \\ & + \sum_{i=9}^{20} \frac{1}{4}(1+\xi_i\xi)(1+\eta_i\eta)(1+\zeta_i\zeta)\left[(1-\xi^2)(1-\xi_i^2)\right. \\ & \left. +(1-\eta^2)(1-\eta_i^2)+(1-\zeta^2)(1-\zeta_i^2)\right]z_i \end{aligned} \tag{4.90}$$

The partial stress field is

$$\boldsymbol{\sigma}_g^e = \mathbf{P}_g \boldsymbol{\beta}^e \tag{4.91}$$

in which, the stress field function matrix $\mathbf{P}_g$ has already been formed by iso-function method in chapter 3. For on-axis orthotropic material, equation (3.259) repeated here is

$$\mathbf{P}_g = \left[\begin{array}{cccccccccccccccccc}
1 & 0 & 0 & \xi & 0 & 0 & \eta & 0 & 0 & \zeta & 0 & 0 & \xi\eta & 0 & 0 & \xi\zeta & 0 & 0 \\
0 & 1 & 0 & 0 & \xi & 0 & 0 & \eta & 0 & 0 & \zeta & 0 & 0 & \xi\eta & 0 & 0 & \xi\zeta & 0 \\
0 & 0 & 1 & 0 & 0 & \xi & 0 & 0 & \eta & 0 & 0 & \zeta & 0 & 0 & \xi\eta & 0 & 0 & \xi\zeta
\end{array}\right.$$

$$\left.\begin{array}{cccccccccccccccccc}
\eta\zeta & 0 & 0 & \xi\eta\zeta & 0 & 0 & \xi^2 & 0 & 0 & \eta^2 & 0 & 0 & \zeta^2 & 0 & 0 & \xi^2\eta & 0 \\
0 & \eta\zeta & 0 & 0 & \xi\eta\zeta & 0 & 0 & \xi^2 & 0 & 0 & \eta^2 & 0 & 0 & \zeta^2 & 0 & 0 & \xi^2\eta \\
0 & 0 & \eta\zeta & 0 & 0 & \xi\eta\zeta & 0 & 0 & \xi^2 & 0 & 0 & \eta^2 & 0 & 0 & \zeta^2 & 0 & 0
\end{array}\right.$$

$$\left.\begin{array}{cccccccccccc}
0 & \xi^2\zeta & 0 & \xi\eta^2 & 0 & 0 & \eta^2\zeta & 0 & \xi\zeta^2 & 0 & \eta\zeta^2 & 0 \\
0 & 0 & \xi^2\zeta & 0 & \xi\eta^2 & 0 & 0 & 0 & 0 & \xi\zeta^2 & 0 & 0 \\
\xi^2\eta & 0 & 0 & 0 & 0 & \xi\eta^2 & 0 & \eta^2\zeta & 0 & 0 & 0 & \eta\zeta^2
\end{array}\right], \tag{4.92}$$

and the corresponding partial stress field parameter vector $\boldsymbol{\beta}^e$ is

$$\boldsymbol{\beta}^e = \left[\begin{array}{cccc} \beta_1, & \beta_2, & \cdots, & \beta_{47} \end{array}\right]^T \tag{4.93}$$

For off-axis orthotropic material, equation (3.315) repeated here is

$$\mathbf{P} = \left[\begin{array}{cccccccccccccccccc}
1 & 0 & 0 & \xi & 0 & 0 & \eta & 0 & 0 & \zeta & 0 & 0 & \xi\eta & 0 & 0 & \xi\zeta & 0 & 0 \\
0 & 1 & 0 & 0 & \xi & 0 & 0 & \eta & 0 & 0 & \zeta & 0 & 0 & \xi\eta & 0 & 0 & \xi\zeta & 0 \\
0 & 0 & 1 & 0 & 0 & \xi & 0 & 0 & \eta & 0 & 0 & \zeta & 0 & 0 & \xi\eta & 0 & 0 & \xi\zeta
\end{array}\right.$$

$$
\begin{bmatrix}
\eta\zeta & 0 & 0 & \xi\eta\zeta & 0 & 0 & \xi^2 & 0 & 0 & \eta^2 & 0 & 0 & \zeta^2 & 0 & 0 & \xi^2\eta & 0 & 0 \\
0 & \eta\zeta & 0 & 0 & \xi\eta\zeta & 0 & 0 & \xi^2 & 0 & 0 & \eta^2 & 0 & 0 & \zeta^2 & 0 & 0 & \xi^2\eta & 0 \\
0 & 0 & \eta\zeta & 0 & 0 & \xi\eta\zeta & 0 & 0 & \xi^2 & 0 & 0 & \eta^2 & 0 & 0 & \zeta^2 & 0 & 0 & \xi^2\eta
\end{bmatrix}
$$

$$
\begin{bmatrix}
\xi^2\zeta & 0 & 0 & \xi\eta^2 & 0 & 0 & \eta^2\zeta & 0 & 0 & \xi\zeta^2 & 0 & 0 & \eta\zeta^2 & 0 & 0 \\
0 & \xi^2\zeta & 0 & 0 & \xi\eta^2 & 0 & 0 & \eta^2\zeta & 0 & 0 & \xi\zeta^2 & 0 & 0 & \eta\zeta^2 & 0 \\
0 & 0 & \xi^2\zeta & 0 & 0 & \xi\eta^2 & 0 & 0 & \eta^2\zeta & 0 & 0 & \xi\zeta^2 & 0 & 0 & \eta\zeta^2
\end{bmatrix}
\tag{4.94}
$$

and the corresponding partial stress field parameter vector $\boldsymbol{\beta}^e$ is

$$
\boldsymbol{\beta}^e = \begin{bmatrix} \beta_1, & \beta_2, & \cdots, & \beta_{51} \end{bmatrix}^T \tag{4.95}
$$

4.3 A Numerical Example

In order to check the efficiency and accuracy of the composite element, interlaminar stresses in a laminate subjected to bending loads are calculated with three dimensional, eight-node composite element developed in section 4.2.1.

The laminated strip considered herein is a three-layer symmetric cross-ply laminate(0/90/0) made of unidirectional fibrous composite material (see Fig.4.4). The laminate is infinitely long in the y direction and simply supported on the ends $x = 0$ and $x = l$ with length to thickness ratio of $S = l/h = 4$.

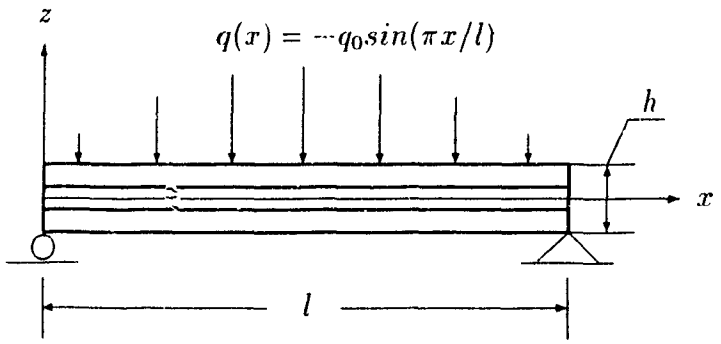

Figure 4.4: The three-layer cross-ply laminate(0/90/0) beam with sinusoidally distributed transverse loading

The material stiffness properties are

$$\begin{aligned} E_L &= 171GPa \\ E_T &= 3.42GPa \\ G_{LT} &= 3.42GPa \\ G_{TT} &= 1.37GPa \\ \nu_{TT} &= \nu_{LT} = 0.25 \end{aligned} \tag{4.96}$$

where, L is the direction parallel to the fibers and T the transverse direction. The Poisson ratio ν_{LT} measuring strain in the transverse direction under uniaxial normal stress in the L direction. A sinusoidally distributed transverse loading

$$q(x) = -q_0 sin(\frac{\pi x}{l})$$

is applied on the top surface of the laminate as shown in fig.4.4.

The boundary conditions are

$$\begin{aligned} \sigma_z(x, h/2) &= q(x) \\ \sigma_z(x, -h/2) &= \sigma_{xz}(x, h/2) = 0 \\ \sigma_x(0, z) &= \sigma_x(l, z) = 0 \end{aligned}$$

$$w(0,z) = w(l,z) = 0$$

Because of symmetry, only half the length l of the laminate is modeled. There are ten uniform elements in the half length, one element in the width and two, four, eight elements per layer in three cases making a total of 60, 120, 240 three dimensional eight node composite elements respectively for three different finite element meshes.

The numerical results will be presented in terms of normalized values which are defined as

$$\begin{aligned}
\bar{\sigma}_x &= \sigma_x(L/2,z)/q_0 \\
\bar{\sigma}_z &= \sigma_z(L/2,z)/q_0 \\
\bar{\sigma}_{xz} &= \sigma_{xz}(0,z)/q_0 \\
\bar{u} &= E_T u(0,z)/(hq_0) \\
\bar{w} &= 100E_T h^3 w(L/2,z)/(q_0 L^4) \\
\bar{z} &= z/h
\end{aligned} \tag{4.97}$$

The distribution of transverse stress σ_{xz} is shown in fig.4.5, which compares the results calculated with 60, 120, 240 8-node composite elements and the results of Pagano's elasticity solution [8]. The comparison of stresses σ_z, σ_x and displacement $\bar{u}$ are shown in fig.4.6, fig.4.7 and fig.4.8 respectively.

The distribution of stress of the same problem was solved by using conventional 3-D displacement formulated element[71], which modeled the laminate with 432 three dimensional, 20-node displacement elements. The results of the shear stress σ_{xz} from the 240, 8-node composite elements and 432 20-node displacement elements are shown in fig.4.9, compared with the results of Pagano's elasticity solution.

Fig.4.5 indicates that the shear stress σ_{xz} of composite element solution quickly

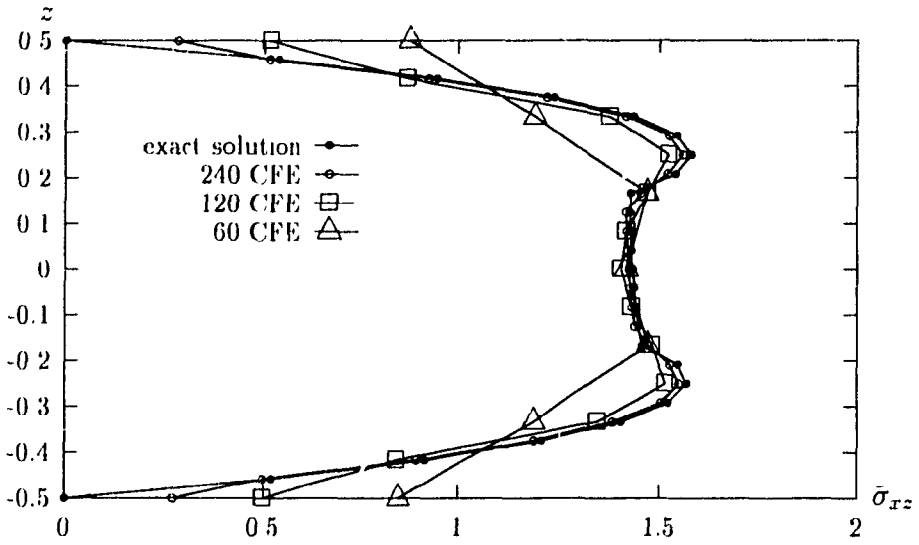

Figure 4.5: Shear stress $\bar{\sigma}_{xz}(x = 0)$, results of 8-node composite element

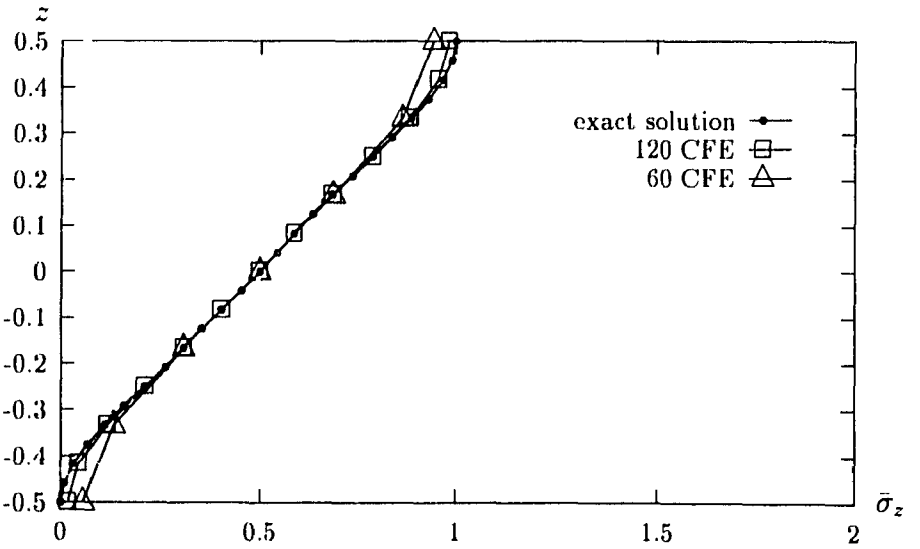

Figure 4.6: stress $\sigma_z(x = l/2)$, results of 8-node composite element

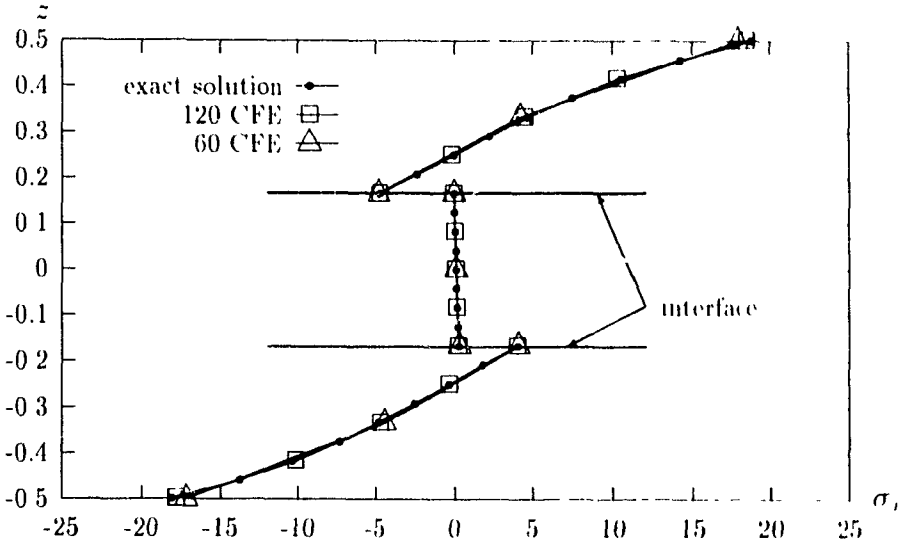

Figure 4.7: Stress $\sigma_x(x = l/2)$, results of 8-node composite element

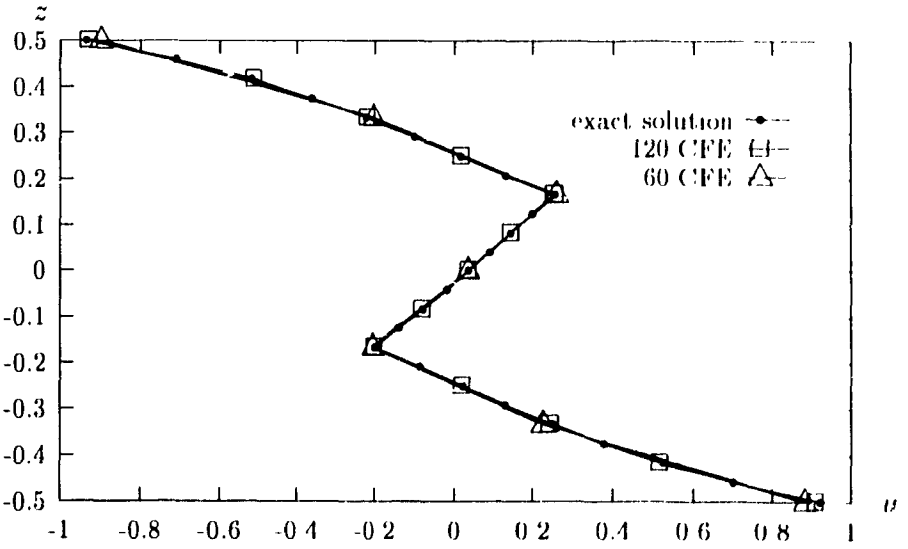

Figure 4.8: Normal displacement at $x = 0$, results of 8-node composite element

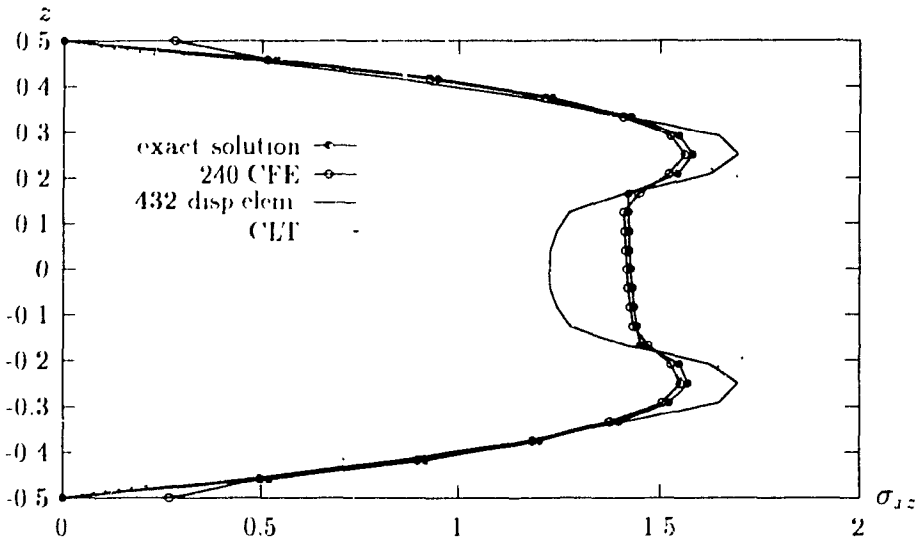

Figure 4.9: Shear stress $\sigma_{xz}(x = 0)$, compared with 20-node displacement element results

converges to the exact elasticity solution as the number of elements increases. The good convergence property of the present CFE is also shown in Fig. 4.10, which shows the results of convergnece study of stress σ_x and σ_{xz}. In the figure, σ_x is the in-plane normal stress at $x = l/2$, $z = h/2$ from CFE, σ_x^p is the corresponding stress from Pagano's exact solution. σ_{xz} is the transverse shear stress at $x = 0$, $z = h/6$(at interface) form CFE, while σ_{xz}^p is the corresponding stress from Pagano's exect solution.

Fig. 4.9 shows the composite element solution is in better agreement with the exact Pagano's elasticity solution, although the composite element solution uses only 240, 8-node while the displacement formulated element solution uses 432, 20-node elements. The CPU time consumed for 240, 8-node composite elements is 2 minutes 58.94 seconds and that for 432, 20-node displacement elements is 18 minutes 2.87 seconds. The programs were run on a VAX 6510 computer.

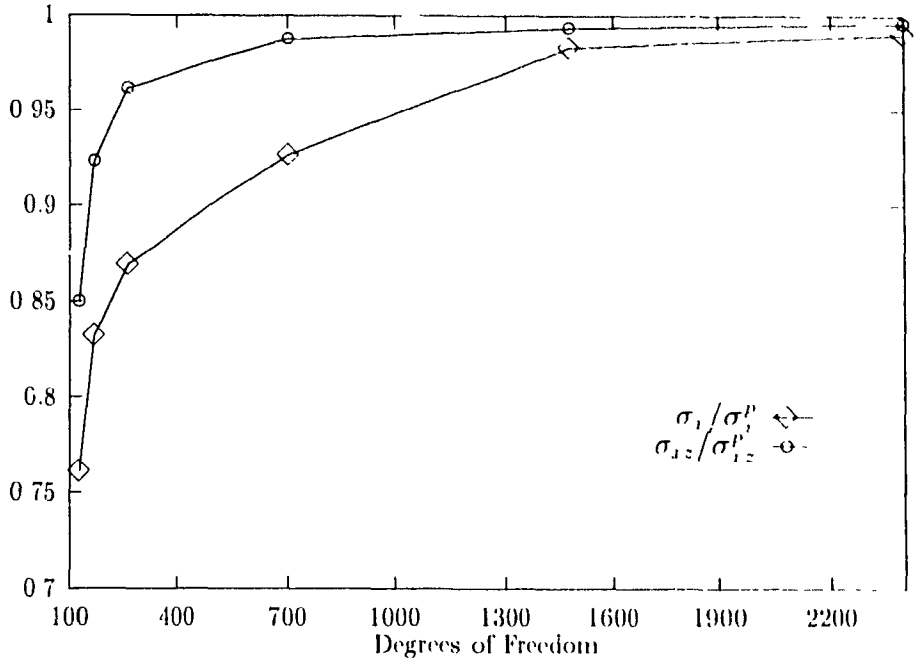

Figure 4.10: Convergence of stress $\sigma_x(x = l/2, z = h/2)$, and stress $\sigma_{xz}(x = 0, z = h/6)$

4.4 Conclusions

This chapter provides the Composite Finite Element technique and gives formulations of three different 3-D composite finite elements with this new technique. The numerical example shown in this chapter clearly exhibits that the composite finite element has the advantages of excellent accuracy and high efficiency over conventional displacement formulated element.

The displacement element can not satisfy the continuity condition at the interface between layers. The composite element does not ensure that this condition is satisfied automatically as mentioned in Chapter 2, except when only one composite element is used to map the whole thickness of a composite laminate.

The numerical results of this chapter also raise the necessity to satisfy the traction

free condition at lower and upper surfaces of a composite laminate. Figure 4.5 shows that the shear stress σ_{xz} at lower or upper surfaces can be as high as 50% of the maximum value when only six elements are used to map through the thickness of the laminate.

However, since the composite finite element model takes the three transverse stresses as basic variables, it is possible to enforce the satisfaction of the continuous condition and traction free condition in advance as will be shown in the next chapter. This is impossible for conventional displacement element method.

Chapter 5

The Multilayer Composite Element for Stress Analysis of Laminates

5.1 Introduction

The numerical analysis of composite finite element developed in the last chapter shows clearly the importance to have a finite element that is traction free at the upper and lower surfaces of composite laminates. It is also obvious that the continuous and natural discontinuous conditions are not satisfied automatically across the interlaminar surfaces. In order to overcome these difficulties, multilayer element technique has been used. Mau et al.[24] developed a laminated thick plate element using hybrid method. However, transverse normal stress was not included in the stress field. Constant transverse displacement through the laminate thickness was also assumed. These assumptions did not agree well with the actual mechanism

of deformation of laminated plates in bending. Spilker[57] developed an eight-node isoparametric multilayer plate element for the analysis of thin to thick composite plates. This model has the generality in describing laminate response but the assumption of constant transverse displacement through laminate thickness still remains. Later, multilayer hybrid elements[31] with linear transverse displacement have been developed for analysis of composite laminates. Usually, those hybrid elements have an assumed stress field of six stress components (full stress field), and has very large assumed stress field. For example, the two types of stress field used by C.T.Sun[30] and W.J.Liou[31] in a three dimensional, eight-node multilayer element have 48 stress parameters and 55 stress parameters respectively. For the specific structure of composite laminates, Reddy and Robbins have also proposed a finite element technique, which they named as the *layerwise theory of Reddy* [20, 21, 22]. However, their works are mainly on the displacement formulated finite elements.

This chapter develops the multilayer composite finite elements based on the composite finite elements provided earlier for interlaminar stress analysis of composite laminates. Since the matrix size of the partial stress field is only a quarter of the full stress field, the mapping matrix for forming the element 'stiffness' matrix in composite element is smaller than that for those elements with a full stress field. Therefore, less computing time is required for formulating the 'stiffness' matrix of partial stress field elements.

In composite finite element, the partial stress field formed with the iso-function method is assumed inside the boundary of an element. It is difficult to apply boundary conditions such as the traction free condition on upper/lower surfaces of a laminate and the traction continuity condition at interlaminar surfaces to the stress field directly. For this reason, a new surface stress field parameter vector is introduced. With the surface stress field parameter vector, the interface traction continuous condition is satisfied automatically and the traction free condition is satisfied simply by assigning zero to a number of stress field parameters at the

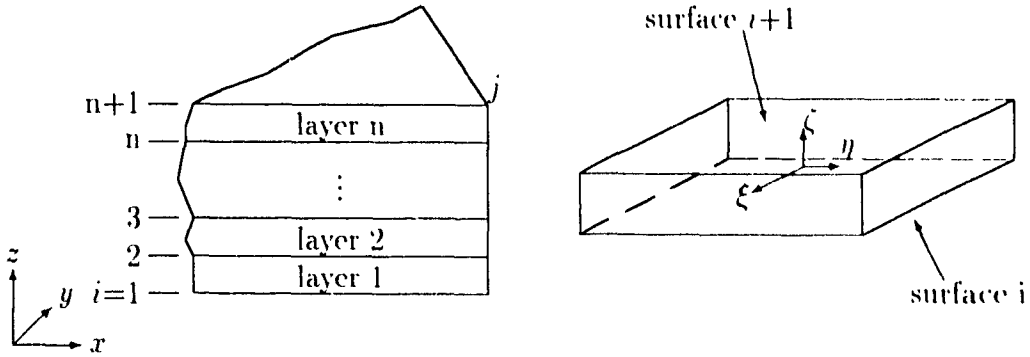

(a) Layer numbering (b) Layer i

Figure 5.1: Geometry and layer numbering conventions for the isoparametric multilayer composite element

upper/lower surfaces of a laminate.

Figure 5.1 shows the geometry structure of a multilayer composite finite element which is composed of n layer elements. The multilayer composite element itself can be seen as a laminate with n perfectly bonded layers (layer elements). In the figure, z corresponds to the transverse direction of the laminate. The layers are numbered from bottom to top of the laminate. Thickness and orientation of the laminate can be varied from lamina to lamina.

The traction free conditions at the top and bottom surface of a laminate are

$$\sigma_{yz}{}^{n} = \sigma_{xz}{}^{n} = 0|_{z=h/2} \tag{5.1}$$

$$\sigma_{yz}{}^{1} = \sigma_{xz}{}^{1} = \sigma_{z}{}^{1} = 0|_{z=-h/2} \tag{5.2}$$

The continuous condition of stresses at the inter-laminar surfaces is

$$\boldsymbol{\sigma}_g{}^{i}|_{\zeta=1} = \boldsymbol{\sigma}_g{}^{i+1}|_{\zeta=-1} \qquad i = 1, 2, \cdots, n-1 \tag{5.3}$$

5.2 Multilayer Composite Finite Element Method

5.2.1 The Partial Stress Field Surface Parameter

Now, let us introduce a new vector of parameters $\boldsymbol{\alpha}$.

$$\boldsymbol{\alpha}^i = \begin{Bmatrix} \alpha_1^i \\ \alpha_2^i \\ \vdots \\ \alpha_r^i \end{Bmatrix} \tag{5.1}$$

in which, r is the number of parameters in the vector $\boldsymbol{\alpha}$.

Assume that $\boldsymbol{\alpha}^i$ is attached to the lower surface of the i-th layer element and $\boldsymbol{\alpha}^{i+1}$ to the upper surface. Thus, for a lamina i, the surface parameter vector is

$$\boldsymbol{\varphi}^i = \begin{Bmatrix} \boldsymbol{\alpha}^i \\ \boldsymbol{\alpha}^{i+1} \end{Bmatrix} \tag{5.5}$$

For the $i-th$ lamina, define

$$\boldsymbol{\beta}^i = \mathbf{U}\boldsymbol{\varphi}^i \tag{5.6}$$

where $\mathbf{U}$ is a transformation matrix of stress field parameter. Now, the partial stress field is

$$\boldsymbol{\sigma}_q{}^i = \mathbf{P}_q\mathbf{U}\boldsymbol{\varphi}^i \tag{5.7}$$

The physical meaning of surface parameter $\boldsymbol{\alpha}^i$ is that, at the lower surface of the i-th layer, we have

$$\boldsymbol{\sigma}_q{}^i|_{\zeta=-1} = \mathbf{P}_q\mathbf{U}\boldsymbol{\alpha}^i|_{\zeta=-1} = \mathbf{A}(\xi,\eta)\boldsymbol{\alpha}^i \tag{5.8}$$

and, at the upper surface of the $i-th$ layer, we have

$$\boldsymbol{\sigma}_g{}^i|_{\zeta=1} = \mathbf{P}_g\mathbf{U}\boldsymbol{\alpha}^i|_{\zeta=1} = \mathbf{A}(\xi,\eta)\boldsymbol{\alpha}^{i+1} \tag{5.9}$$

Thus, at the interface between the i-th and the $(i+1)$-th lamina, we have

$$\boldsymbol{\sigma}_g{}^i|_{\zeta=1} = \mathbf{A}(\xi,\eta)\boldsymbol{\alpha}^{i+1} = \boldsymbol{\sigma}_g{}^{i+1}|_{\zeta=-1}. \tag{5.10}$$

This is to say the traction continuous condition is satisfied automatically.

The transformation matrix can be derived directly by satisfying equation 5.10. The detailed derivation procedure will be shown later in sections of the 4-node multilayer composite element and 8-node multilayer composite element.

Now, with the introduction of the partial stress field parameter vector $\boldsymbol{\alpha}^i$, the partial stress field in the i-th layer is

$$\boldsymbol{\sigma}_g{}^i = \tilde{\mathbf{P}}_g\boldsymbol{\varphi}^i \tag{5.11}$$

where

$$\tilde{\mathbf{P}}_g = \mathbf{P}_g\mathbf{U} \tag{5.12}$$

5.2.2 The Variational Functional and Element Equation of Composite Element Method

The variational functional given in equation 2.56 repeated here is

$$\begin{aligned} \delta\Pi_c &= 0 \\ \Pi_C &= \sum_j \left[\int_{v_j} (\frac{1}{2}\mathbf{q}^T\mathbf{R}\mathbf{q} + \boldsymbol{\sigma}_g{}^T\overline{\mathbf{B}}_c\mathbf{u} - \mathbf{F}^T\mathbf{u})dv_j - \int_{s_{j\sigma}} \overline{\mathbf{T}}^T\mathbf{u}ds_j \right]. \end{aligned} \tag{5.13}$$

For multilayer element, the functional can be written as

$$\Pi_C = \sum_j \sum_{i=1}^{n} \left[\int_{v_j^i} (\frac{1}{2}\mathbf{q}^{iT}\mathbf{R}^i\mathbf{q}^i + \boldsymbol{\sigma}_g^{iT}\overline{\mathbf{B}}_c\mathbf{u}^i - \mathbf{F}^{iT}\mathbf{u}^i)dv_j^i - \int_{s_{j\sigma}^i} \overline{\mathbf{T}}^{iT}\mathbf{u}^i ds_j^i \right]. \quad (5.14)$$

In this equation, j is used to count the number of multilayer elements, while i is used to count the number of layers in the j-th multilayer element (i is used to count accross the thickness ot the laminate, j is used to count with the plane of the laminate). v_j^i is the volume of the i-th layer in the j-th multilayer element. s_j^i is the surface of the i-th layer in the j-th multilayer element.

Because

$$\begin{aligned}
\tfrac{1}{2}\mathbf{q}^{iT}\mathbf{R}^i\mathbf{q}^i &= \frac{1}{2}\begin{bmatrix} \boldsymbol{\epsilon}_g^{iT}, & \boldsymbol{\sigma}_g^{iT} \end{bmatrix} \begin{bmatrix} \mathbf{R}_1^i & \mathbf{R}_2^i \\ \mathbf{R}_3^i & \mathbf{R}_4^i \end{bmatrix} \begin{Bmatrix} \boldsymbol{\epsilon}_g^i \\ \boldsymbol{\sigma}_g^i \end{Bmatrix} \\
&= \frac{1}{2}\begin{bmatrix} \boldsymbol{\epsilon}_g^{iT}\mathbf{R}_1^i + \boldsymbol{\sigma}_g^{iT}\mathbf{R}_3^i, & \boldsymbol{\epsilon}_g^{iT}\mathbf{R}_2^i + \boldsymbol{\sigma}_g^{iT}\mathbf{R}_4^i \end{bmatrix} \begin{Bmatrix} \boldsymbol{\epsilon}_g^i \\ \boldsymbol{\sigma}_g^i \end{Bmatrix} \\
&= \frac{1}{2}\left(\boldsymbol{\epsilon}_g^{iT}\mathbf{R}_1^i\boldsymbol{\epsilon}_g^i + \boldsymbol{\sigma}_g^{iT}\mathbf{R}_3^i\boldsymbol{\epsilon}_g^i + \boldsymbol{\epsilon}_g^{iT}\mathbf{R}_2^i\boldsymbol{\sigma}_g^i + \boldsymbol{\sigma}_g^{iT}\mathbf{R}_4^i\boldsymbol{\sigma}_g^i\right), \quad (5.15)
\end{aligned}$$

and because

$$\mathbf{R}_2^{iT} = \mathbf{R}_3^i, \quad (5.16)$$

we have

$$\frac{1}{2}\mathbf{q}^{iT}\mathbf{R}^i\mathbf{q}^i = \frac{1}{2}\left(\boldsymbol{\epsilon}_g^{iT}\mathbf{R}_1^i\boldsymbol{\epsilon}_g^i + 2\boldsymbol{\sigma}_g^{iT}\mathbf{R}_3^i\boldsymbol{\epsilon}_g^i + \boldsymbol{\sigma}_g^{iT}\mathbf{R}_4^i\boldsymbol{\sigma}_g^i\right). \quad (5.17)$$

Substitute 5.17 into equation 5.14, we have

$$\begin{aligned}
\Pi_C = \sum_j \sum_{i=1}^{n} \Bigg[\int_{v_j^i} \Big(&\frac{1}{2}\boldsymbol{\epsilon}_g^{iT}\mathbf{R}_1^i\boldsymbol{\epsilon}_g^i + \frac{1}{2}\boldsymbol{\sigma}_g^{iT}\mathbf{R}_4^i\boldsymbol{\sigma}_g^i + \boldsymbol{\sigma}_g^{iT}\mathbf{R}_3^i\boldsymbol{\epsilon}_g^i \\
&+ \boldsymbol{\sigma}_g^{iT}\overline{\mathbf{B}}_c\mathbf{u}^i - \mathbf{F}^{iT}\mathbf{u}^i\Big) dv_j^i - \int_{s_{j\sigma}^i} \overline{\mathbf{T}}^{iT}\mathbf{u}^i ds_j^i \Bigg]. \quad (5.18)
\end{aligned}$$

Because

$$\boldsymbol{\epsilon}_g{}^t = \mathbf{B}_g \boldsymbol{\delta}^t, \tag{5.19}$$

$$\boldsymbol{\sigma}_g{}^t = \tilde{\mathbf{P}}_g \boldsymbol{\varphi}^t, \tag{5.20}$$

$$\mathbf{u}^t = \mathbf{N}\boldsymbol{\delta}^t, \tag{5.21}$$

equation 5.18 becomes

$$\begin{aligned} \Pi^t = \sum_j \sum_{i=1}^{n} \Bigg\{ \int_{v_j^t} \Big[& \frac{1}{2} \boldsymbol{\delta}^{t^T} \mathbf{B}_g{}^T \mathbf{R}_1^t \mathbf{B}_g \boldsymbol{\delta}^t + \frac{1}{2} \boldsymbol{\varphi}^{t^T} \tilde{\mathbf{P}}_g^T \mathbf{R}_1^t \tilde{\mathbf{P}}_g \boldsymbol{\varphi}^t \\ & + \boldsymbol{\varphi}^{t^T} \tilde{\mathbf{P}}_g^T \left(\mathbf{R}_3^t \mathbf{B}_g + \mathbf{B}_c \right) \boldsymbol{\delta}^t - \boldsymbol{\delta}^{t^T} \mathbf{N}^T \mathbf{F}^t \Big] dv_j^t \\ & - \int_{s_{j\sigma}^t} \boldsymbol{\delta}^{t^T} \mathbf{N}^T \mathbf{T}^t ds_j^t \Bigg\}. \end{aligned} \tag{5.22}$$

Define

$$\mathbf{K}_d{}^t = \int_{v_j^t} \mathbf{B}_g{}^T \mathbf{R}_1^t \mathbf{B}_g dv_j^t \tag{5.23}$$

$$\mathbf{H}^t = -\int_{v_j^t} \tilde{\mathbf{P}}_g^T \mathbf{R}_4^t \tilde{\mathbf{P}}_g^t dv_j^t \tag{5.24}$$

$$\mathbf{G}^t = \int_{v_j^t} \tilde{\mathbf{P}}_g^T \left(\mathbf{B}_c + \mathbf{R}_3^t \mathbf{B}_g \right) dv_j^t \tag{5.25}$$

$$\mathbf{f}^t = \int_{v_j^t} \mathbf{N}^T \mathbf{F}^t dv_j^t + \int_{s_{j\sigma}^t} \mathbf{N}^T \mathbf{T}^t ds_j^t, \tag{5.26}$$

and substitute them into equation(5.22), the functional takes the form:

$$\Pi_C = \sum_j \sum_{i=1}^{n} \left[\frac{1}{2} \boldsymbol{\delta}^{t^T} \mathbf{K}_d{}^t \boldsymbol{\delta}^t - \frac{1}{2} \boldsymbol{\varphi}^{t^T} \mathbf{H}^t \boldsymbol{\varphi}^t + \boldsymbol{\varphi}^{t^T} \mathbf{G}^t \boldsymbol{\delta}^t - \boldsymbol{\delta}^{t^T} \mathbf{f}^t \right] \tag{5.27}$$

Assembling all the layers in the j-th multilayer element from 1 to n, and defining

the assembling rule as

$$\boldsymbol{\delta} = \begin{Bmatrix} \mathbf{d}^1 \\ \mathbf{d}^2 \\ \mathbf{d}^3 \\ \vdots \\ \mathbf{d}^{(n+1)} \end{Bmatrix} \tag{5.28}$$

where $\mathbf{d}^k$, is the nodal displacement vector at the k-th faces

$$\mathbf{d}^k = \begin{Bmatrix} u_1^k \\ v_1^k \\ w_1^k \\ u_2^k \\ \vdots \\ u_m^k \\ v_m^k \\ w_m^k \end{Bmatrix} \tag{5.29}$$

in which, $k = 1, 2, \cdots, n+1$, m is the number of nodes at surface k that is contained in a multilayer composite element, and

$$\boldsymbol{\varphi} = \begin{Bmatrix} \boldsymbol{\alpha}^1 \\ \boldsymbol{\alpha}^2 \\ \boldsymbol{\alpha}^3 \\ \vdots \\ \boldsymbol{\alpha}^{n+1} \end{Bmatrix} \tag{5.30}$$

According to these two assembling rules (eq.5.29, 5.30), at the multilayer element level, we have

$$\mathbf{K}_d = \sum_{i=1}^{n} \mathbf{K}_d{}^i \tag{5.31}$$

$$\mathbf{H} = \sum_{i=1}^{n} \mathbf{H}^i \tag{5.32}$$

$$\mathbf{G} = \sum_{i=1}^{n} \mathbf{G}^i \tag{5.33}$$

$$\mathbf{f} = \sum_{i=1}^{n} \mathbf{f}^i \tag{5.34}$$

Then, eq.5.27 can be written as

$$\Pi_C = \sum_J \left(\frac{1}{2} \boldsymbol{\delta}^T \mathbf{K}_d \boldsymbol{\delta} - \frac{1}{2} \boldsymbol{\varphi}^T \mathbf{H} \boldsymbol{\varphi} + \boldsymbol{\varphi}^T \mathbf{G} \boldsymbol{\delta} - \boldsymbol{\delta}^T \mathbf{f} \right) \tag{5.35}$$

To satisfy the traction free conditions, some components of the bottom surface parameter vector $\boldsymbol{\alpha}^1$ and top surface parameter vector $\boldsymbol{\alpha}^{n+1}$ should be zero. Eliminating these zero surface parameter form $\boldsymbol{\varphi}$, we have a reduced $\tilde{\boldsymbol{\varphi}}$, and $\tilde{\mathbf{H}}$, $\tilde{\mathbf{G}}$ from $\mathbf{H}$, $\mathbf{G}$ respectively. Thus eq.5.35 becomes

$$\Pi_C = \sum_J \left(\frac{1}{2} \boldsymbol{\delta}^T \mathbf{K}_d \boldsymbol{\delta} - \frac{1}{2} \tilde{\boldsymbol{\varphi}}^T \tilde{\mathbf{H}} \tilde{\boldsymbol{\varphi}} + \tilde{\boldsymbol{\varphi}}^T \tilde{\mathbf{G}} \boldsymbol{\delta} - \boldsymbol{\delta}^T \mathbf{f} \right) \tag{5.36}$$

Equation 5.36 gives a variational functional based on the laminate level. The functional takes three transverse stresses and three in-plane strains as basic variables and impose that the stresses in the laminate automatically satisfy continuous conditions between lamina and traction free conditions at top and bottom surfaces of the laminate.

Using one of the partial stationary conditions of Π_C

$$\frac{\partial \Pi_C}{\partial \tilde{\boldsymbol{\varphi}}} = 0 \tag{5.37}$$

we have

$$\tilde{\boldsymbol{\varphi}} = \tilde{\mathbf{H}}^{-1} \tilde{\mathbf{G}} \boldsymbol{\delta} \tag{5.38}$$

Substitute it into eq.5.36, the functional become

$$\Pi_C = \sum_j \left(\frac{1}{2}\delta^T \mathbf{K}_d \delta + \frac{1}{2}\delta^T \widetilde{\mathbf{G}}^T \widetilde{\mathbf{H}}^{-1} \widetilde{\mathbf{G}} \delta - \delta^T \mathbf{f} \right) \tag{5.39}$$

Applying another partial stationary condition of Π_C

$$\frac{\partial \Pi_C}{\partial \delta} = 0 \tag{5.40}$$

We have the multilayer composite finite element equation

$$\mathbf{K}_m \delta = \mathbf{f} \tag{5.41}$$

where

$$\mathbf{K}_m = \mathbf{K}_d + \widetilde{\mathbf{G}}^T \widetilde{\mathbf{H}}^{-1} \widetilde{\mathbf{G}} \tag{5.42}$$

is the 'stiffness' matrix of a multilayer composite element which exactly is a kind of super-element laminated by n layer elements.

5.2.3 Formulation Procedures

The procedure required to formulate a multilayer composite finite element includes the following steps

1. Set up coordinate relations and displacement field,
2. Set up partial stress field and transform the field parameter β^i into surface parameter vector φ^i to enforce the continuity condition
3. Form element matrices at layer level
4. Form element matrices at laminate level

5. adjust element matrices to satisfy traction free condition

Coordinate Relations and Displacement Field

Consider the multilayer element composed of n perfectly bonded laminae as shown in fig 5.1. To achieve general applicability, an isoparametric finite element formulation is adopted, which interpolates the element coordinates and element displacements through the natural coordinates. For a typical i-th lamina, assuming the displacements u, v, and w to vary linearly through thickness of each lamina, the coordinate relation can be expressed as

$$x = \sum_{j=1}^{m} N_j x_j \tag{5.43}$$

$$y = \sum_{j=1}^{m} N_j y_j \tag{5.44}$$

$$z = \frac{(1-\zeta)}{2} z^i + \frac{(1+\zeta)}{2} z^{i+1} \tag{5.45}$$

where m is the number of nodes at a surface in a multilayer composite element,

The displacement field can be assumed as

$$u^i = \sum_{j=1}^{m} N_j(\xi,\eta)\left[\frac{(1-\zeta)}{2} u_j^i + \frac{(1+\zeta)}{2} u_j^{i+1}\right] \tag{5.46}$$

$$v^i = \sum_{j=1}^{m} N_j(\xi,\eta)\left[\frac{(1-\zeta)}{2} v_j^i + \frac{(1+\zeta)}{2} v_j^{i+1}\right] \tag{5.47}$$

$$w^i = \sum_{j=1}^{m} N_j(\xi,\eta)\left[\frac{(1-\zeta)}{2} w_j^i + \frac{(1+\zeta)}{2} w_j^{i+1}\right] \tag{5.48}$$

where N_j is shape function.

$$N_j = \begin{cases} 0 & \text{at any node except j;} \\ 1 & \text{at the } j\text{-th node.} \end{cases} \tag{5.49}$$

Partial Stress Field and Transformation Matrix

For the i th lamina, the partial stress field given by the iso-function method is

$$\boldsymbol{\sigma}_g^i = \mathbf{P}_g \boldsymbol{\beta}^i \tag{5.50}$$

Transform the partial stress parameter vector $\boldsymbol{\beta}^i$ into the surface parameter vector $\boldsymbol{\varphi}^i$ through a linear transformation

$$\boldsymbol{\beta}^i = \mathbf{U} \boldsymbol{\varphi}^i \tag{5.51}$$

Thus the partial stress field of the i-th lamina in terms of partial stress field surface parameter vector is

$$\boldsymbol{\sigma}_g^i = \tilde{\mathbf{P}}_g \boldsymbol{\varphi}^i \tag{5.52}$$

where

$$\tilde{\mathbf{P}}_g = \mathbf{P}_g \mathbf{U} \tag{5.53}$$

Element Matrices at Lamina Level

After setting up the displacement field and the partial stress field, the element matrices at lamina level are calculated as

$$\mathbf{K}_d^i = \int_{v_j^i} \mathbf{B}_g^T \mathbf{R}_1^i \mathbf{B}_g dv_j^i \tag{5.54}$$

$$\mathbf{H}^i = -\int_{v_j^i} \tilde{\mathbf{P}}_g^T \mathbf{R}_4^i \tilde{\mathbf{P}}_g^i dv_j^i \tag{5.55}$$

$$\mathbf{G}^i = \int_{v_j^i} \tilde{\mathbf{P}}_g^i \left(\mathbf{B}_c + \mathbf{R}_3^i \mathbf{B}_g \right) dv_j^i \tag{5.56}$$

$$\mathbf{f}^i = \int_{v_j^i} \mathbf{N}^T \mathbf{F}^i dv_j^i + \int_{s_{j\sigma}^i} \mathbf{N}^T \mathbf{T}^i ds_j^i. \tag{5.57}$$

Element Matrices at Laminate Level

Assembling all these element matrices of the i-th lamina from 1 to n, and defining

the assembling rule as

$$\boldsymbol{\delta} = \begin{Bmatrix} \mathbf{d}^1 \\ \mathbf{d}^2 \\ \mathbf{d}^3 \\ \vdots \\ \mathbf{d}^{(n+1)} \end{Bmatrix} \tag{5.58}$$

where $\mathbf{d}^k$, is the nodal displacement vector at the k-th surface

$$\mathbf{d}^k = \begin{Bmatrix} u_1^k \\ v_1^k \\ w_1^k \\ u_2^k \\ \vdots \\ u_m^k \\ v_m^k \\ w_m^k \end{Bmatrix} \tag{5.59}$$

in which, $k = 1, 2, \cdots, n+1$, m is number of nodes at a surface in a multilayer composite element, and

$$\boldsymbol{\varphi} = \begin{Bmatrix} \boldsymbol{\alpha}^1 \\ \boldsymbol{\alpha}^2 \\ \boldsymbol{\alpha}^3 \\ \vdots \\ \boldsymbol{\alpha}^{n+1} \end{Bmatrix} \tag{5.60}$$

According these two assembling rules (eq.5.59, 5.60), at the laminate level, we have

$$\mathbf{K}_q = \sum_{i=1}^{n} \mathbf{K}_q^i \tag{5.61}$$

$$\mathbf{H} = \sum_{i=1}^{n} \mathbf{H}^i \tag{5.62}$$

$$\mathbf{G} = \sum_{i=1}^{n} \mathbf{G}^i \tag{5.63}$$

$$\mathbf{f} = \sum_{i=1}^{n} \mathbf{f}^i \tag{5.61}$$

Stiffness Matrix

Before formulating the stiffness matrix of multilayer composite element, some adjustment is needed to satisfying traction free conditions.

At upper surface of laminate, the transverse stresses are

$$\boldsymbol{\sigma}_g{}^n|_{\zeta=1} = \mathbf{A}(\xi,\eta)\alpha^{n+1}. \tag{5.65}$$

At lower surface of laminate, the transverse stresses is

$$\boldsymbol{\sigma}_g{}^1|_{\zeta=-1} = \mathbf{A}(\xi,\eta)\alpha^1 \tag{5.66}$$

Forcing these transverse stresses to satisfy traction free conditions will yield some zero parameters in surface vector α^1 and α^{n+1}. Eliminating these zero surface parameters from $\boldsymbol{\varphi}$, we have a reduced vector $\tilde{\boldsymbol{\varphi}}$ from $\boldsymbol{\varphi}$, and $\widetilde{\mathbf{H}}$, $\widetilde{\mathbf{G}}$ from $\mathbf{H}$, $\mathbf{G}$ respectively.

Thus, the stiffness matrix of multilayer composite element is calculated as

$$\mathbf{K}_m = \mathbf{K}_d + \widetilde{\mathbf{G}}^T\widetilde{\mathbf{H}}^{-1}\widetilde{\mathbf{G}} \tag{5.67}$$

The element equation is

$$\mathbf{K}_m\boldsymbol{\delta} = \mathbf{f} \tag{5.68}$$

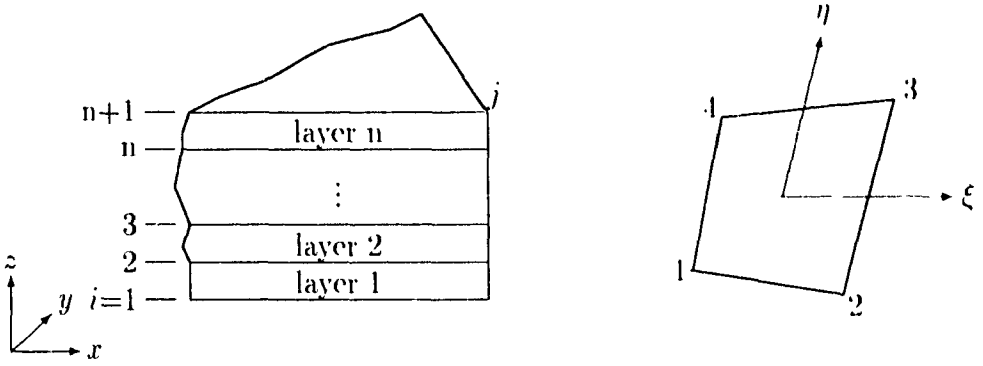

(a) Layer numbering (b) Top view

Figure 5.2: The 4-node, 3-D multilayer composite element

5.3 3-D, 4-Node Multilayer Composite Element

A four-node three dimensional laminate is shown in the fig.5.2.

Coordinate Relations

$$x = \sum_{j=1}^{4} N_j x_j \tag{5.69}$$

$$y = \sum_{j=1}^{4} N_j y_j \tag{5.70}$$

$$z = \frac{(1-\zeta)}{2} z^i + \frac{(1+\zeta)}{2} z^{i+1} \tag{5.71}$$

Displacement Interpolation and Shape Function

$$u^i = \sum_{j=1}^{4} N_j(\xi,\eta) \left[\frac{(1-\zeta)}{2} u_j^i + \frac{(1+\zeta)}{2} u_j^{i+1} \right] \tag{5.72}$$

$$v^i = \sum_{j=1}^{4} N_j(\xi,\eta) \left[\frac{(1-\zeta)}{2} v_j^i + \frac{(1+\zeta)}{2} v_j^{i+1} \right] \tag{5.73}$$

$$w^i = \sum_{j=1}^{4} N_j(\xi,\eta) \left[\frac{(1-\zeta)}{2} w_j^i + \frac{(1+\zeta)}{2} w_j^{i+1} \right] \tag{5.74}$$

where the shape function for four node element is

$$N_j(\xi,\eta)=\frac{1}{4}\left(1+\xi_j\xi\right)\left(1+\eta_j\eta\right), \qquad j=1,2,3,4 \tag{5.75}$$

Partial Stress Field

Actually, every layer element in a 4-node multilayer element is a three dimensional 8-node element, for which the partial stress field for off-axis orthotropic material has already been given by the iso-function method, equation (3.98) repeated here as

$$\boldsymbol{\sigma}_g=\mathbf{P}_g\boldsymbol{\beta} \tag{5.76}$$

where

$$\mathbf{P}_g=\begin{bmatrix} 1 & 0 & 0 & \xi & 0 & 0 & \eta & 0 & 0 & \zeta & 0 & 0 \\ 0 & 1 & 0 & 0 & \xi & 0 & 0 & \eta & 0 & 0 & \zeta & 0 \\ 0 & 0 & 1 & 0 & 0 & \xi & 0 & 0 & \eta & 0 & 0 & \zeta \end{bmatrix}$$

$$\begin{bmatrix} \xi\eta & 0 & 0 & \eta\zeta & 0 & 0 & \xi\zeta & 0 & 0 \\ 0 & \xi\eta & 0 & 0 & \eta\zeta & 0 & 0 & \xi\zeta & 0 \\ 0 & 0 & \xi\eta & 0 & 0 & \eta\zeta & 0 & 0 & \xi\zeta \end{bmatrix} \tag{5.77}$$

and the partial stress field parameter vector $\boldsymbol{\beta}$ is

$$\boldsymbol{\beta}=\begin{Bmatrix} \beta_1 \\ \beta_2 \\ \beta_3 \\ \vdots \\ \beta_{21} \end{Bmatrix} \tag{5.78}$$

So for the $i-th$ layer element, the transverse stresses are

$$\sigma^i_\zeta = \beta^i_1 + \beta^i_4\xi + \beta^i_7\eta + \beta^i_{10}\zeta + \beta^i_{13}\xi\eta + \beta^i_{16}\eta\zeta + \beta^i_{19}\xi\zeta \tag{5.79}$$

$$\sigma^i_{\eta\zeta} = \beta^i_2 + \beta^i_5\xi + \beta^i_8\eta + \beta^i_{11}\zeta + \beta^i_{14}\xi\eta + \beta^i_{17}\eta\zeta + \beta^i_{20}\xi\zeta \tag{5.80}$$

$$\sigma^i_{\xi\zeta} = \beta^i_3 + \beta^i_6\xi + \beta^i_9\eta + \beta^i_{12}\zeta + \beta^i_{15}\xi\eta + \beta^i_{18}\eta\zeta + \beta^i_{21}\xi\zeta \tag{5.81}$$

At the upper surface of the $i-th$ layer element, $\zeta = 1$, the stresses are

$$\sigma^i_\zeta = (\beta^i_1 + \beta^i_{10}) + (\beta^i_4 + \beta^i_{19})\xi + (\beta^i_7 + \beta^i_{16})\eta + \beta^i_{13}\xi\eta \tag{5.82}$$

$$\sigma^i_{\eta\zeta} = (\beta^i_2 + \beta^i_{11}) + (\beta^i_5 + \beta^i_{20})\xi + (\beta^i_8 + \beta^i_{17})\eta + \beta^i_{14}\xi\eta \tag{5.83}$$

$$\sigma^i_{\xi\zeta} = (\beta^i_3 + \beta^i_{12}) + (\beta^i_6 + \beta^i_{21})\xi + (\beta^i_9 + \beta^i_{18})\eta + \beta^i_{15}\xi\eta \tag{5.84}$$

At the lower surfaces of the $i-th$ layer element, $\zeta = -1$, the stresses are

$$\sigma^i_\zeta = (\beta^i_1 - \beta^i_{10}) + (\beta^i_4 - \beta^i_{19})\xi + (\beta^i_7 - \beta^i_{16})\eta + \beta^i_{13}\xi\eta \tag{5.85}$$

$$\sigma^i_{\eta\zeta} = (\beta^i_2 - \beta^i_{11}) + (\beta^i_5 - \beta^i_{20})\xi + (\beta^i_8 - \beta^i_{17})\eta + \beta^i_{14}\xi\eta \tag{5.86}$$

$$\sigma^i_{\xi\zeta} = (\beta^i_3 - \beta^i_{12}) + (\beta^i_6 - \beta^i_{21})\xi + (\beta^i_9 - \beta^i_{18})\eta + \beta^i_{15}\xi\eta \tag{5.87}$$

Traction Free Conditions and Continuous Conditions

The traction free conditions at the top and bottom surface of a laminate are

$$\sigma^n_{\eta\zeta} = \sigma^n_{\xi\zeta} = 0|_{z=h/2} \tag{5.88}$$

$$\sigma^1_{\eta\zeta} = \sigma^1_{\xi\zeta} = \sigma^1_\zeta = 0|_{z=-h/2} \tag{5.89}$$

To satisfy these conditions, we have

$$\beta^n_2 + \beta^n_{11} = 0$$

$$
\begin{aligned}
&\beta_5^n + \beta_{20}^n = 0 \\
&\beta_8^n + \beta_{17}^n = 0 \\
&\beta_{14}^n = 0 \\
&\beta_3^n + \beta_{12}^n = 0 \\
&\beta_6^n + \beta_{21}^n = 0 \\
&\beta_9^n + \beta_{18}^n = 0 \\
&\beta_{15}^n = 0
\end{aligned}
\tag{5.90}
$$

and

$$
\begin{aligned}
&\beta_1^1 - \beta_{10}^1 = 0 \\
&\beta_4^1 - \beta_{19}^1 = 0 \\
&\beta_7^1 - \beta_{16}^1 = 0 \\
&\beta_{13}^1 = 0 \\
&\beta_2^1 - \beta_{11}^1 = 0 \\
&\beta_5^1 - \beta_{20}^1 = 0 \\
&\beta_8^1 - \beta_{17}^1 = 0 \\
&\beta_{14}^1 = 0 \\
&\beta_3^1 - \beta_{12}^1 = 0 \\
&\beta_6^1 - \beta_{21}^1 = 0 \\
&\beta_9^1 - \beta_{18}^1 = 0 \\
&\beta_{15}^1 = 0
\end{aligned}
\tag{5.91}
$$

The continuous conditions at the inter-lamina surfaces are

$$
\boldsymbol{\sigma}_g{}^i|_{\zeta=1} = \boldsymbol{\sigma}_g{}^{i+1}|_{\zeta=-1} \qquad i = 1, 2, \cdots, n-1 \tag{5.92}
$$

Thus, we have

$$
\begin{aligned}
\beta_1^t + \beta_{10}^t &= \beta_1^{t+1} - \beta_{10}^{t+1} \\
\beta_4^t + \beta_{19}^t &= \beta_4^{t+1} - \beta_{19}^{t+1} \\
\beta_7^t + \beta_{16}^t &= \beta_7^{t+1} - \beta_{16}^{t+1} \\
\beta_{13}^t &= \beta_{13}^{t+1} \\
\beta_2^t + \beta_{11}^t &= \beta_2^{t+1} - \beta_{11}^{t+1} \\
\beta_5^t + \beta_{20}^t &= \beta_5^{t+1} - \beta_{20}^{t+1} \\
\beta_8^t + \beta_{17}^t &= \beta_8^{t+1} - \beta_{17}^{t+1} \\
\beta_{14}^t &= \beta_{11}^{t+1} \\
\beta_3^t + \beta_{12}^t &= \beta_3^{t+1} - \beta_{12}^{t+1} \\
\beta_6^t + \beta_{21}^t &= \beta_6^{t+1} - \beta_{21}^{t+1} \\
\beta_9^t + \beta_{18}^t &= \beta_9^{t+1} - \beta_{18}^{t+1} \\
\beta_{15}^t &= \beta_{15}^{t+1}
\end{aligned}
\tag{5.93}
$$

From above equations(eq. 5.90, 5.91 and 5.93), it could be deduced that

$$
\beta_{13}^t = \beta_{14}^t = \beta_{15}^t = 0 \tag{5.94}
$$

Thus, the partial stress field could be simplified as

$$
\boldsymbol{\sigma}_g{}^t = \dot{\mathbf{P}}_g \dot{\boldsymbol{\beta}}^t \tag{5.95}
$$

where the stress function is

$$
\dot{\mathbf{P}}_g = \begin{bmatrix}
1 & 0 & 0 & \xi & 0 & 0 & \eta & 0 & 0 & \zeta & 0 & 0 & \eta\zeta & 0 & 0 & \xi\zeta & 0 & 0 \\
0 & 1 & 0 & 0 & \xi & 0 & 0 & \eta & 0 & 0 & \zeta & 0 & 0 & \eta\zeta & 0 & 0 & \xi\zeta & 0 \\
0 & 0 & 1 & 0 & 0 & \xi & 0 & 0 & \eta & 0 & 0 & \zeta & 0 & 0 & \eta\zeta & 0 & 0 & \xi\zeta
\end{bmatrix} \tag{5.96}
$$

and the new partial stress field parameter vector $\acute{\boldsymbol{\beta}}$ is

$$\acute{\boldsymbol{\beta}}^{i} = \begin{Bmatrix} \acute{\beta}_1^i \\ \acute{\beta}_2^i \\ \vdots \\ \acute{\beta}_{18}^i \end{Bmatrix} \tag{5.97}$$

In order for the element to be traction free on the upper/lower surfaces and continuous at the interlaminar surfaces in a laminate, corresponding to equation 5.93, equation 5.91 and equation 5.90, the parameters of the simplified partial stress field of layer element should satisfy following equations.

$$\begin{aligned}
\acute{\beta}_1^i + \acute{\beta}_{10}^i &= \acute{\beta}_1^{i+1} - \acute{\beta}_{10}^{i+1} \\
\acute{\beta}_4^i + \acute{\beta}_{16}^i &= \acute{\beta}_4^{i+1} - \acute{\beta}_{16}^{i+1} \\
\acute{\beta}_7^i + \acute{\beta}_{13}^i &= \acute{\beta}_7^{i+1} - \acute{\beta}_{13}^{i+1} \\
\acute{\beta}_2^i + \acute{\beta}_{11}^i &= \acute{\beta}_2^{i+1} - \acute{\beta}_{11}^{i+1} \\
\acute{\beta}_5^i + \acute{\beta}_{17}^i &= \acute{\beta}_5^{i+1} - \acute{\beta}_{17}^{i+1} \\
\acute{\beta}_8^i + \acute{\beta}_{14}^i &= \acute{\beta}_8^{i+1} - \acute{\beta}_{14}^{i+1} \\
\acute{\beta}_3^i + \acute{\beta}_{12}^i &= \acute{\beta}_3^{i+1} - \acute{\beta}_{12}^{i+1} \\
\acute{\beta}_6^i + \acute{\beta}_{18}^i &= \acute{\beta}_6^{i+1} - \acute{\beta}_{18}^{i+1} \\
\acute{\beta}_9^i + \acute{\beta}_{15}^i &= \acute{\beta}_9^{i+1} - \acute{\beta}_{15}^{i+1}
\end{aligned} \tag{5.98}$$

where, $i = 2, 3, \cdots, n-1$, and for $i = 1$:

$$\begin{aligned}
\acute{\beta}_1^1 - \acute{\beta}_{10}^1 &= 0 \\
\acute{\beta}_4^1 - \acute{\beta}_{16}^1 &= 0 \\
\acute{\beta}_7^1 - \acute{\beta}_{13}^1 &= 0 \\
\acute{\beta}_2^1 - \acute{\beta}_{11}^1 &= 0 \\
\acute{\beta}_5^1 - \acute{\beta}_{17}^1 &= 0
\end{aligned} \tag{5.99}$$

$$\beta_8^1 - \beta_{14}^1 = 0$$
$$\beta_3^1 - \beta_{12}^1 = 0$$
$$\beta_6^1 - \beta_{18}^1 = 0$$
$$\beta_9^1 - \beta_{15}^1 = 0$$

for $i = r_e$:

$$\begin{aligned}
\beta_2^n + \beta_{11}^n &= 0 \\
\beta_5^n + \beta_{17}^n &= 0 \\
\beta_8^n + \beta_{14}^n &= 0 \\
\beta_3^n + \beta_{12}^n &= 0 \\
\beta_6^n + \beta_{18}^n &= 0 \\
\beta_9^n + \beta_{15}^n &= 0
\end{aligned} \tag{5.100}$$

Now, lets introduce a new vector of parameter $\boldsymbol{\varphi}$,

$$\boldsymbol{\varphi}^i = \left\{ \begin{array}{c} \boldsymbol{\alpha}^i \\ \boldsymbol{\alpha}^{i+1} \end{array} \right\} \tag{5.101}$$

where

$$\boldsymbol{\alpha}^i = \left\{ \begin{array}{c} \alpha_1^i \\ \alpha_2^i \\ \vdots \\ \alpha_9^i \end{array} \right\} \tag{5.102}$$

$$\boldsymbol{\alpha}^{i+1} = \left\{ \begin{array}{c} \alpha_1^{i+1} \\ \alpha_2^{i+1} \\ \vdots \\ \alpha_9^{i+1} \end{array} \right\} \tag{5.103}$$

Assume that $\boldsymbol{\alpha}^i$ is attached in the lower surface of the i-th layer element and $\boldsymbol{\alpha}^{i+1}$ in the upper surface, and defining α_k^i, α_k^{i+1} $(k = 1, 2, \cdots, 9)$ as

$$
\begin{aligned}
\alpha_1^{i+1} &= \beta_1^i + \beta_{10}^i = \beta_1^{i+1} - \beta_{10}^{i+1} \\
\alpha_1^i &= \beta_1^i - \beta_{10}^i = \beta_1^{i-1} + \beta_{10}^{i-1} \\
\alpha_2^{i+1} &= \beta_4^i + \beta_{16}^i = \beta_4^{i+1} - \beta_{16}^{i+1} \\
\alpha_2^i &= \beta_4^i - \beta_{16}^i = \beta_4^{i-1} + \beta_{16}^{i-1} \\
\alpha_3^{i+1} &= \beta_7^i + \beta_{13}^i = \beta_7^{i+1} - \beta_{13}^{i+1} \\
\alpha_3^i &= \beta_7^i - \beta_{13}^i = \beta_7^{i-1} + \beta_{13}^{i-1} \\
\alpha_4^{i+1} &= \beta_2^i + \beta_{11}^i = \beta_2^{i+1} - \beta_{11}^{i+1} \\
\alpha_4^i &= \beta_2^i - \beta_{11}^i = \beta_2^{i-1} + \beta_{11}^{i-1} \\
\alpha_5^{i+1} &= \beta_5^i + \beta_{17}^i = \beta_5^{i+1} - \beta_{17}^{i+1} \\
\alpha_5^i &= \beta_5^i - \beta_{17}^i = \beta_5^{i-1} + \beta_{17}^{i-1} \\
\alpha_6^{i+1} &= \beta_8^i + \beta_{14}^i = \beta_8^{i+1} - \beta_{14}^{i+1} \\
\alpha_6^i &= \beta_8^i - \beta_{14}^i = \beta_8^{i-1} + \beta_{14}^{i-1} \\
\alpha_7^{i+1} &= \beta_3^i + \beta_{12}^i = \beta_3^{i+1} - \beta_{12}^{i+1} \\
\alpha_7^i &= \beta_3^i - \beta_{12}^i = \beta_3^{i-1} + \beta_{12}^{i-1} \\
\alpha_8^{i+1} &= \beta_6^i + \beta_{18}^i = \beta_6^{i+1} - \beta_{18}^{i+1} \\
\alpha_8^i &= \beta_6^i - \beta_{18}^i = \beta_6^{i-1} + \beta_{18}^{i-1} \\
\alpha_9^{i+1} &= \beta_9^i + \beta_{15}^i = \beta_9^{i+1} - \beta_{15}^{i+1} \\
\alpha_9^i &= \beta_9^i - \beta_{15}^i = \beta_9^{i-1} + \beta_{15}^{i-1}
\end{aligned}
\tag{5.104}
$$

So we have

$$
\begin{aligned}
\beta_1^i &= \frac{1}{2}\left(\alpha_1^{i+1} + \alpha_1^i\right) \\
\beta_{10}^i &= \frac{1}{2}\left(\alpha_1^{i+1} - \alpha_1^i\right)
\end{aligned}
$$

$$
\begin{aligned}
\beta_4^{'} &= \frac{1}{2}\left(\alpha_2^{i+1} + \alpha_2^{i}\right) \\
\beta_{16}^{'} &= \frac{1}{2}\left(\alpha_2^{i+1} - \alpha_2^{i}\right) \\
\beta_7^{'} &= \frac{1}{2}\left(\alpha_3^{i+1} + \alpha_3^{i}\right) \\
\beta_{13}^{'} &= \frac{1}{2}\left(\alpha_3^{i+1} - \alpha_3^{i}\right) \\
\beta_2^{'} &= \frac{1}{2}\left(\alpha_4^{i+1} + \alpha_4^{i}\right) \\
\beta_{11}^{'} &= \frac{1}{2}\left(\alpha_4^{i+1} - \alpha_4^{i}\right) \\
\beta_5^{'} &= \frac{1}{2}\left(\alpha_5^{i+1} + \alpha_5^{i}\right) \\
\beta_{17}^{'} &= \frac{1}{2}\left(\alpha_5^{i+1} - \alpha_5^{i}\right) \\
\beta_8^{'} &= \frac{1}{2}\left(\alpha_6^{i+1} + \alpha_6^{i}\right) \\
\beta_{14}^{'} &= \frac{1}{2}\left(\alpha_6^{i+1} - \alpha_6^{i}\right) \\
\beta_3^{'} &= \frac{1}{2}\left(\alpha_7^{i+1} + \alpha_7^{i}\right) \\
\beta_{12}^{'} &= \frac{1}{2}\left(\alpha_7^{i+1} - \alpha_7^{i}\right) \\
\beta_6^{'} &= \frac{1}{2}\left(\alpha_8^{i+1} + \alpha_8^{i}\right) \\
\beta_{18}^{'} &= \frac{1}{2}\left(\alpha_8^{i+1} - \alpha_8^{i}\right) \\
\beta_9^{'} &= \frac{1}{2}\left(\alpha_9^{i+1} + \alpha_9^{i}\right) \\
\beta_{15}^{'} &= \frac{1}{2}\left(\alpha_9^{i+1} - \alpha_9^{i}\right)
\end{aligned}
\tag{5.105}
$$

Above equations give a relation between $\boldsymbol{\beta}^{'}$ and $\boldsymbol{\alpha}$, which in matrix form is

$$
\left\{\boldsymbol{\beta}^{'}\right\} = [\mathbf{U}]\left\{\begin{array}{c} \boldsymbol{\alpha}^{i} \\ \boldsymbol{\alpha}^{i+1} \end{array}\right\} \tag{5.106}
$$

where

$$\mathbf{U}=\frac{1}{2}\begin{bmatrix}
a & 0 & 0 & 0 & 0 & 0 & 0 & 0 & 0 & a & 0 & 0 & 0 & 0 & 0 & 0 & 0 & 0\\
0 & 0 & 0 & a & 0 & 0 & 0 & 0 & 0 & 0 & 0 & 0 & a & 0 & 0 & 0 & 0 & 0\\
0 & 0 & 0 & 0 & 0 & 0 & a & 0 & 0 & 0 & 0 & 0 & 0 & 0 & 0 & a & 0 & 0\\
0 & a & 0 & 0 & 0 & 0 & 0 & 0 & 0 & 0 & a & 0 & 0 & 0 & 0 & 0 & 0 & 0\\
0 & 0 & 0 & 0 & a & 0 & 0 & 0 & 0 & 0 & 0 & 0 & 0 & a & 0 & 0 & 0 & 0\\
0 & 0 & 0 & 0 & 0 & 0 & 0 & a & 0 & 0 & 0 & 0 & 0 & 0 & 0 & 0 & a & 0\\
0 & 0 & a & 0 & 0 & 0 & 0 & 0 & 0 & 0 & 0 & a & 0 & 0 & 0 & 0 & 0 & 0\\
0 & 0 & 0 & 0 & 0 & a & 0 & 0 & 0 & 0 & 0 & 0 & 0 & 0 & a & 0 & 0 & 0\\
0 & 0 & 0 & 0 & 0 & 0 & 0 & 0 & a & 0 & 0 & 0 & 0 & 0 & 0 & 0 & 0 & a\\
b & 0 & 0 & 0 & 0 & 0 & 0 & 0 & 0 & a & 0 & 0 & 0 & 0 & 0 & 0 & 0 & 0\\
0 & 0 & 0 & b & 0 & 0 & 0 & 0 & 0 & 0 & 0 & 0 & a & 0 & 0 & 0 & 0 & 0\\
0 & 0 & 0 & 0 & 0 & 0 & b & 0 & 0 & 0 & 0 & 0 & 0 & 0 & 0 & a & 0 & 0\\
0 & 0 & b & 0 & 0 & 0 & 0 & 0 & 0 & 0 & 0 & a & 0 & 0 & 0 & 0 & 0 & 0\\
0 & 0 & 0 & 0 & 0 & b & 0 & 0 & 0 & 0 & 0 & 0 & 0 & 0 & a & 0 & 0 & 0\\
0 & 0 & 0 & 0 & 0 & 0 & 0 & 0 & b & 0 & 0 & 0 & 0 & 0 & 0 & 0 & 0 & a\\
0 & b & 0 & 0 & 0 & 0 & 0 & 0 & 0 & 0 & a & 0 & 0 & 0 & 0 & 0 & 0 & 0\\
0 & 0 & 0 & 0 & b & 0 & 0 & 0 & 0 & 0 & 0 & 0 & 0 & a & 0 & 0 & 0 & 0\\
0 & 0 & 0 & 0 & 0 & 0 & 0 & b & 0 & 0 & 0 & 0 & 0 & 0 & 0 & 0 & a & 0
\end{bmatrix} \tag{5.107}$$

in which $a=1$, $b=-1$.

Equation 5.106 transfers partial stress parameter $\acute{\boldsymbol{\beta}}^{i}(i=1,2,\cdots,n)$ to $\boldsymbol{\alpha}^{i}(i=1,2,\cdots,n+1)$, which are assumed to exist on the boundaries (interlaminar faces) of layer elements. The new partial stress field which ensure the continuity between layers is

$$\boldsymbol{\sigma}_g{}^{i}=\acute{\mathbf{P}}_g\mathbf{U}\begin{Bmatrix}\boldsymbol{\alpha}^{i}\\ \boldsymbol{\alpha}^{i+1}\end{Bmatrix} \tag{5.108}$$

For convenience, it is rewritten as

$$\boldsymbol{\sigma}_g{}^{i}=\tilde{\mathbf{P}}_g\boldsymbol{\varphi}^{i} \tag{5.109}$$

where

$$\tilde{\mathbf{P}}_g = \acute{\mathbf{P}}_g \mathbf{U} \tag{5.110}$$

$$\boldsymbol{\varphi}^i = \left\{ \begin{array}{c} \boldsymbol{\alpha}^i \\ \boldsymbol{\alpha}^{i+1} \end{array} \right\} \tag{5.111}$$

Thus by taking $\boldsymbol{\varphi}^i$ instead of $\acute{\boldsymbol{\beta}}^i$ as unknown stress parameters, the continuity conditions of transverse stresses are automatically satisfied. This could be proved as follows:

Since the 1-st to 9-th columns of $\acute{\mathbf{P}}_g|_{\zeta=1}\mathbf{U}$ are zero as can be seen by performing the multiplication using equation (5.96) and (5.107),

$$\acute{\mathbf{P}}_g|_{\zeta=1}\mathbf{U} = \begin{bmatrix} 0 & 0 & 0 & 0 & 0 & 0 & 0 & 0 & 0 & 1 & \xi & \eta & 0 & 0 & 0 & 0 & 0 & 0 \\ 0 & 0 & 0 & 0 & 0 & 0 & 0 & 0 & 0 & 0 & 0 & 0 & 1 & \xi & \eta & 0 & 0 & 0 \\ 0 & 0 & 0 & 0 & 0 & 0 & 0 & 0 & 0 & 0 & 0 & 0 & 0 & 0 & 0 & 1 & \xi & \eta \end{bmatrix} \tag{5.112}$$

we have

$$\begin{aligned} \boldsymbol{\sigma}_g{}^i|_{\zeta=1} &= \tilde{\mathbf{P}}_g \boldsymbol{\varphi}^i|_{\zeta=1} \\ &= \acute{\mathbf{P}}_g|_{\zeta=1}\mathbf{U} \left\{ \begin{array}{c} \boldsymbol{\alpha}^i \\ \boldsymbol{\alpha}^{i+1} \end{array} \right\} \\ &= \begin{bmatrix} 1 & \xi & \eta & 0 & 0 & 0 & 0 & 0 & 0 \\ 0 & 0 & 0 & 1 & \xi & \eta & 0 & 0 & 0 \\ 0 & 0 & 0 & 0 & 0 & 0 & 1 & \xi & \eta \end{bmatrix} \left\{ \boldsymbol{\alpha}^{i+1} \right\} \end{aligned} \tag{5.113}$$

and for $\zeta = -1$, the 10-th to 18 th columns of $\dot{\mathbf{P}}_g|_{\zeta=-1}\mathbf{U}$ are zero,

$$\dot{\mathbf{P}}_g|_{\zeta=-1}\mathbf{U} = \begin{bmatrix} 1 & \xi & \eta & 0 & 0 & 0 & 0 & 0 & 0 & 0 & 0 & 0 & 0 & 0 & 0 & 0 & 0 & 0 \\ 0 & 0 & 0 & 1 & \xi & \eta & 0 & 0 & 0 & 0 & 0 & 0 & 0 & 0 & 0 & 0 & 0 & 0 \\ 0 & 0 & 0 & 0 & 0 & 0 & 1 & \xi & \eta & 0 & 0 & 0 & 0 & 0 & 0 & 0 & 0 & 0 \end{bmatrix} \tag{5.114}$$

so we have

$$\begin{aligned} \boldsymbol{\sigma}_g{}^{i+1}|_{\zeta=-1} &= \tilde{\mathbf{P}}_g \boldsymbol{\varphi}^{i+1}|_{\zeta=-1} \\ &= \dot{\mathbf{P}}_g|_{\zeta=-1}\mathbf{U} \begin{Bmatrix} \boldsymbol{\alpha}^{i+1} \\ \boldsymbol{\alpha}^{i+2} \end{Bmatrix} \\ &= \begin{bmatrix} 1 & \xi & \eta & 0 & 0 & 0 & 0 & 0 & 0 \\ 0 & 0 & 0 & 1 & \xi & \eta & 0 & 0 & 0 \\ 0 & 0 & 0 & 0 & 0 & 0 & 1 & \xi & \eta \end{bmatrix} \left\{ \boldsymbol{\alpha}^{i+1} \right\}. \end{aligned} \tag{5.115}$$

Thus

$$\boldsymbol{\sigma}_g{}^{i}|_{\zeta=1} = \boldsymbol{\sigma}_g{}^{i+1}|_{\zeta=-1} \tag{5.116}$$

This completes the proof for transverse stress continuity.

To satisfy surface traction free conditions as defined in equations (5.88) and (5.89),

from equations (5.99), (5.100) and (5.101), we have

$$\boldsymbol{\alpha}^1 = \left\{ \begin{array}{c} \alpha_1^1 \\ \alpha_2^1 \\ \alpha_3^1 \\ \alpha_4^1 \\ \alpha_5^1 \\ \alpha_6^1 \\ \alpha_7^1 \\ \alpha_8^1 \\ \alpha_9^1 \end{array} \right\} = 0 \tag{5.117}$$

and

$$\left\{ \begin{array}{c} \alpha_4^{n+1} \\ \alpha_5^{n+1} \\ \alpha_6^{n+1} \\ \alpha_7^{n+1} \\ \alpha_8^{n+1} \\ \alpha_9^{n+1} \end{array} \right\} = 0 \tag{5.118}$$

Similarly, for on-axis orthotropic material by satisfying the traction free condition (5.88, 5.89) and continuous condition (5.92), we have

$$\dot{\mathbf{P}}_g = \begin{bmatrix} 1 & 0 & 0 & \xi & 0 & \eta & 0 & \zeta & 0 & 0 & \eta\zeta & 0 & \xi\zeta & 0 \\ 0 & 1 & 0 & 0 & \xi & 0 & 0 & 0 & \zeta & 0 & 0 & 0 & 0 & \xi\zeta \\ 0 & 0 & 1 & 0 & 0 & 0 & \eta & 0 & 0 & \zeta & 0 & \eta\zeta & 0 & 0 \end{bmatrix} \tag{5.119}$$

and by introducing a new vector of parameter $\boldsymbol{\varphi}$,

$$\boldsymbol{\varphi}^i = \left\{ \begin{array}{c} \boldsymbol{\alpha}^i \\ \boldsymbol{\alpha}^{i+1} \end{array} \right\} \tag{5.120}$$

in which

$$\boldsymbol{\alpha}^{i} = \begin{Bmatrix} \alpha_1^i \\ \alpha_2^i \\ \vdots \\ \alpha_7^i \end{Bmatrix} \tag{5.121}$$

$$\boldsymbol{\alpha}^{i+1} = \begin{Bmatrix} \alpha_1^{i+1} \\ \alpha_2^{i+1} \\ \vdots \\ \alpha_7^{i+1} \end{Bmatrix} \tag{5.122}$$

we have the partial stress field as

$$\boldsymbol{\sigma}_g{}^{i} = \tilde{\mathbf{P}}_g \boldsymbol{\varphi}^{i} \tag{5.123}$$

where

$$\tilde{\mathbf{P}}_g = \mathbf{P}_g' \mathbf{U} \tag{5.124}$$

$$\mathbf{U} = \frac{1}{2} \begin{bmatrix} 1 & 0 & 0 & 0 & 0 & 0 & 0 & 1 & 0 & 0 & 0 & 0 & 0 & 0 \\ 0 & 0 & 0 & 1 & 0 & 0 & 0 & 0 & 0 & 0 & 1 & 0 & 0 & 0 \\ 0 & 0 & 0 & 0 & 0 & 1 & 0 & 0 & 0 & 0 & 0 & 0 & 1 & 0 \\ 0 & 1 & 0 & 0 & 0 & 0 & 0 & 0 & 1 & 0 & 0 & 0 & 0 & 0 \\ 0 & 0 & 0 & 0 & 1 & 0 & 0 & 0 & 0 & 0 & 0 & 1 & 0 & 0 \\ 0 & 0 & 1 & 0 & 0 & 0 & 0 & 0 & 0 & 1 & 0 & 0 & 0 & 0 \\ 0 & 0 & 0 & 0 & 0 & 0 & 1 & 0 & 0 & 0 & 0 & 0 & 0 & 1 \\ -1 & 0 & 0 & 0 & 0 & 0 & 0 & 1 & 0 & 0 & 0 & 0 & 0 & 0 \\ 0 & 0 & 0 & -1 & 0 & 0 & 0 & 0 & 0 & 0 & 1 & 0 & 0 & 0 \\ 0 & 0 & 0 & 0 & 0 & -1 & 0 & 0 & 0 & 0 & 0 & 0 & 1 & 0 \\ 0 & 0 & -1 & 0 & 0 & 0 & 0 & 0 & 0 & 1 & 0 & 0 & 0 & 0 \\ 0 & 0 & 0 & 0 & 0 & 0 & -1 & 0 & 0 & 0 & 0 & 0 & 0 & 1 \\ 0 & -1 & 0 & 0 & 0 & 0 & 0 & 0 & 1 & 0 & 0 & 0 & 0 & 0 \\ 0 & 0 & 0 & 0 & -1 & 0 & 0 & 0 & 0 & 0 & 0 & 1 & 0 & 0 \end{bmatrix} \tag{5.125}$$

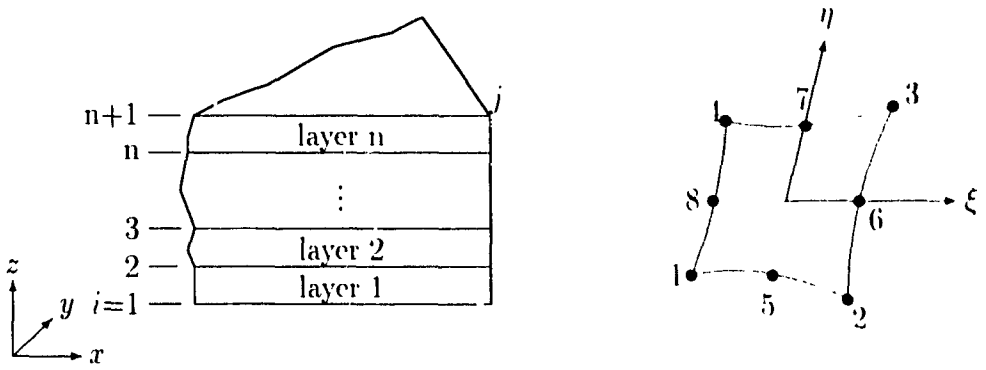

(a) Layer numbering (b) Top view

Figure 5.3: The 8-node, 3-D multilayer composite element

5.4 3-D, 8-node Multilayer Composite Element

The eight-node three dimensional laminate is shown in the figure 5.3.

Coordinate Relations

$$x = \sum_{j=1}^{8} N_j x_j \tag{5.126}$$

$$y = \sum_{j=1}^{8} N_j y_j \tag{5.127}$$

$$z = \frac{(1-\zeta)}{2} z^i + \frac{(1+\zeta)}{2} z^{i+1} \tag{5.128}$$

Displacement Interpolation and Shape Function

$$u^i = \sum_{j=1}^{8} N_j(\xi,\eta) \left[\frac{(1-\zeta)}{2} u_j^i + \frac{(1+\zeta)}{2} u_j^{i+1} \right] \tag{5.129}$$

$$v^i = \sum_{j=1}^{8} N_j(\xi,\eta) \left[\frac{(1-\zeta)}{2} v_j^i + \frac{(1+\zeta)}{2} v_j^{i+1} \right] \tag{5.130}$$

$$w^i = \sum_{j=1}^{8} N_j(\xi,\eta) \left[\frac{(1-\zeta)}{2} w_j^i + \frac{(1+\zeta)}{2} w_j^{i+1} \right] \tag{5.131}$$

where the shape function for the eight node element is

$$N_1(\xi,\eta) = \frac{1}{4}(1-\xi)(1-\eta)(-1-\xi-\eta), \tag{5.132}$$

$$N_2(\xi,\eta) = \frac{1}{4}(1+\xi)(1-\eta)(-1+\xi-\eta), \tag{5.133}$$

$$N_3(\xi,\eta) = \frac{1}{4}(1+\xi)(1+\eta)(-1+\xi+\eta), \tag{5.134}$$

$$N_4(\xi,\eta) = \frac{1}{4}(1-\xi)(1+\eta)(-1-\xi+\eta), \tag{5.135}$$

$$N_5(\xi,\eta) = \frac{1}{2}(1-\xi^2)(1-\eta), \tag{5.136}$$

$$N_6(\xi,\eta) = \frac{1}{2}(1+\xi)(1-\eta^2), \tag{5.137}$$

$$N_7(\xi,\eta) = \frac{1}{2}(1-\xi^2)(1+\eta), \tag{5.138}$$

$$N_8(\xi,\eta) = \frac{1}{2}(1-\xi)(1-\eta^2), \tag{5.139}$$

Partial Stress Field

Actually, every layer element in a 8-node multilayer element is a three dimensional 16-node element, for which the partial stress field for off-axis orthotropic material has already been derived using the iso-function method as shown in equation 3.199 and repeated here as

$$\boldsymbol{\sigma}_g = \mathbf{P}_g\boldsymbol{\beta} \tag{5.140}$$

where

$$\mathbf{P} = \begin{bmatrix} 1 & 0 & 0 & \xi & 0 & 0 & \eta & 0 & 0 & \zeta & 0 & 0 & \xi\eta & 0 & 0 & \xi\zeta & 0 & 0 \\ 0 & 1 & 0 & 0 & \xi & 0 & 0 & \eta & 0 & 0 & \zeta & 0 & 0 & \xi\eta & 0 & 0 & \xi\zeta & 0 \\ 0 & 0 & 1 & 0 & 0 & \xi & 0 & 0 & \eta & 0 & 0 & \zeta & 0 & 0 & \xi\eta & 0 & 0 & \xi\zeta \end{bmatrix}$$

$$\begin{matrix} \eta\zeta & 0 & 0 & \xi\eta\zeta & 0 & 0 & \xi^2 & 0 & 0 & \eta^2 & 0 & 0 & \xi^2\eta & 0 & 0 \\ 0 & \eta\zeta & 0 & 0 & \xi\eta\zeta & 0 & 0 & \xi^2 & 0 & 0 & \eta^2 & 0 & 0 & \xi^2\eta & 0 \\ 0 & 0 & \eta\zeta & 0 & 0 & \xi\eta\zeta & 0 & 0 & \xi^2 & 0 & 0 & \eta^2 & 0 & 0 & \xi^2\eta \end{matrix}$$

$$\begin{bmatrix} \xi^2\zeta & 0 & 0 & \xi\eta^2 & 0 & 0 & \eta^2\zeta & 0 & 0 \\ 0 & \xi^2\zeta & 0 & 0 & \xi\eta^2 & 0 & 0 & \eta^2\zeta & 0 \\ 0 & 0 & \xi^2\zeta & 0 & 0 & \xi\eta^2 & 0 & 0 & \eta^2\zeta \end{bmatrix} \tag{5.141}$$

and the partial stress field parameter vector $\boldsymbol{\beta}$ is

$$\boldsymbol{\beta} = \begin{Bmatrix} \beta_1 \\ \beta_2 \\ \vdots \\ \beta_{42} \end{Bmatrix} \tag{5.142}$$

So for the $i-th$ layer element, the transverse stresses are

$$\begin{aligned} \sigma^i_\zeta &= \beta^i_1 + \beta^i_4\xi + \beta^i_7\eta + \beta^i_{10}\zeta + \beta^i_{13}\xi\eta + \beta^i_{16}\xi\zeta + \beta^i_{19}\eta\zeta + \beta^i_{22}\xi\eta\zeta \\ &\quad + \beta^i_{25}\xi^2 + \beta^i_{28}\eta^2 + \beta^i_{31}\xi^2\eta + \beta^i_{34}\xi^2\zeta + \beta^i_{37}\xi\eta^2 + \beta^i_{40}\eta^2\zeta \qquad (5.143) \\ \sigma^i_{\eta\zeta} &= \beta^i_2 + \beta^i_5\xi + \beta^i_8\eta + \beta^i_{11}\zeta + \beta^i_{14}\xi\eta + \beta^i_{17}\xi\zeta + \beta^i_{20}\eta\zeta + \beta^i_{23}\xi\eta\zeta \\ &\quad + \beta^i_{26}\xi^2 + \beta^i_{29}\eta^2 + \beta^i_{32}\xi^2\eta + \beta^i_{35}\xi^2\zeta + \beta^i_{38}\xi\eta^2 + \beta^i_{41}\eta^2\zeta \qquad (5.144) \\ \sigma^i_{\xi\zeta} &= \beta^i_3 + \beta^i_6\xi + \beta^i_9\eta + \beta^i_{12}\zeta + \beta^i_{15}\xi\eta + \beta^i_{18}\xi\zeta + \beta^i_{21}\eta\zeta + \beta^i_{24}\xi\eta\zeta \\ &\quad + \beta^i_{27}\xi^2 + \beta^i_{30}\eta^2 + \beta^i_{33}\xi^2\eta + \beta^i_{36}\xi^2\zeta + \beta^i_{39}\xi\eta^2 + \beta^i_{42}\eta^2\zeta \qquad (5.145) \end{aligned}$$

At the upper surfaces of the $i-th$ layer element, $\zeta = 1$, the stresses are

$$\begin{aligned} \sigma^i_\zeta &= (\beta^i_1 + \beta^i_{10}) + (\beta^i_4 + \beta^i_{16})\xi + (\beta^i_7 + \beta^i_{19})\eta + (\beta^i_{13} + \beta^i_{22})\xi\eta \\ &\quad + (\beta^i_{25} + \beta^i_{34})\xi^2 + (\beta^i_{28} + \beta^i_{40})\eta^2 + \beta^i_{31}\xi^2\eta + \beta^i_{37}\xi\eta^2 \qquad (5.146) \\ \sigma^i_{\eta\zeta} &= (\beta^i_2 + \beta^i_{11}) + (\beta^i_5 + \beta^i_{17})\xi + (\beta^i_8 + \beta^i_{20})\eta + (\beta^i_{14} + \beta^i_{23})\xi\eta \\ &\quad + (\beta^i_{26} + \beta^i_{35})\xi^2 + (\beta^i_{29} + \beta^i_{41})\eta^2 + \beta^i_{32}\xi^2\eta + \beta^i_{38}\xi\eta^2 \qquad (5.147) \\ \sigma^i_{\xi\zeta} &= (\beta^i_3 + \beta^i_{12}) + (\beta^i_6 + \beta^i_{18})\xi + (\beta^i_9 + \beta^i_{21})\eta + (\beta^i_{15} + \beta^i_{24})\xi\eta \\ &\quad + (\beta^i_{27} + \beta^i_{36})\xi^2 + (\beta^i_{30} + \beta^i_{42})\eta^2 + \beta^i_{33}\xi^2\eta + \beta^i_{39}\xi\eta^2 \qquad (5.148) \end{aligned}$$

At the lower surfaces of the $i-th$ layer element, $\zeta = -1$, the stresses are

$$\begin{aligned}
\sigma^1_\zeta &= (\beta^1_1 - \beta^1_{10}) + (\beta^1_4 - \beta^1_{16})\xi + (\beta^1_7 - \beta^1_{19})\eta + (\beta^1_{13} - \beta^1_{22})\xi\eta \\
&\quad + (\beta^1_{25} - \beta^1_{34})\xi^2 + (\beta^1_{28} - \beta^1_{40})\eta^2 + \beta^1_{31}\xi^2\eta + \beta^1_{37}\xi\eta^2 \qquad (5.149) \\
\sigma^1_{\eta\zeta} &= (\beta^1_2 - \beta^1_{11}) + (\beta^1_5 - \beta^1_{17})\xi + (\beta^1_8 - \beta^1_{20})\eta + (\beta^1_{14} - \beta^1_{23})\xi\eta \\
&\quad + (\beta^1_{26} - \beta^1_{35})\xi^2 + (\beta^1_{29} - \beta^1_{41})\eta^2 + \beta^1_{32}\xi^2\eta + \beta^1_{38}\xi\eta^2 \qquad (5.150) \\
\sigma^1_{\xi\zeta} &= (\beta^1_3 - \beta^1_{12}) + (\beta^1_6 - \beta^1_{18})\xi + (\beta^1_9 - \beta^1_{21})\eta + (\beta^1_{15} - \beta^1_{24})\xi\eta \\
&\quad + (\beta^1_{27} - \beta^1_{36})\xi^2 + (\beta^1_{30} - \beta^1_{42})\eta^2 + \beta^1_{33}\xi^2\eta + \beta^1_{39}\xi\eta^2 \qquad (5.151)
\end{aligned}$$

Traction Free Conditions and Continuous Conditions

The traction free conditions at the top and bottom surface of a laminate are

$$\sigma^n_{\eta\zeta} = \sigma^n_{\xi\zeta} = 0|_{z=h/2} \qquad (5.152)$$

$$\sigma^1_{\eta\zeta} = \sigma^1_{\xi\zeta} = \sigma^1_\zeta = 0|_{z=-h/2} \qquad (5.153)$$

To satisfy these conditions, we have

$$\begin{aligned}
\beta^n_2 + \beta^n_{11} &= 0, & \beta^n_5 + \beta^n_{17} &= 0, \\
\beta^n_8 + \beta^n_{20} &= 0, & \beta^n_{14} + \beta^n_{23} &= 0, \\
\beta^n_{26} + \beta^n_{35} &= 0, & \beta^n_{29} + \beta^n_{41} &= 0, \\
\beta^n_{32} &= 0, & \beta^n_{38} &= 0, \\
\beta^n_3 + \beta^n_{12} &= 0, & \beta^n_6 + \beta^n_{18} &= 0, \qquad (5.154) \\
\beta^n_9 + \beta^n_{21} &= 0, & \beta^n_{15} + \beta^n_{24} &= 0, \\
\beta^n_{27} + \beta^n_{36} &= 0, & \beta^n_{30} + \beta^n_{42} &= 0, \\
\beta^n_{33} &= 0, & \beta^n_{39} &= 0,
\end{aligned}$$

and

$$
\begin{aligned}
\beta_1^1 - \beta_{10}^1 &= 0, & \beta_4^1 - \beta_{16}^1 &= 0,\\
\beta_7^1 - \beta_{19}^1 &= 0, & \beta_{13}^1 - \beta_{22}^1 &= 0,\\
\beta_{25}^1 - \beta_{31}^1 &= 0, & \beta_{28}^1 - \beta_{40}^1 &= 0,\\
\beta_{31}^1 &= 0, & \beta_{37}^1 &= 0,\\
\beta_2^1 - \beta_{11}^1 &= 0, & \beta_5^1 - \beta_{17}^1 &= 0,\\
\beta_8^1 - \beta_{20}^1 &= 0, & \beta_{14}^1 - \beta_{23}^1 &= 0,\\
\beta_{26}^1 - \beta_{35}^1 &= 0, & \beta_{29}^1 - \beta_{41}^1 &= 0,\\
\beta_{32}^1 &= 0, & \beta_{38}^1 &= 0,\\
\beta_3^1 - \beta_{12}^1 &= 0, & \beta_6^1 - \beta_{18}^1 &= 0,\\
\beta_9^1 - \beta_{21}^1 &= 0, & \beta_{15}^1 - \beta_{24}^1 &= 0,\\
\beta_{27}^1 - \beta_{36}^1 &= 0, & \beta_{30}^1 - \beta_{42}^1 &= 0,\\
\beta_{33}^1 &= 0, & \beta_{39}^1 &= 0.
\end{aligned}
\tag{5.155}
$$

The continuous condition between the inter-lamina surfaces is

$$
\boldsymbol{\sigma}_g{}^i|_{\zeta=1} = \boldsymbol{\sigma}_g{}^{i+1}|_{\zeta=-1} \qquad i = 1, 2, \cdots, n-1 \tag{5.156}
$$

Thus, we have

$$
\begin{aligned}
\beta_1^i + \beta_{10}^i &= \beta_1^{i+1} - \beta_{10}^{i+1} & \beta_4^i + \beta_{16}^i &= \beta_4^{i+1} - \beta_{16}^{i+1}\\
\beta_7^i + \beta_{19}^i &= \beta_7^{i+1} - \beta_{19}^{i+1} & \beta_{13}^i + \beta_{22}^i &= \beta_{13}^{i+1} - \beta_{22}^{i+1}\\
\beta_{25}^i + \beta_{34}^i &= \beta_{25}^{i+1} - \beta_{34}^{i+1} & \beta_{28}^i + \beta_{40}^i &= \beta_{28}^{i+1} - \beta_{40}^{i+1}\\
\beta_{31}^i &= \beta_{31}^{i+1} & \beta_{37}^i &= \beta_{37}^{i+1}\\
\beta_2^i + \beta_{11}^i &= \beta_2^{i+1} - \beta_{11}^{i+1} & \beta_5^i + \beta_{17}^i &= \beta_5^{i+1} - \beta_{17}^{i+1}\\
\beta_8^i + \beta_{20}^i &= \beta_8^{i+1} - \beta_{20}^{i+1} & \beta_{14}^i + \beta_{23}^i &= \beta_{14}^{i+1} - \beta_{23}^{i+1}
\end{aligned}
$$

$$\beta^1_{26} + \beta^1_{35} = \beta^{1+1}_{26} - \beta^{1+1}_{35} \qquad \beta^1_{29} + \beta^1_{41} = \beta^{1+1}_{29} - \beta^{1+1}_{41} \tag{5.157}$$

$$\beta^1_{32} = \beta^{1+1}_{32} \qquad \beta^1_{38} = \beta^{1+1}_{38}$$

$$\beta^1_{3} + \beta^1_{12} = \beta^{1+1}_{3} - \beta^{1+1}_{12} \qquad \beta^1_{6} + \beta^1_{18} = \beta^{1+1}_{6} - \beta^{1+1}_{18}$$

$$\beta^1_{9} + \beta^1_{21} = \beta^{1+1}_{9} - \beta^{1+1}_{21} \qquad \beta^1_{15} + \beta^1_{24} = \beta^{1+1}_{15} - \beta^{1+1}_{24}$$

$$\beta^1_{27} + \beta^1_{36} = \beta^{1+1}_{27} - \beta^{1+1}_{36} \qquad \beta^1_{30} + \beta^1_{42} = \beta^{1+1}_{30} - \beta^{1+1}_{42}$$

$$\beta^1_{33} = \beta^{1+1}_{33} \qquad \beta^1_{39} = \beta^{1+1}_{39}$$

From above equations(eq. 5.154, 5.155 and 5.157), it could be deduced that

$$\beta^1_{31} = \beta^1_{32} = \beta^1_{33} = \beta^1_{37} = \beta^1_{38} = \beta^1_{39} = 0 \tag{5.158}$$

Thus, the partial stress field could be simplified as

$$\boldsymbol{\sigma}_g{}^1 = \acute{\mathbf{P}}_g \acute{\boldsymbol{\beta}}^1 \tag{5.159}$$

where the stress function is

$$\acute{\mathbf{P}}_g = \begin{bmatrix}
1 & 0 & 0 & \xi & 0 & 0 & \eta & 0 & 0 & \zeta & 0 & 0 & \xi\eta & 0 & 0 & \xi\zeta & 0 & 0 \\
0 & 1 & 0 & 0 & \xi & 0 & 0 & \eta & 0 & 0 & \zeta & 0 & 0 & \xi\eta & 0 & 0 & \xi\zeta & 0 \\
0 & 0 & 1 & 0 & 0 & \xi & 0 & 0 & \eta & 0 & 0 & \zeta & 0 & 0 & \xi\eta & 0 & 0 & \xi\zeta
\end{bmatrix}$$

$$\begin{bmatrix}
\eta\zeta & 0 & 0 & \xi\eta\zeta & 0 & 0 & \xi^2 & 0 & 0 & \eta^2 & 0 & 0 \\
0 & \eta\zeta & 0 & 0 & \xi\eta\zeta & 0 & 0 & \xi^2 & 0 & 0 & \eta^2 & 0 \\
0 & 0 & \eta\zeta & 0 & 0 & \xi\eta\zeta & 0 & 0 & \xi^2 & 0 & 0 & \eta^2
\end{bmatrix}$$

$$\begin{bmatrix}
\xi^2\zeta & 0 & 0 & \eta^2\zeta & 0 & 0 \\
0 & \xi^2\zeta & 0 & 0 & \eta^2\zeta & 0 \\
0 & 0 & \xi^2\zeta & 0 & 0 & \eta^2\zeta
\end{bmatrix} \tag{5.160}$$

and the new partial stress field parameter vector $\dot{\boldsymbol{\beta}}$ is

$$\dot{\boldsymbol{\beta}}^{i} = \begin{Bmatrix} \dot{\beta}_1^{i} \\ \dot{\beta}_2^{i} \\ \dot{\beta}_3^{i} \\ \vdots \\ \dot{\beta}_{36}^{i} \end{Bmatrix} \tag{5.161}$$

In order to be traction free on the upper/lower surfaces and continuous on the interlaminar surfaces in a laminate, corresponding to eq.5.157, eq.5.155, eq.5.154, the parameters of the simplified partial stress field of layer element should satisfy following equations.

$$\begin{aligned}
\dot{\beta}_1^{i} + \dot{\beta}_{10}^{i} &= \dot{\beta}_1^{i+1} - \dot{\beta}_{10}^{i+1} \\
\dot{\beta}_4^{i} + \dot{\beta}_{16}^{i} &= \dot{\beta}_4^{i+1} - \dot{\beta}_{16}^{i+1} \\
\dot{\beta}_7^{i} + \dot{\beta}_{19}^{i} &= \dot{\beta}_7^{i+1} - \dot{\beta}_{19}^{i+1} \\
\dot{\beta}_{13}^{i} + \dot{\beta}_{22}^{i} &= \dot{\beta}_{13}^{i+1} - \dot{\beta}_{22}^{i+1} \\
\dot{\beta}_{25}^{i} + \dot{\beta}_{31}^{i} &= \dot{\beta}_{25}^{i+1} - \dot{\beta}_{31}^{i+1} \\
\dot{\beta}_{28}^{i} + \dot{\beta}_{34}^{i} &= \dot{\beta}_{28}^{i+1} - \dot{\beta}_{34}^{i+1} \\
\dot{\beta}_2^{i} + \dot{\beta}_{11}^{i} &= \dot{\beta}_2^{i+1} - \dot{\beta}_{11}^{i+1} \\
\dot{\beta}_5^{i} + \dot{\beta}_{17}^{i} &= \dot{\beta}_5^{i+1} - \dot{\beta}_{17}^{i+1} \\
\dot{\beta}_8^{i} + \dot{\beta}_{20}^{i} &= \dot{\beta}_8^{i+1} - \dot{\beta}_{20}^{i+1} \\
\dot{\beta}_{14}^{i} + \dot{\beta}_{23}^{i} &= \dot{\beta}_{14}^{i+1} - \dot{\beta}_{23}^{i+1} \\
\dot{\beta}_{26}^{i} + \dot{\beta}_{32}^{i} &= \dot{\beta}_{26}^{i+1} - \dot{\beta}_{32}^{i+1} \\
\dot{\beta}_{29}^{i} + \dot{\beta}_{35}^{i} &= \dot{\beta}_{29}^{i+1} - \dot{\beta}_{35}^{i+1} \\
\dot{\beta}_3^{i} + \dot{\beta}_{12}^{i} &= \dot{\beta}_3^{i+1} - \dot{\beta}_{12}^{i+1} \\
\dot{\beta}_6^{i} + \dot{\beta}_{18}^{i} &= \dot{\beta}_6^{i+1} - \dot{\beta}_{18}^{i+1} \\
\dot{\beta}_9^{i} + \dot{\beta}_{21}^{i} &= \dot{\beta}_9^{i+1} - \dot{\beta}_{21}^{i+1}
\end{aligned} \tag{5.162}$$

$$\acute{\beta}^i_{15} + \acute{\beta}^i_{24} = \acute{\beta}^{i+1}_{15} - \acute{\beta}^{i+1}_{24}$$
$$\acute{\beta}^i_{27} + \acute{\beta}^i_{33} = \acute{\beta}^{i+1}_{27} - \acute{\beta}^{i+1}_{33}$$
$$\acute{\beta}^i_{30} + \acute{\beta}^i_{36} = \acute{\beta}^{i+1}_{30} - \acute{\beta}^{i+1}_{36}$$

where, $i = 2, 3, \cdots, n-1$.

For $i = 1$:

$$\begin{aligned}
&\acute{\beta}^1_1 - \acute{\beta}^1_{10} = 0 \\
&\acute{\beta}^1_4 - \acute{\beta}^1_{16} = 0 \\
&\acute{\beta}^1_7 - \acute{\beta}^1_{19} = 0 \\
&\acute{\beta}^1_{13} - \acute{\beta}^1_{22} = 0 \\
&\acute{\beta}^1_{25} - \acute{\beta}^1_{31} = 0 \\
&\acute{\beta}^1_{28} - \acute{\beta}^1_{34} = 0 \\
&\acute{\beta}^1_2 - \acute{\beta}^1_{11} = 0 \\
&\acute{\beta}^1_5 - \acute{\beta}^1_{17} = 0 \\
&\acute{\beta}^1_8 - \acute{\beta}^1_{20} = 0 \\
&\acute{\beta}^1_{14} - \acute{\beta}^1_{23} = 0 \\
&\acute{\beta}^1_{26} - \acute{\beta}^1_{32} = 0 \\
&\acute{\beta}^1_{29} - \acute{\beta}^1_{35} = 0 \\
&\acute{\beta}^1_3 - \acute{\beta}^1_{12} = 0 \\
&\acute{\beta}^1_6 - \acute{\beta}^1_{18} = 0 \\
&\acute{\beta}^1_9 - \acute{\beta}^1_{21} = 0 \\
&\acute{\beta}^1_{15} - \acute{\beta}^1_{24} = 0 \\
&\acute{\beta}^1_{27} - \acute{\beta}^1_{33} = 0 \\
&\acute{\beta}^1_{30} - \acute{\beta}^1_{36} = 0
\end{aligned} \tag{5.163}$$

For $i = n$:

$$\begin{aligned}
\beta_2^n + \beta_{11}^n &= 0 \\
\beta_5^n + \beta_{17}^n &= 0 \\
\beta_8^n + \beta_{20}^n &= 0 \\
\beta_{14}^n + \beta_{23}^n &= 0 \\
\beta_{26}^n + \beta_{32}^n &= 0 \\
\beta_{29}^n + \beta_{35}^n &= 0 \\
\beta_3^n + \beta_{12}^n &= 0 \\
\beta_6^n + \beta_{18}^n &= 0 \\
\beta_9^n + \beta_{21}^n &= 0 \\
\beta_{15}^n + \beta_{24}^n &= 0 \\
\beta_{27}^n + \beta_{33}^n &= 0 \\
\beta_{30}^n + \beta_{36}^n &= 0
\end{aligned} \tag{5.161}$$

Now, lets introduce a new vector of parameter φ,

$$\varphi^i = \begin{Bmatrix} \alpha^i \\ \alpha^{i+1} \end{Bmatrix} \tag{5.165}$$

where

$$\alpha^i = \begin{Bmatrix} \alpha_1^i \\ \alpha_2^i \\ \vdots \\ \alpha_{18}^i \end{Bmatrix} \tag{5.166}$$

$$\boldsymbol{\alpha}^{i+1} = \begin{Bmatrix} \alpha_1^{i+1} \\ \alpha_2^{i+1} \\ \vdots \\ \alpha_{18}^{i+1} \end{Bmatrix} \tag{5.167}$$

Assume that $\boldsymbol{\alpha}^i$ is attached in the lower surface of the i-th layer element and $\boldsymbol{\alpha}^{i+1}$ in the upper surface, and define α_1^i, α_1^{i+1} as

$$\alpha_1^{i+1} = \beta_1^i + \beta_{10}^i = \beta_1^{i+1} - \beta_{10}^{i+1} \tag{5.168}$$

$$\alpha_1^i = \beta_1^i - \beta_{10}^i = \beta_1^{i-1} + \beta_{10}^{i-1} \tag{5.169}$$

So we have

$$\beta_1^i = \frac{1}{2}\left(\alpha_1^{i+1} + \alpha_1^i\right) \tag{5.170}$$

$$\beta_{10}^i = \frac{1}{2}\left(\alpha_1^{i+1} - \alpha_1^i\right) \tag{5.171}$$

In the same way, define the rest of α_k^i, α_k^{i+1} $(k = 2, 3, 4, \cdots, 18)$ as

$$\alpha_2^{i+1} = \beta_4^i + \beta_{16}^i = \beta_4^{i+1} - \beta_{16}^{i+1}$$

$$\alpha_2^i = \beta_4^i - \beta_{16}^i = \beta_4^{i-1} + \beta_{16}^{i-1}$$

$$\alpha_3^{i+1} = \beta_7^i + \beta_{19}^i = \beta_7^{i+1} - \beta_{19}^{i+1}$$

$$\alpha_3^i = \beta_7^i - \beta_{19}^i = \beta_7^{i-1} + \beta_{19}^{i-1}$$

$$\alpha_4^{i+1} = \beta_{13}^i + \beta_{22}^i = \beta_{13}^{i+1} - \beta_{22}^{i+1}$$

$$\alpha_4^i = \beta_{13}^i - \beta_{22}^i = \beta_{13}^{i-1} + \beta_{22}^{i-1}$$

$$\alpha_5^{i+1} = \beta_{25}^i + \beta_{31}^i = \beta_{25}^{i+1} - \beta_{31}^{i+1}$$

$$\alpha_5^i = \beta_{25}^i - \beta_{31}^i = \beta_{25}^{i-1} + \beta_{31}^{i-1}$$

$$\alpha_6^{i+1} = \beta_{28}^i + \beta_{34}^i = \beta_{28}^{i+1} - \beta_{34}^{i+1}$$

$$\alpha_6^i = \beta_{28}^i - \beta_{34}^i = \beta_{28}^{i-1} + \beta_{34}^{i-1}$$

$$
\begin{aligned}
\alpha_7^{i+1} &= \beta_2^i + \beta_{11}^i = \beta_2^{i+1} - \beta_{11}^{i+1} \\
\alpha_7^i &= \beta_2^i - \beta_{11}^i = \beta_2^{i-1} + \beta_{11}^{i-1} \\
\alpha_8^{i+1} &= \beta_5^i + \beta_{17}^i = \beta_5^{i+1} - \beta_{17}^{i+1} \\
\alpha_8^i &= \beta_5^i - \beta_{17}^i = \beta_5^{i-1} + \beta_{17}^{i-1} \\
\alpha_9^{i+1} &= \beta_8^i + \beta_{20}^i = \beta_8^{i+1} - \beta_{20}^{i+1} \\
\alpha_9^i &= \beta_8^i - \beta_{20}^i = \beta_8^{i-1} + \beta_{20}^{i-1} \\
\alpha_{10}^{i+1} &= \beta_{14}^i + \beta_{23}^i = \beta_{14}^{i+1} - \beta_{23}^{i+1} \\
\alpha_{10}^i &= \beta_{14}^i - \beta_{23}^i = \beta_{14}^{i-1} + \beta_{23}^{i-1} \\
\alpha_{11}^{i+1} &= \beta_{26}^i + \beta_{32}^i = \beta_{26}^{i+1} - \beta_{32}^{i+1} \\
\alpha_{11}^i &= \beta_{26}^i - \beta_{32}^i = \beta_{26}^{i-1} + \beta_{32}^{i-1} \\
\alpha_{12}^{i+1} &= \beta_{29}^i + \beta_{35}^i = \beta_{29}^{i+1} - \beta_{35}^{i+1} \\
\alpha_{12}^i &= \beta_{29}^i - \beta_{35}^i = \beta_{29}^{i-1} + \beta_{35}^{i-1} \\
\alpha_{13}^{i+1} &= \beta_3^i + \beta_{12}^i = \beta_3^{i+1} - \beta_{12}^{i+1} \\
\alpha_{13}^i &= \beta_3^i - \beta_{12}^i = \beta_3^{i-1} + \beta_{12}^{i-1} \\
\alpha_{14}^{i+1} &= \beta_6^i + \beta_{18}^i = \beta_6^{i+1} - \beta_{18}^{i+1} \\
\alpha_{14}^i &= \beta_6^i - \beta_{18}^i = \beta_6^{i-1} + \beta_{18}^{i-1} \\
\alpha_{15}^{i+1} &= \beta_9^i + \beta_{21}^i = \beta_9^{i+1} - \beta_{21}^{i+1} \\
\alpha_{15}^i &= \beta_9^i - \beta_{21}^i = \beta_9^{i-1} + \beta_{21}^{i-1} \\
\alpha_{16}^{i+1} &= \beta_{15}^i + \beta_{24}^i = \beta_{15}^{i+1} - \beta_{24}^{i+1} \\
\alpha_{16}^i &= \beta_{15}^i - \beta_{24}^i = \beta_{15}^{i-1} + \beta_{24}^{i-1} \\
\alpha_{17}^{i+1} &= \beta_{27}^i + \beta_{33}^i = \beta_{27}^{i+1} - \beta_{33}^{i+1} \\
\alpha_{17}^i &= \beta_{27}^i - \beta_{33}^i = \beta_{27}^{i-1} + \beta_{33}^{i-1} \\
\alpha_{18}^{i+1} &= \beta_{30}^i + \beta_{36}^i = \beta_{30}^{i+1} - \beta_{36}^{i+1} \\
\alpha_{18}^i &= \beta_{30}^i - \beta_{36}^i = \beta_{30}^{i-1} + \beta_{36}^{i-1}
\end{aligned}
\tag{5.172}
$$

we have

$$
\begin{aligned}
\acute{\beta}^i_4 &= \frac{1}{2}\left(\alpha^{i+1}_2 + \alpha^i_2\right), & \acute{\beta}^i_{16} &= \frac{1}{2}\left(\alpha^{i+1}_2 - \alpha^i_2\right),\\
\acute{\beta}^i_7 &= \frac{1}{2}\left(\alpha^{i+1}_3 + \alpha^i_3\right), & \acute{\beta}^i_{19} &= \frac{1}{2}\left(\alpha^{i+1}_3 - \alpha^i_3\right),\\
\acute{\beta}^i_{13} &= \frac{1}{2}\left(\alpha^{i+1}_4 + \alpha^i_4\right), & \acute{\beta}^i_{22} &= \frac{1}{2}\left(\alpha^{i+1}_4 - \alpha^i_4\right),\\
\acute{\beta}^i_{25} &= \frac{1}{2}\left(\alpha^{i+1}_5 + \alpha^i_5\right), & \acute{\beta}^i_{31} &= \frac{1}{2}\left(\alpha^{i+1}_5 - \alpha^i_5\right),\\
\acute{\beta}^i_{28} &= \frac{1}{2}\left(\alpha^{i+1}_6 + \alpha^i_6\right), & \acute{\beta}^i_{34} &= \frac{1}{2}\left(\alpha^{i+1}_6 - \alpha^i_6\right),\\
\acute{\beta}^i_2 &= \frac{1}{2}\left(\alpha^{i+1}_7 + \alpha^i_7\right), & \acute{\beta}^i_{11} &= \frac{1}{2}\left(\alpha^{i+1}_7 - \alpha^i_7\right),\\
\acute{\beta}^i_5 &= \frac{1}{2}\left(\alpha^{i+1}_8 + \alpha^i_8\right), & \acute{\beta}^i_{17} &= \frac{1}{2}\left(\alpha^{i+1}_8 - \alpha^i_8\right),\\
\acute{\beta}^i_8 &= \frac{1}{2}\left(\alpha^{i+1}_9 + \alpha^i_9\right), & \acute{\beta}^i_{20} &= \frac{1}{2}\left(\alpha^{i+1}_9 - \alpha^i_9\right),\\
\acute{\beta}^i_{14} &= \frac{1}{2}\left(\alpha^{i+1}_{10} + \alpha^i_{10}\right), & \acute{\beta}^i_{23} &= \frac{1}{2}\left(\alpha^{i+1}_{10} - \alpha^i_{10}\right),\\
\acute{\beta}^i_{26} &= \frac{1}{2}\left(\alpha^{i+1}_{11} + \alpha^i_{11}\right), & \acute{\beta}^i_{32} &= \frac{1}{2}\left(\alpha^{i+1}_{11} - \alpha^i_{11}\right),\\
\acute{\beta}^i_{29} &= \frac{1}{2}\left(\alpha^{i+1}_{12} + \alpha^i_{12}\right), & \acute{\beta}^i_{35} &= \frac{1}{2}\left(\alpha^{i+1}_{12} - \alpha^i_{12}\right),\\
\acute{\beta}^i_3 &= \frac{1}{2}\left(\alpha^{i+1}_{13} + \alpha^i_{13}\right), & \acute{\beta}^i_{12} &= \frac{1}{2}\left(\alpha^{i+1}_{13} - \alpha^i_{13}\right),\\
\acute{\beta}^i_6 &= \frac{1}{2}\left(\alpha^{i+1}_{14} + \alpha^i_{14}\right), & \acute{\beta}^i_{18} &= \frac{1}{2}\left(\alpha^{i+1}_{14} - \alpha^i_{14}\right),\\
\acute{\beta}^i_9 &= \frac{1}{2}\left(\alpha^{i+1}_{15} + \alpha^i_{15}\right), & \acute{\beta}^i_{21} &= \frac{1}{2}\left(\alpha^{i+1}_{15} - \alpha^i_{15}\right),\\
\acute{\beta}^i_{15} &= \frac{1}{2}\left(\alpha^{i+1}_{16} + \alpha^i_{16}\right), & \acute{\beta}^i_{24} &= \frac{1}{2}\left(\alpha^{i+1}_{16} - \alpha^i_{16}\right).\\
\acute{\beta}^i_{27} &= \frac{1}{2}\left(\alpha^{i+1}_{17} + \alpha^i_{17}\right), & \acute{\beta}_{33} &= \frac{1}{2}\left(\alpha^{i+1}_{17} - \alpha^i_{17}\right).\\
\acute{\beta}^i_{30} &= \frac{1}{2}\left(\alpha^{i+1}_{18} + \alpha^i_{18}\right), & \acute{\beta}^i_{36} &= \frac{1}{2}\left(\alpha^{i+1}_{18} - \alpha^i_{18}\right).
\end{aligned}
\tag{5.173}
$$

Above equations give a relation between $\acute{\boldsymbol{\beta}}^i$ and $\boldsymbol{\alpha}^i$, which in matrix form is

$$
\acute{\boldsymbol{\beta}}^i = \mathbf{U}\left\{\begin{array}{c}\boldsymbol{\alpha}^i\\ \boldsymbol{\alpha}^{i+1}\end{array}\right\} \tag{5.174}
$$

where

$$\mathbf{U} = \frac{1}{2}[u(i,j)] \tag{5.175}$$

in which

$$u(i,j) = 0, \qquad i,j = 1,2,\cdots,36 \tag{5.176}$$

except

$$\begin{array}{llll}
u(1,1)=1, & u(1,19)=1, & u(2,7)=1, & u(2,25)=1, \\
u(3,13)=1 & u(3,31)=1, & u(4,2)=1, & u(4,20)=1, \\
u(5,8)=1, & u(5,26)=1, & u(6,14)=1, & u(6,32)=1, \\
u(7,3)=1, & u(7,21)=1, & u(8,9)=1, & u(8,27)=1, \\
u(9,15)=1, & u(9,33)=1, & u(10,1)=-1, & u(10,19)=1, \\
u(11,7)=-1, & u(11,25)=1, & u(12,13)=-1, & u(12,31)=1, \\
u(13,4)=1, & u(13,22)=1, & u(14,10)=1, & u(14,28)=1, \\
u(15,16)=1, & u(15,34)=1 & u(16,2)=-1, & u(16,20)=1, \\
u(17,8)=-1, & u(17,26)=1, & u(18,14)=-1, & u(18,32)=1, \\
u(19,3)=-1, & u(19,21)=1, & u(20,9)=-1, & u(20,27)=1, \\
u(21,15)=-1, & u(21,33)=1, & u(22,4)=-1, & u(22,22)=1, \\
u(23,10)=-1, & u(23,28)=1, & u(24,16)=-1, & u(24,34)=1, \\
u(25,5)=1, & u(25,23)=1, & u(26,11)=1, & u(26,29)=1, \\
u(27,17)=1, & u(27,35)=1, & u(28,6)=1, & u(28,24)=1, \\
u(29,12)=1, & u(29,30)=1, & u(30,18)=1, & u(30,36)=1, \\
u(31,5)=-1, & u(31,23)=1, & u(32,11)=-1, & u(32,29)=1, \\
u(33,17)=-1, & u(33,35)=1, & u(34,6)=-1, & u(34,24)=1, \\
u(35,12=-1, & u(35,30)=1, & u(36,18)=-1, & u(36,36)=1,
\end{array} \tag{5.177}$$

Equation(5.174) transfers partial stress parameter $\hat{\boldsymbol{\beta}}^{\mathrm{I}}$ $(i = 1,2,\cdots,n)$ to $\boldsymbol{\alpha}^{\mathrm{I}}$ $(i = 1,2,\cdots,n+1)$, which are assumed to exist on the boundaries (interlaminar faces) of layer elements. The new partial stress field which ensure the continuity between

layers is

$$\boldsymbol{\sigma}_g{}^i = \acute{\mathbf{P}}_g \mathbf{U} \left\{ \begin{array}{c} \boldsymbol{\alpha}^i \\ \boldsymbol{\alpha}^{i+1} \end{array} \right\} \tag{5.178}$$

For convenience, it is rewritten as

$$\boldsymbol{\sigma}_g{}^i = \tilde{\mathbf{P}}_g \boldsymbol{\varphi}^i \tag{5.179}$$

where

$$\tilde{\mathbf{P}}_g = \acute{\mathbf{P}}_g \mathbf{U} \tag{5.180}$$

$$\boldsymbol{\varphi}^i = \left\{ \begin{array}{c} \boldsymbol{\alpha}^i \\ \boldsymbol{\alpha}^{i+1} \end{array} \right\} \tag{5.181}$$

Thus by taking $\boldsymbol{\varphi}^i$ instead of $\acute{\boldsymbol{\beta}}^i$ as unknown stress parameters, the continuity conditions of transverse stresses are automatically satisfied. This could be proved as follows:

Since the 1-th to 18-th column of $\acute{\mathbf{P}}_g|_{\zeta=}.\mathbf{U}$ are zero as can be seen by performing the multiplication using equation(5.160) and (5.175),

$$\acute{\mathbf{P}}_g|_{\zeta=1}\mathbf{U} = \left[\begin{array}{cccccccccccccccccc} 0 & 0 & 0 & 0 & 0 & 0 & 0 & 0 & 0 & 0 & 0 & 0 & 0 & 0 & 0 & 0 & 0 & 1 & \xi \\ 0 & 0 & 0 & 0 & 0 & 0 & 0 & 0 & 0 & 0 & 0 & 0 & 0 & 0 & 0 & 0 & 0 & 0 & 0 \\ 0 & 0 & 0 & 0 & 0 & 0 & 0 & 0 & 0 & 0 & 0 & 0 & 0 & 0 & 0 & 0 & 0 & 0 & 0 \end{array} \right.$$

$$\left. \begin{array}{cccccccccccccccccc} \eta & \xi\eta & \xi^2 & \eta^2 & 0 & 0 & 0 & 0 & 0 & 0 & 0 & 0 & 0 & 0 & 0 & 0 \\ 0 & 0 & 0 & 0 & 1 & \xi & \eta & \xi\eta & \xi^2 & \eta^2 & 0 & 0 & 0 & 0 & 0 & 0 \\ 0 & 0 & 0 & 0 & 0 & 0 & 0 & 0 & 0 & 0 & 1 & \xi & \eta & \xi\eta & \xi^2 & \eta^2 \end{array} \right] \tag{5.182}$$

we have

$$\boldsymbol{\sigma}_g{}^{i}|_{\zeta=1} = \tilde{\mathbf{P}}_g \boldsymbol{\varphi}^{i}|_{\zeta=1} = \acute{\mathbf{P}}_g|_{\zeta=1}\mathbf{U}\left\{\begin{array}{c}\boldsymbol{\alpha}^{i}\\ \boldsymbol{\alpha}^{i+1}\end{array}\right\}$$

$$= \begin{bmatrix} 1 & \xi & \eta & \xi\eta & \xi^2 & \eta^2 & 0 & 0 & 0 & 0 & 0 & 0 & 0 & 0 & 0 & 0 & 0 & 0 \\ 0 & 0 & 0 & 0 & 0 & 0 & 1 & \xi & \eta & \xi\eta & \xi^2 & \eta^2 & 0 & 0 & 0 & 0 & 0 & 0 \\ 0 & 0 & 0 & 0 & 0 & 0 & 0 & 0 & 0 & 0 & 0 & 0 & 1 & \xi & \eta & \xi\eta & \xi^2 & \eta^2 \end{bmatrix} \{\boldsymbol{\alpha}^{i+1}\} \tag{5.183}$$

and for $\zeta = -1$, the 19-th to 36-th column of $\acute{\mathbf{P}}_g|_{\zeta=-1}\mathbf{U}$ are zero,

$$\acute{\mathbf{P}}_g|_{\zeta=-1}\mathbf{U} = \begin{bmatrix} 1 & \xi & \eta & \xi\eta & \xi^2 & \eta^2 & 0 & 0 & 0 & 0 & 0 & 0 & 0 & 0 & 0 & 0 \\ 0 & 0 & 0 & 0 & 0 & 0 & 1 & \xi & \eta & \xi\eta & \xi^2 & \eta^2 & 0 & 0 & 0 & 0 \\ 0 & 0 & 0 & 0 & 0 & 0 & 0 & 0 & 0 & 0 & 0 & 0 & 1 & \xi & \eta & \xi\eta \end{bmatrix}$$

$$\begin{bmatrix} 0 & 0 & 0 & 0 & 0 & 0 & 0 & 0 & 0 & 0 & 0 & 0 & 0 & 0 & 0 & 0 & 0 & 0 & 0 & 0 \\ 0 & 0 & 0 & 0 & 0 & 0 & 0 & 0 & 0 & 0 & 0 & 0 & 0 & 0 & 0 & 0 & 0 & 0 & 0 & 0 \\ \xi^2 & \eta^2 & 0 & 0 & 0 & 0 & 0 & 0 & 0 & 0 & 0 & 0 & 0 & 0 & 0 & 0 & 0 & 0 & 0 & 0 \end{bmatrix} \tag{5.184}$$

we have

$$\boldsymbol{\sigma}_g{}^{i+1}|_{\zeta=-1} = \tilde{\mathbf{P}}_g \boldsymbol{\varphi}^{i+1}|_{\zeta=-1} = \acute{\mathbf{P}}_g|_{\zeta=-1}\mathbf{U}\left\{\begin{array}{c}\boldsymbol{\alpha}^{i+1}\\ \boldsymbol{\alpha}^{i+2}\end{array}\right\}$$

$$= \begin{bmatrix} 1 & \xi & \eta & \xi\eta & \xi^2 & \eta^2 & 0 & 0 & 0 & 0 & 0 & 0 & 0 & 0 & 0 & 0 & 0 & 0 \\ 0 & 0 & 0 & 0 & 0 & 0 & 1 & \xi & \eta & \xi\eta & \xi^2 & \eta^2 & 0 & 0 & 0 & 0 & 0 & 0 \\ 0 & 0 & 0 & 0 & 0 & 0 & 0 & 0 & 0 & 0 & 0 & 0 & 1 & \xi & \eta & \xi\eta & \xi^2 & \eta^2 \end{bmatrix} \{\boldsymbol{\alpha}^{i+1}\} \tag{5.185}$$

Thus

$$\boldsymbol{\sigma}_g{}^{1}|_{\zeta=1} = \boldsymbol{\sigma}_g{}^{i+1}|_{\zeta=-1} \tag{5.186}$$

This completes the proof for transverse stress continuity.

To satisfy traction free conditions as defined in equations (5.152) and (5.153), from equation (5.163) and (5.164), we have

$$\boldsymbol{\alpha}^1 = \left\{ \begin{array}{c} \alpha_1^1 \\ \alpha_2^1 \\ \alpha_3^1 \\ \vdots \\ \alpha_{18}^1 \end{array} \right\} = 0 \tag{5.187}$$

and

$$\left\{ \begin{array}{c} \alpha_7^{n+1} \\ \alpha_8^{n+1} \\ \alpha_9^{n+1} \\ \vdots \\ \alpha_{18}^{n+1} \end{array} \right\} = 0 \tag{5.188}$$

Chapter 6

Applications of Multilayer Composite Elements

6.1 Cylindrical Bending of a Simply Supported Long Strip

The laminated strip considered herein is a three-layer symmetric cross-ply laminate(0/90/0) made of unidirectional fibrous composite material(fig.6.1). The laminate is infinitely long in the y direction and simply supported on the ends $x = 0$ and $x = L$ with length to thickness ratio $S = L/h$.

The material stiffness properties are

$$\begin{aligned} E_L &= 174.6GPa, \\ E_T &= 7GPa, \\ G_{LT} &= 3.5GPa, \end{aligned} \tag{6.1}$$

$$G_{TT} = 1.4GPa,$$

$$\nu_{TT} = \nu_{LT} = 0.25.$$

where, L is the direction parallel to the fibers and T the transverse direction. The Possion ratio ν_{LT} measuring strain in the transverse direction under uniaxial normal stress in the L direction.

A sinusoidally distributed transverse loading

$$q = q_0 sin(\pi x/L) \tag{6.2}$$

is applied on the top surface of the laminate as shown in fig.6.1.

The numerical results will be presented in terms of normalized values which are defined as

$$\begin{aligned}
\sigma_x &= \sigma_x(L/2, z)/q_0 \\
\sigma_z &= \sigma_z(L/2, z)/q_0 \\
\sigma_{xz} &= \sigma_{xz}(0, z)/q_0 \\
\bar{u} &= E_T u(0, z)/(h q_0) \\
w &= 100 E_T h^3 w(L/2, z)/(q_0 L^4) \\
z &= z/h
\end{aligned} \tag{6.3}$$

The maximum central transverse deflection w with respect to S is shown in table 6.1, where the surface number indicates the location of each surface of laminate starting from bottom to top of the laminate. Normal displacement $\bar{u}$ and in-plane normal stress σ_x are shown in fig.6.2 and fig.6.4. Through-thickness transverse shear stress σ_{xz} and transverse normal stress σ_z are shown in fig.6.3 and fig.6.5. The $\bar{\sigma}_z$ of CLT is computed by invoking equilibrium considerations. The elasticity exact solutions are evaluated by using the same procedures as given in [8]. The results predicted

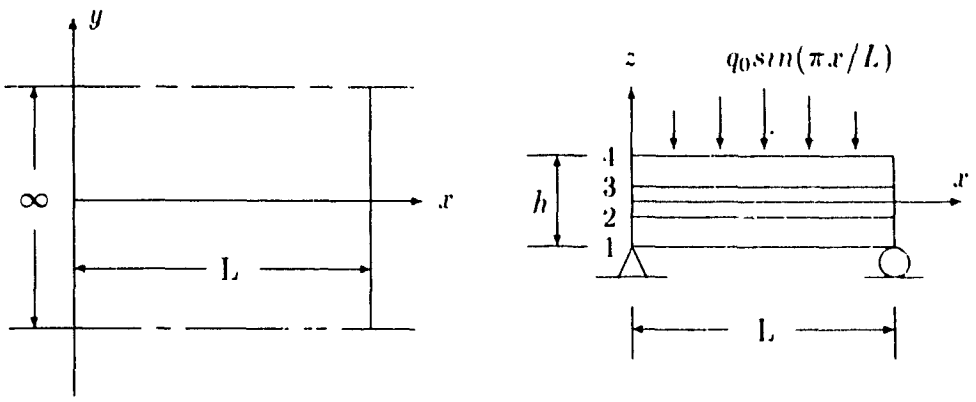

(a) Top view (b) Side view

Figure 6.1: The three layer cross-ply simply supported long strip under sinusoidal loading

by hybrid finite element method with full stress field are from [31]. The table shows that the results based on classical lamination theory, which is independent of the span-to-thickness ratio, are accurate only for the thin plates(i.e. S is larger than 50). Excellent agreement with exact solution is found both for the hybrid element and for present multilayer composite element.

The distribution of stress of the same problem was solved by using conventional 3-D displacement formulated element in [71], which modeled the laminate with 432 three dimensional, 20-node displacement elements. Fig.6.6 compares the shear stress σ_{xz} from the 8-node multilayer composite element and from the displacement elements. It shows the multilayer composite element solution is in better agreement with the exact Pagano's elasticity solution, although the multilayer composite element solution is using fewer elements (5 8-node multilayer composite elements, one in y-direction, 5 in x-direction. Every multilayer element is composed of 12 layer elements).

The CPU time required for the 8-node multilayer composite element solution is 2 min 10.07 s on a VAX 6510 computer compared with 24 minute 2.87 second CPU time for the 432 conventional 20-node finite element solution(15279 Degree

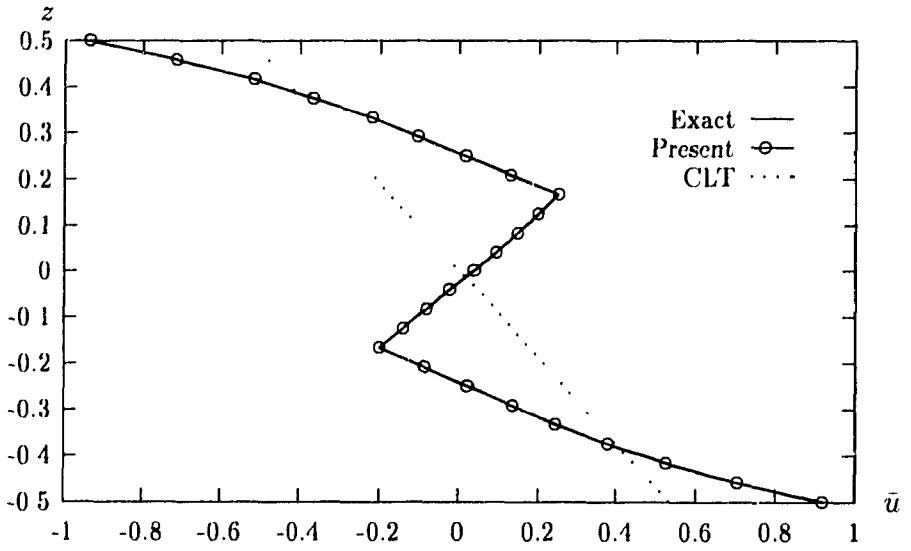

(a) Normal displacement

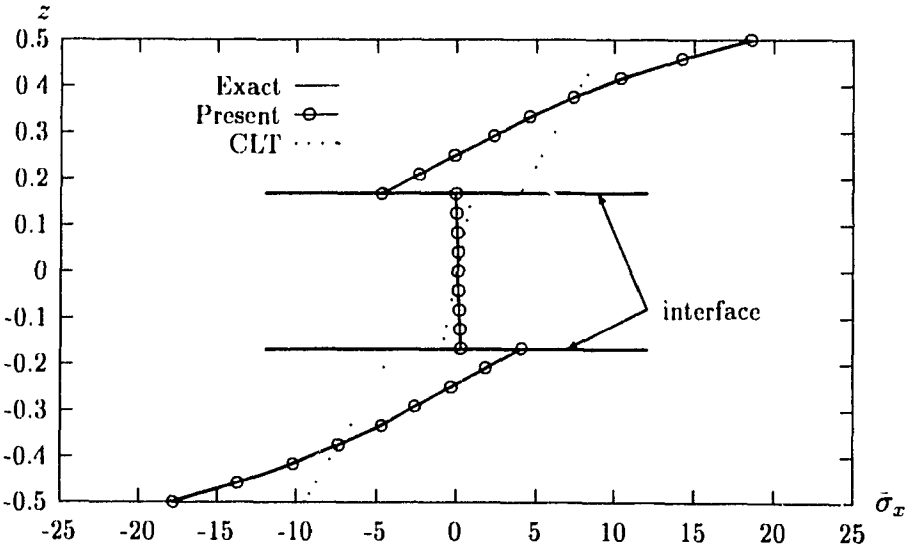

(b) Normal stress

Figure 6.2: Through-thickness in-plane normal displacement and normal stress distributions for S=4

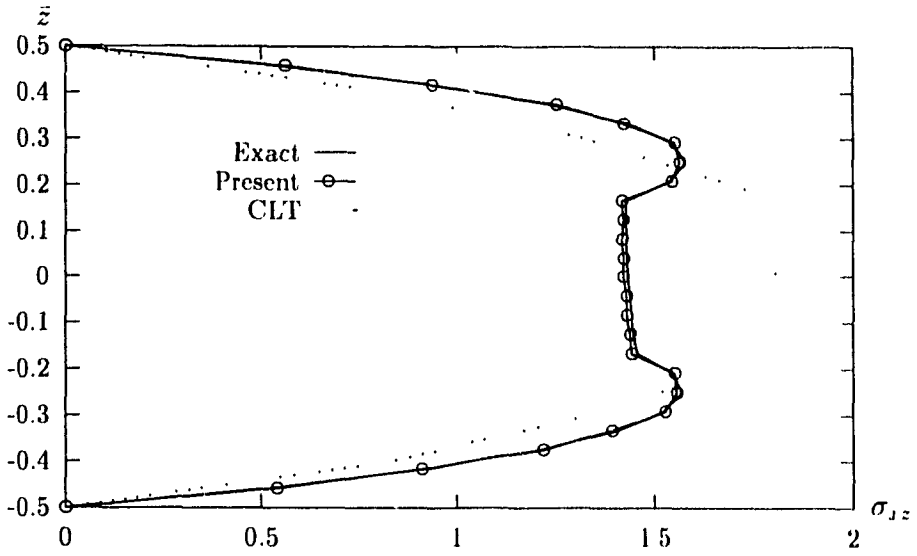

(c) Transverse shear stress

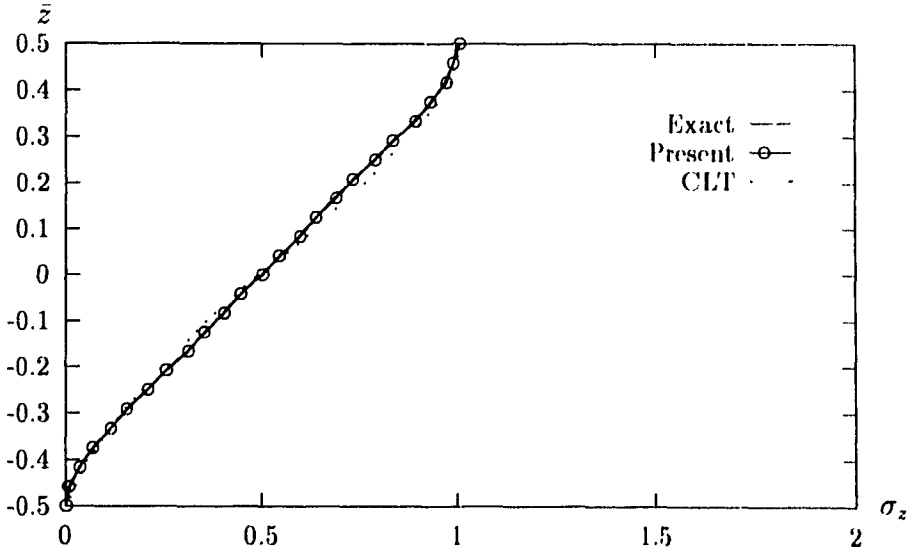

(d) Transverse normal stress

Figure 6.3: Through-thickness Transverse shear stress and normal stress distributions for S=4

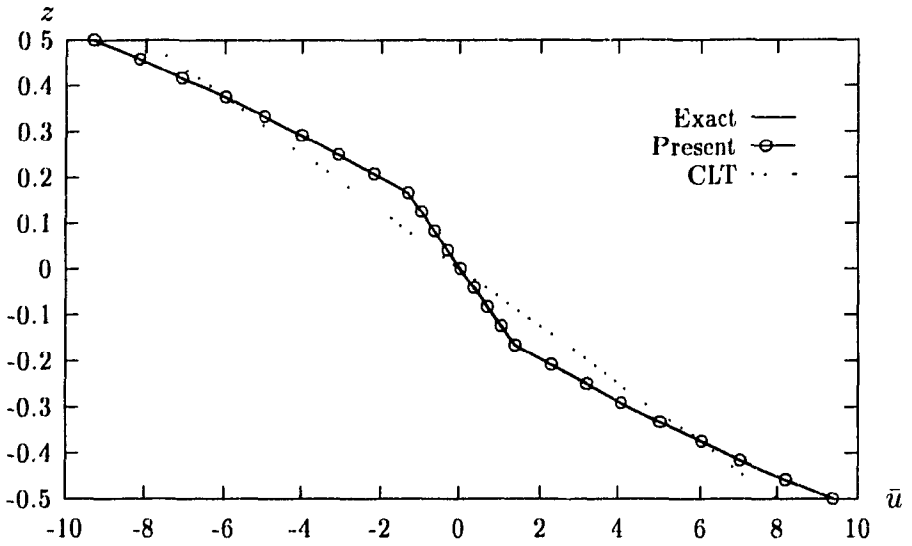

(a) Normal displacement

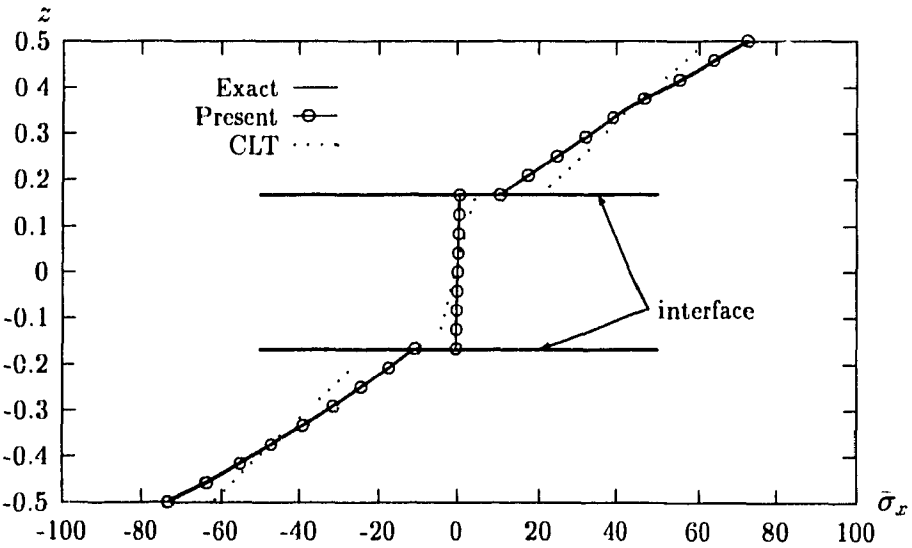

(b) Normal stress

Figure 6.4: Through-thickness in-plane normal displacement and normal stress distributions for S=10

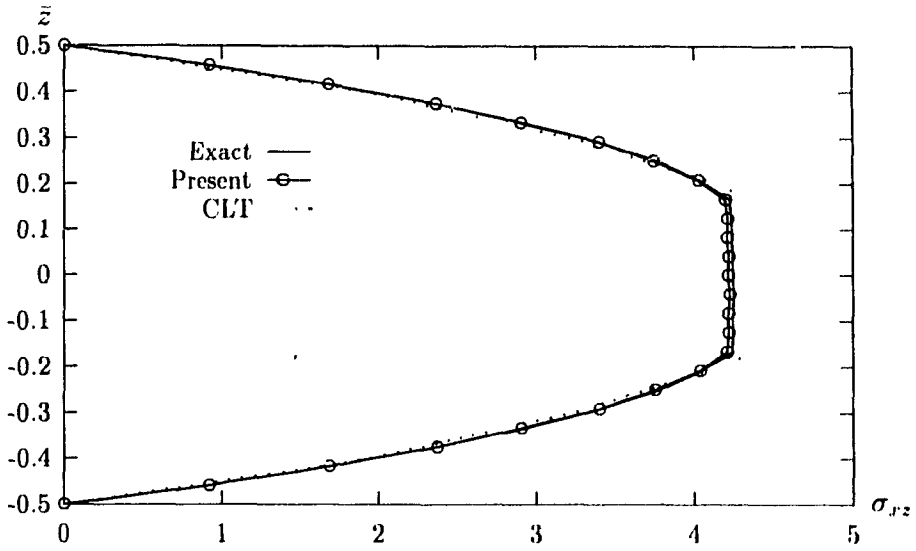

(c) Transverse shear stress

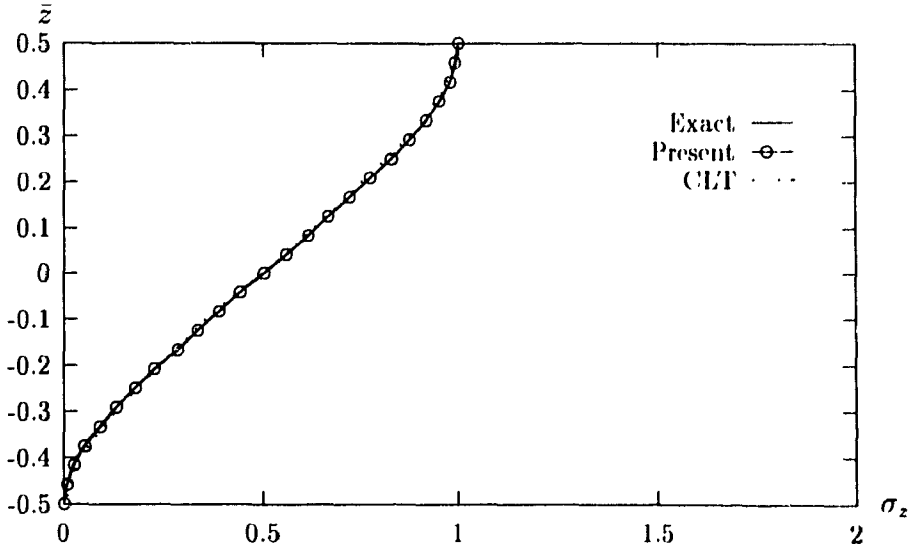

(d) Transverse normal stress

Figure 6.5: Through-thickness transverse shear stress and normal stress distributions for S=10

Table 6.1: Maximum transverse central deflection $\bar{w}$ for different S

S	No.	Exact	Hybrid	Present	CLT
4	4	3.023	3.022	3.029	0.5096
	3	2.925	2.931	2.923	0.5096
	2	2.864	2.868	2.862	0.5096
	1	2.839	2.849	2.838	0.5096
10	4	0.934	0.933	0.933	0.5096
	3	0.933	0.932	0.932	0.5096
	2	0.931	0.931	0.930	0.5096
	1	0.929	0.927	0.929	0.5096
50	4	0.527	0.527	0.527	0.5096
	3	0.527	0.527	0.527	0.5096
	2	0.527	0.527	0.527	0.5096
	1	0.527	0.527	0.527	0.5096

No.: Surface number

Exact: Pagano's elasticity exact solution[8]

Hybrid: Hybrid finite element method[31]

Present: the present Multilayer Composite Element method

CLT: Classical Lamination Theory

Of Freedom). Almost same accurate results have been obtained with 10 4-node multilayer composite element (10 in x-direction, 1 in y-direction, every multilayer element was composed of 12 layer elements, 1452 DOF), which took 2 minute 57.54 second.

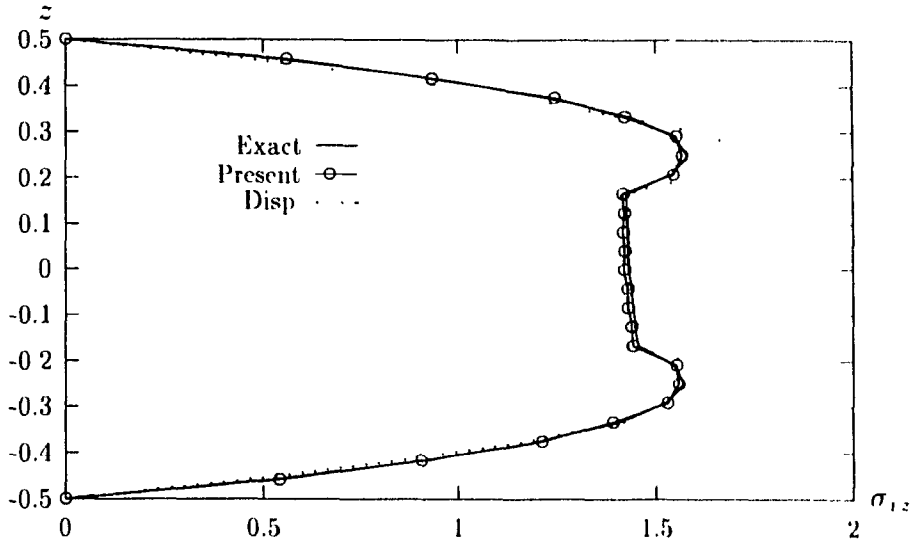

Figure 6.6: Shear stress σ_{xz}, compared with 20-node displacement element (S 1)

6.2 Bending of Simply Supported Rectangular Laminates

The second example analysed with the laminated finite element method is the bending of a simply supported rectangular laminated plate(fig.6.7). This type of problem has been investigated by Pagano[111] with anisotropic elastic theory, by Reddy[112] with higher order shear deformation theory and late by Liou and Sun[31] with hybrid finite element method. To validate the accuracy of the present method, the results are compared with these previous works. The plate is a symmetric three layer cross-ply (0/90/0) laminated plate subjected to sinusoidally distributed loading

$$q(x,y) = q_0 sin(\pi x/a) sin(\pi y/b), \tag{6.4}$$

and lamina material properties are the same as in previous example. The predicted results are presented in Table 6.2 and 6.3, where the elasticity solution[111], higher

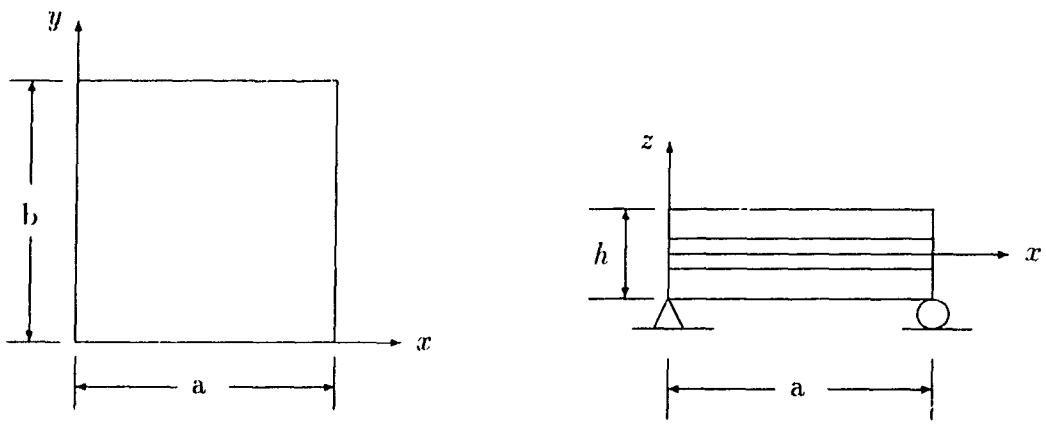

(a) Top view (b) Side view

Figure 6.7: Bending of a simply supported rectangular laminated plate under sinusoidal loading

order shear deformation solution[112], hybrid finite element solution[31] and classic lamination theory solution are also included for comparison. The normalized quantities are expressed as

$$\begin{aligned} (\sigma_x, \sigma_y, \sigma_{xy}) &= (\sigma_x, \sigma_y, \sigma_{xy})/(q_0 S^2) \\ (\sigma_{yz}, \sigma_{xz}) &= (\sigma_{yz}, \sigma_{xz})/(q_0 S) \\ \bar{w} &= 100 E_T w/q_0 h S^4 \\ z &= z/h \\ S &= a/h \end{aligned} \tag{6.5}$$

A quarter of the plate is modeled with a 4 by 4 mesh on the plane of the plate and twelve layer elements through the thickness of the plate. For the case of S=20, b=3a, the aspect ratio of the layer element is as high as 180, and still high accuracy of interlaminar stresses is observed.

Table 6.2 and Table 6.3 show the excellent accuracy of the present laminated finite element. The CLT solution is accurate only for thin plates; the disagreement is

significant when the span-to-thickness ratio S is small.

Table 6.2: Normalized deflection and stresses in a square laminate (b=a)

S	Source	$\bar{\sigma}_x\left(\frac{a}{2},\frac{b}{2},\pm\frac{h}{2}\right)$	$\bar{\sigma}_y\left(\frac{a}{2},\frac{b}{2},\pm\frac{h}{2}\right)$	$\sigma_{xz}\left(0,\frac{b}{2},0\right)$	$\sigma_{yz}\left(\frac{a}{2},0,0\right)$	$w\left(\frac{a}{2},\frac{b}{2},0\right)$
4	Pagano	0.801	0.534	0.256	0.217	
		-0.755	-0.556			
	Hybrid	0.717	0.517	0.263	0.221	2.020
		-0.679	-0.541			
	Reddy	0.7346			0.1832	1.9218
	Present	0.806	0.538	0.262	0.220	2.041
		-0.760	-0.561			
10	Pagano	0.590	0.285	0.357	0.1228	
		-0.590	-0.288			
	Hybrid	0.580	0.285	0.367	0.127	0.7548
		-0.580	-0.289			
	Reddy	0.5684			0.1033	.7125
	Present	0.590	0.283	0.360	0.126	0.7592
		-0.589	-0.287			
20	Pagano	±0.552	±0.210	0.385	0.0938	
	Hybrid	±0.553	±0.210	0.395	0.0998	0.5170
	Present	±0.552	±0.210	0.385	0.0971	0.5167
	CLT	±0.539	±0.180	0.395	0.0823	

Pagano: elasticity exact solution[8].

Hybrid: Hybrid finite element method[31].

Reddy: High order shear deformation theory[112], σ_x is given at $\sigma_x\left(\frac{a}{2},\frac{b}{2},\frac{h}{2}\right)$, and σ_y is given at $\sigma_x\left(\frac{a}{2},\frac{b}{2},\frac{h}{6}\right)$

Present: The current partial stress finite element model.

CLT: classical lamination theory.

Table 6.3: Normalized deflection and stresses in a rectangular laminate (b=3a)

S	Source	$\bar{\sigma}_x\left(\frac{a}{2},\frac{b}{2},\pm\frac{h}{2}\right)$	$\bar{\sigma}_y\left(\frac{a}{2},\frac{b}{2},\pm\frac{h}{2}\right)$	$\bar{\sigma}_{xz}\left(0,\frac{b}{2},0\right)$	$\bar{\sigma}_{yz}\left(\frac{a}{2},0,0\right)$	$\bar{w}\left(\frac{a}{2},\frac{b}{2},0\right)$
4	Pagano	1.14	0.109	0.351	0.0334	2.82
		-1.10	-0.119			
	Hybrid	1.717	0.108	0.360	0.0326	2.828
		-0.975	-0.118			
	Reddy	1.0356	0.1028	0.2724	0.0348	2.6411
	Present	1.13	0.106	0.350	0.0325	2.829
		-1.08	-0.121			
10	Pagano	0.726	0.0418	0.420	0.0152	0.919
		-0.725	-0.0435			
	Hybrid	0.709	0.0429	0.428	0.0151	0.921
		-0.707	-0.0448			
	Reddy	0.6924	0.0398	0.2859	0.0170	0.8622
	Present	0.718	0.0410	0.417	0.0151	0.917
		-0.717	-0.0435			
20	Pagano	0.650	0.0294	0.434	0.0119	0.610
		-0.650	-0.0299			
	Hybrid	0.653	0.0298	0.450	0.0118	0.611
		-0.646	-0.0304			
	Reddy	0.6407	0.0289	0.2880	0.0139	0.5937
	Present	0.647	0.0291	0.431	0.0119	0.607
		-0.647	-0.0298			
	CLT	$\pm$0.623	$\pm$0.0252	0.440	0.0108	0.503

Pagano: elasticity exact solution[8].

Hybrid: Hybrid finite element method[31].

Reddy: High order shear deformation theory[112], $\bar{\sigma}_x$ is given at $\bar{\sigma}_x\left(\frac{a}{2},\frac{b}{2},\frac{h}{2}\right)$, and σ_y is given at $\sigma_x\left(\frac{a}{2},\frac{b}{2},\frac{h}{6}\right)$

Present: The current partial stress finite element model.

CLT: classical lamination theory.

6.3 Analysis of Edge Effects in Angle-Ply Laminates

This section applies the multilayer composite finite element technique to predict free edge effects on interlaminar stresses of a composite laminates under uniaxial extension. The new finite element approach is focused on exact satisfaction of traction free condition at upper/lower surfaces of laminate, continuous condition of three transverse stresses and three in-plane strains, and natural discontinuity condition of three transverse strains and three in-plane stresses at interfaces. Stress distributions of symmetric angle-ply and cross-ply laminates are analysed. Predicted stresses also satisfy the traction-free-condition at free edge.

6.3.1 Introduction

The edge effect on stress distribution has long been of concern in the study of the failure behavior of composite structures. This problem is very difficult to solve for it involves geometric and material discontinuities.

Many numerical analysises have been done on the stress distribution in the vicinity of traction free edges in a laminate subjected to uniform axial strain. In ref.[9], a finite difference scheme was used to analyse the edge effect problem of a $[\pm 45]_s$ laminate. In ref.[23], a three dimensional finite element method was used to analyse the edge effects in $[\pm 45]_s$ and $[90/0]_s$ laminates. In ref.[113, 114], a quasi-three-dimensional finite element analysis was used to analyse the edge effects problem. The methods used in the above analysis can all be classified as displacement formulated method, which can not exactly satisfy interlaminar traction continuity and upper/lower surface traction-free conditions. To satisfy these conditions, a hybrid-stress model is used in many studies [115, 116, 69], which, if the stress field is composed of all six

stress variables as usual, may not satisfy the natural discontinuous condition. There are also works on satisfying traction-free-edge (TFE) condition [113, 117]. Certain similarities are observed in results obtained by all these investigators. However, there are also a number of discrepancies, and it appears no uniformly acceptable solution has yet been found even for this problem.

From previous studies, it is found that there are four conditions of stress distributions should be satisfied in the study of edge effects of composite laminates. These are

1, Traction free condition at upper/lower surfaces of a laminate,

2, Continuous condition of three transverse stresses and three in-plane strains at interfaces,

3, Natural discontinuity condition of three transverse strains and three in-plane stresses at interfaces,

4, zero value of stress σ_y, σ_{xy}, and σ_{yz} at free edges, or so called as traction-free-edge condition.

The multilayer composite finite element technique developed in previous chapters exactly satisfy the first three conditions in advance. Here the new finite element technique is applied for the analysis of the free edge effects of angle-ply composite laminates and cross-ply composite laminates. It is noticed that stress distribution predicted by this finite element technique also satisfy the traction-free-edge condition in both cases.

6.3.2 Edge effects in angle-ply composite laminates

The problem to be analysed is a four layer finite width symmetric angle-ply laminate subject to a prescribed uniform in-plane normal strain ϵ_x (Fig.6.8). The laminate

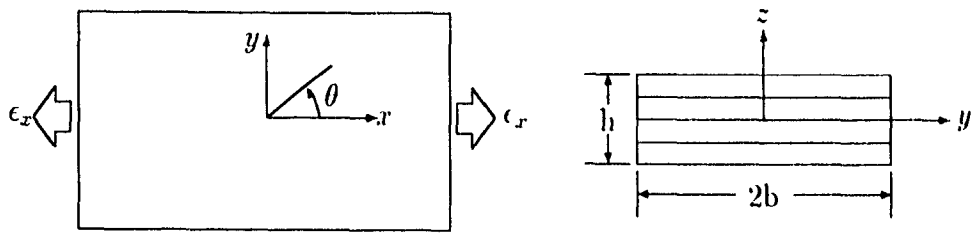

(a) Top view (b) Side view

Figure 6.8: Laminate geometry

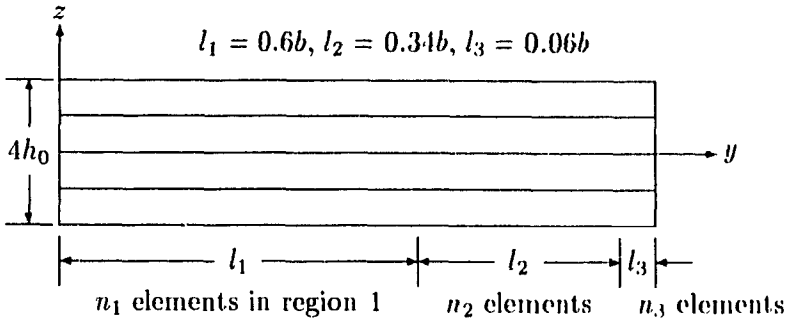

mesh 1: $n_1 = 3, n_2 = 4, n_3 = 2$
mesh 2: $n_1 = 3, n_2 = 6, n_3 = 4$
mesh 3: $n_1 = 3, n_2 = 8, n_3 = 10$

Figure 6.9: Finite element meshes

consists of four identical plies symmetrically stacked in $[45/-45]_s$ sequence. The elastic constants with respect to principal material axes of each ply are

$$\begin{aligned} E_{11} &= 20.0 \times 10^6 \text{psi} \\ E_{22} &= 2.1 \times 10^6 \text{psi} \\ \nu_{12} &= \nu_{31} = \nu_{23} = 0.21 \\ G_{12} &= G_{31} = G_{23} = 0.85 \times 10^6 \text{psi}. \end{aligned} \tag{6.6}$$

The thickness of each ply is denoted by h_0 so that the total thickness of a laminate is $4h_0$, and width is $2b$. The ratio of the width to thickness of a laminate is 4; i.e. $b = 8h_0$. The finite element meshes used for analysis are shown in Fig.6.9.

The results of stress distributions on the mid-plane ($z = 0$) and on the interface ($z = h_0$) are shown in Fig.6.10 and Fig.6.11 respectively. At the mid-plane, the stresses predicted by using three different meshes are the same. At the interface, the stresses from three finite element meshes only show differences in the very vicinity of traction free edge of the laminate. Three in-plane stresses σ_x, σ_y, σ_{xy} show a moderate 'rise' as y/b approaches 1, but decrease to some finite value at y/b=1. The maximum value of σ_x amounts to about 10% over the average σ_x of the laminate and the maximum value of σ_{xy} is about 15% over the average value of σ_{xy} at the interface of $z = h_0$.

At free edge y/b=1, comparing the results predicted with three different meshes, a high stress concentration of transverse shear stress σ_{xz} and a singular behavior of transverse normal stress $\sigma_z$are found. Transverse shear stress σ_{yz} is almost zero along the width of the laminate. It is checked that the self-equilibrium condition,

$$\int_0^b \sigma_z(y, h_0)dy = 0 \tag{6.7}$$

$$\int_0^b \sigma_{yz}(y, h_0)dy = 0 \tag{6.8}$$

are satisfied.

At free edge $y/b = 1$, we have the traction-free-edge conditions as follows,

$$\sigma_y(b, z) = 0 \tag{6.9}$$

$$\sigma_{xy}(b, z) = 0 \tag{6.10}$$

$$\sigma_{yz}(b, z) = 0 \tag{6.11}$$

It is checked that the first and second condition are exactly satisfied. At the corner of interface ($z = h_0$) and free edge, there are two nor zero shear stresses σ_{xy} with same magnitude but opposite direction (see Fig.6.12). Thus the total shear stress σ_{xy} at that point is zero and the third condition is still satisfied with neglecting a very small value at free edge. It is checked that this value converges to zero as fine mesh is used. Through the thickness, the condition

$$\int_{-h/2}^{h/2} \sigma_{xy}(y = b, z)dz = 0 \tag{6.12}$$

is also satisfied.

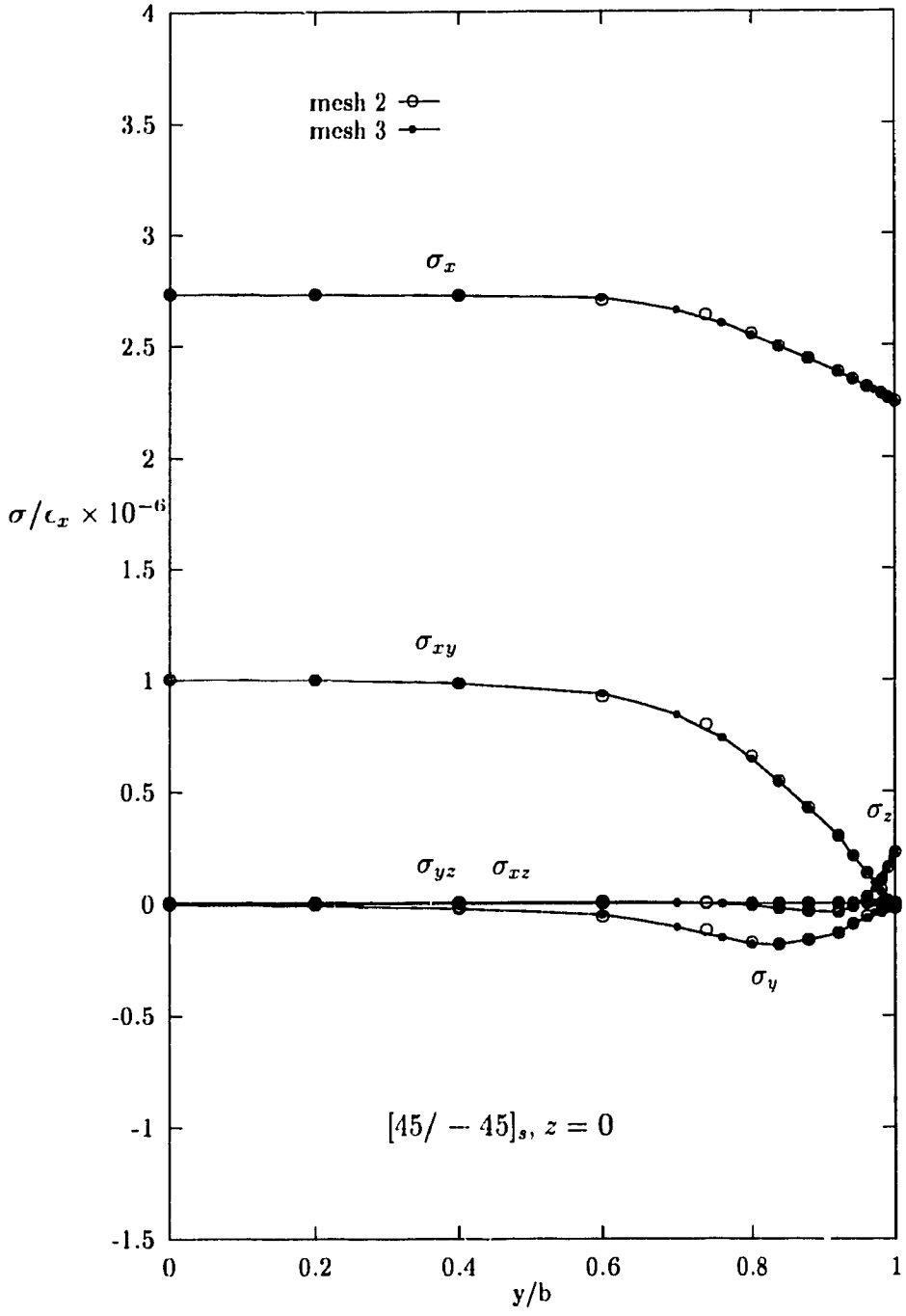

Figure 6.10: Stresses at the midplane $z = 0$

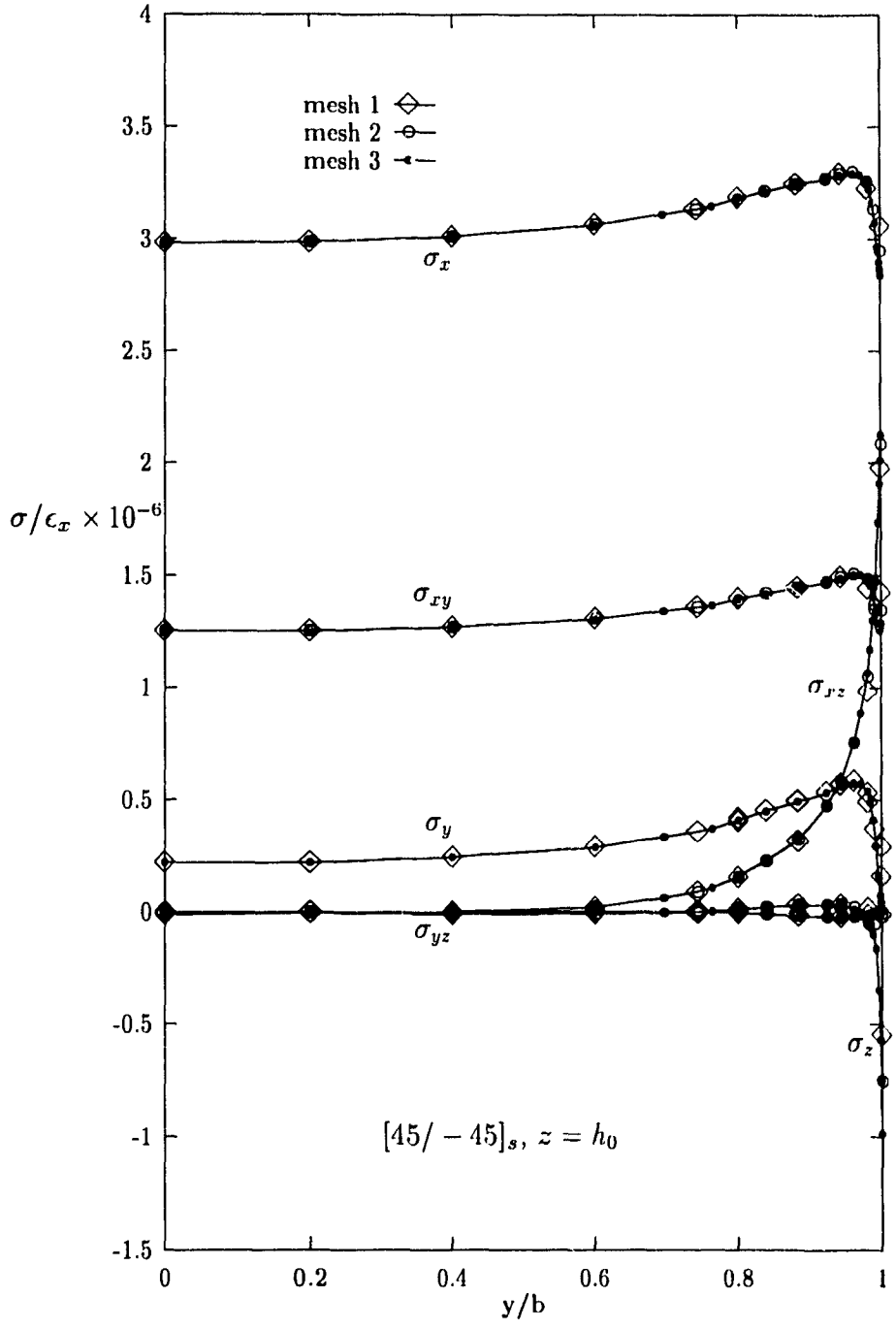

Figure 6.11: Stresses at the interface $z = h_0$

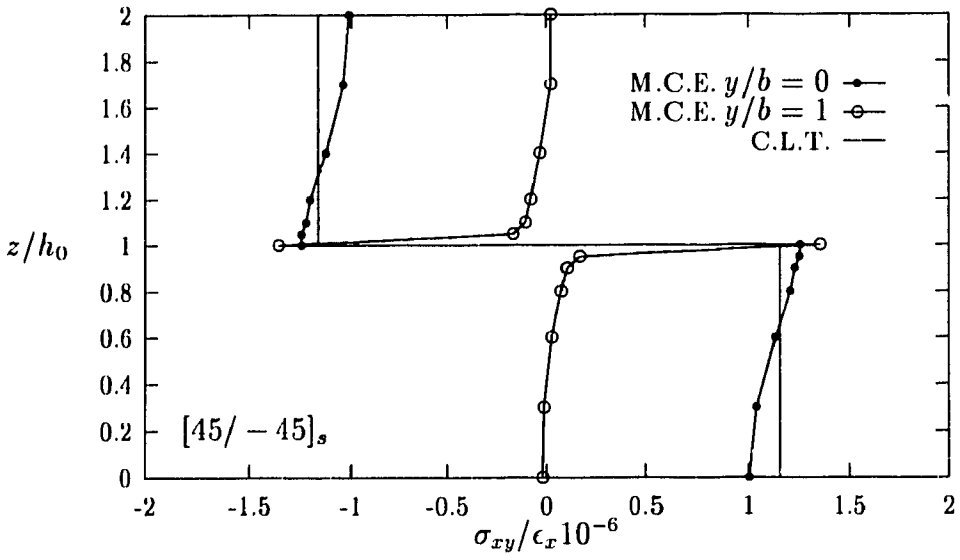

Figure 6.12: Stress σ_{xy} at free edge

6.3.3 Edge effects in cross-ply composite laminates

The problem to be analysed is the same as that given in previous section except that the stacking sequence of four identical plies in this case in $[0/90]_s$ or $[90/0]_s$. The results of stress distribution of σ_z, σ_{yz} and σ_y along interface ($z = h_0$) are shown in Fig.6.13, Fig.6.14 and Fig.6.15 respectively. These three stresses show steep gradients in the vicinity of free edge at interface. Other three stresses are in a normal behavior, that means their values are similar to those predicted with Classical Lamination Theory (σ_{xy}=σ_{xz}=0, σ_x is almost a constant in a ply, see table reftb6.4).

The Fig.6.13 shows that stress σ_z rises sharply towards the free edge in a possible singular behavior for both laminates ($[0/90]_s$ and $[90/0]_s$). In Fig.6.14, the magnitudes of stress σ_{yz} for both laminates also increase towards the free edge, achieve the maximum value at $y/b = 0.988$ and then decrease to zero quickly. Fig.6.15 gives the distribution of in-plane stress σ_y which also rises sharply in the vicinity of free edge for both laminates in a possible singular behavior.

As for the traction-free-edge condition (eq.6.9 to eq.6.11) at free edge $y = b$, it is checked that the eq.6.10 and 6.11 are exactly satisfied. At the corner of interface ($z = h_0$) and free edge, there are two nor zero stresses σ_y with same magnitude

Table 6.4: Normal stress $\sigma_x/\epsilon_x \times 10^6$ (psi) in $[0/90]_s$ laminate

	in the middle (y=0)		at free edge (y=b)	
Ply	0	90	0	90
CLT	20.08	2.09	20.08	2.09
MCE	20 08	2.09	20.10	2.17

Ply: means ply orientation.
CLT: Classical Lamination Theory.
MCE: the present Multilayer Composite finite Element method.

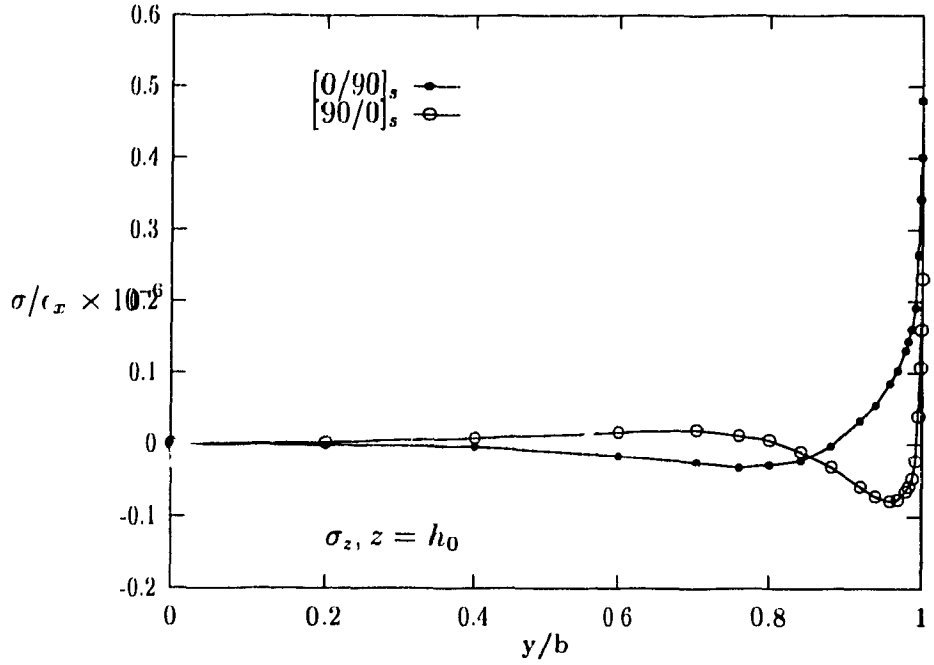

Figure 6.13: Stress σ_z at the interface $z = h_0$

but opposite direction (see Fig.6.16). Thus the total stress σ_y at that point ($y = b$, $z = h_0$) is zero and eq.6.9 is still satisfied with neglecting a very small value at free edge. It is found that, with fine element mesh used, this value converges to zero while the magnitude of two opposite direction σ_y increases. Through the thickness, the condition

$$\int_{-h/2}^{h/2} \sigma_y(y = b, z)dz = 0 \tag{6.13}$$

is also satisfied.

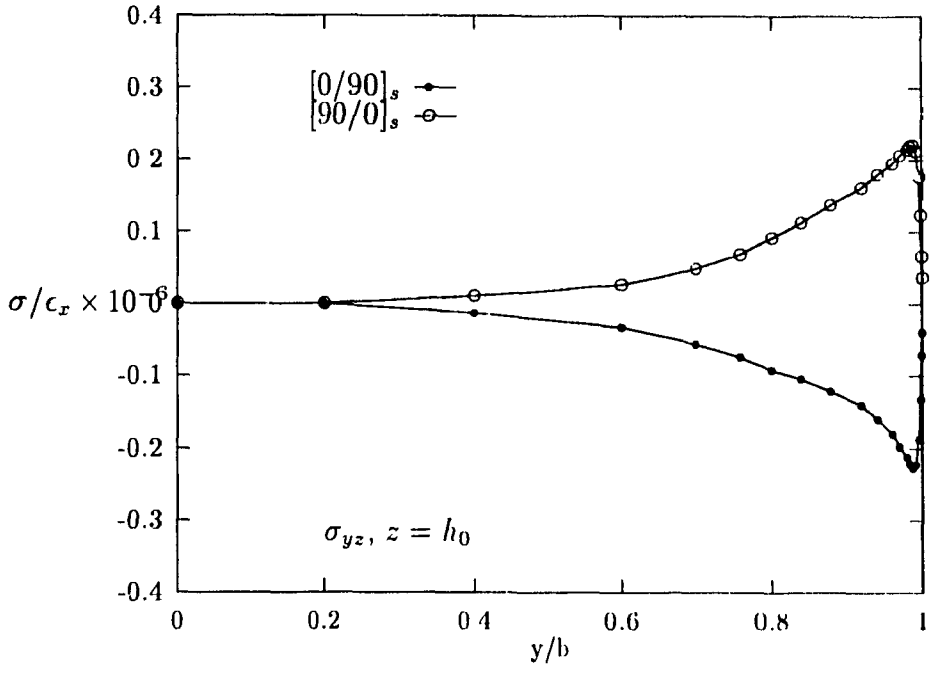

Figure 6.14: Stress σ_{yz} at the interface $z = h_0$

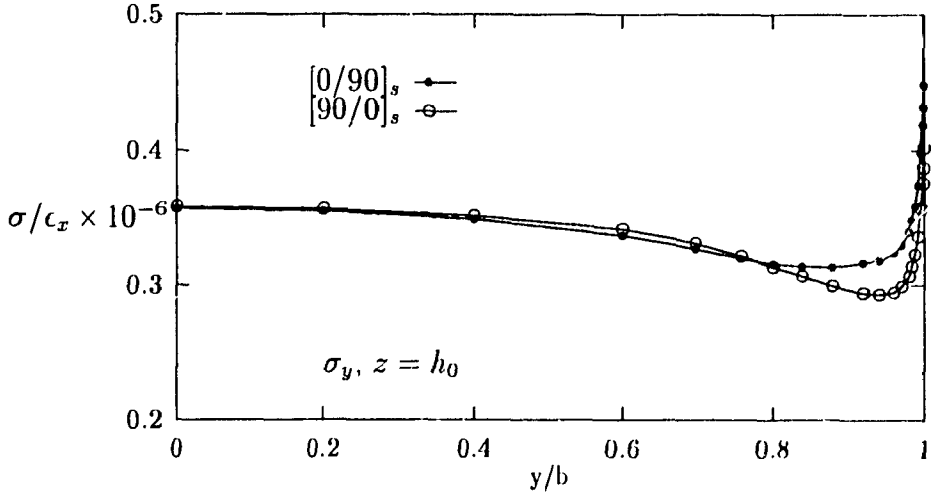

Figure 6.15: Stress σ_y at the interface $z = h_0$

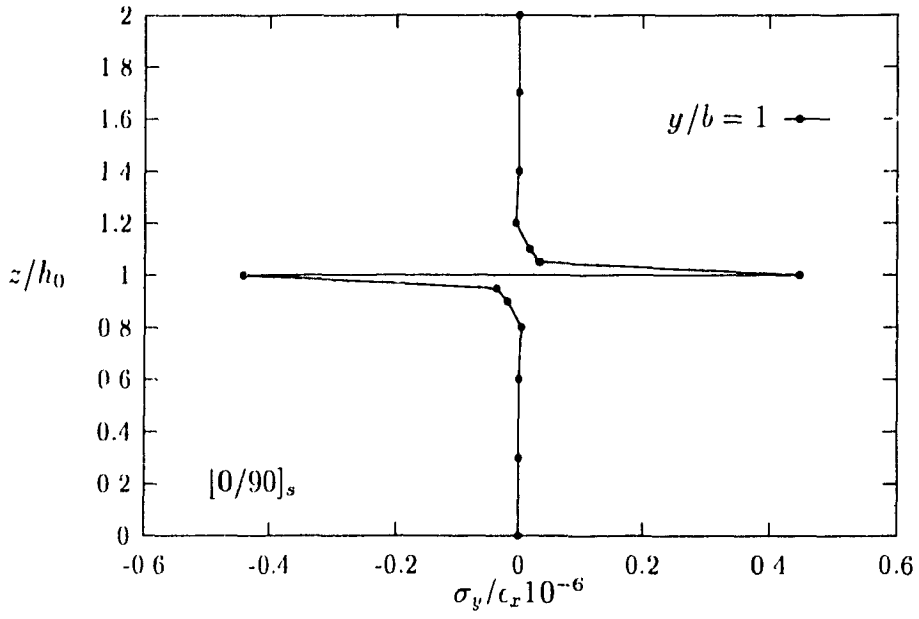

Figure 6.16: Stress σ_y near free edge

6.4 Conclusion

In this chapter, the multilayer composite finite element has been introduced for the stress analysis of laminated composite plates. For any composite laminate, the stress distribution should satisfy the following three conditions: the continuity condition of three transverse stresses and in-plane strains, natural discontinuity condition of three transverse strains and three in-plane stress at interlaminar surfaces and traction free condition at laminate upper/lower surfaces. The multilayer composite finite element technique satisfies all above three conditions exactly in advance.

Interlaminar stresses of three examples have been calculated with the present finite element approach. Results have been compared with available solutions using various analytical methods. Excellent accuracy and fast convergence of the multilayer composite element model have been observed.

As for the free edge problem, there is an extra condition named as traction-free-edge condition, which concern the stress behavior at free edge. The numerical results predicted by the current finite element are also found to satisfy the traction free-edge condition.

For angle-ply laminate, present study shows that interlaminar stresses σ_{xz} and σ_z rise sharply towards the free edge but σ_{xz} shows convergence to a finite value while σ_z seems to be singular at free edge.

For cross-ply laminate, it is found that interlaminar stresses σ_{yz}, σ_z and in-plane stress σ_y also rise sharply towards the free edge but σ_{yz} achieves its maximum value at $y/b = 0.988$ then decreases quickly to zero, while σ_z and σ_y increase in a possible singular behavior at free edge.

Chapter 7

Contribution And Suggestion For Future Work

In this thesis, following have been done:

- A hybrid variational functional of partial stress model have been used and revised for the formulation of composite and multilayer composite finite element for 3-D stress analysis of composite laminates.
- Introduction of the iso-function method to set up the partial stress field. The iso-function scheme gives an easy and simple way to form a stress field and ensures that the stress field is free from zero-energy modes.
- Formulation of 8-nodes, 16-nodes and 20-nodes three dimensional composite finite elements, which consists of two semi-stiffness matrix, one is semi-displacement stiffness matrix, another is semi-hybrid stiffness matrix.
- Introduction of the concept of partial stress surface parameter vector which is associated to the upper and lower surfaces of a layer. The multilayer composite

finite element was formulated.

- Interlaminar stress analysis of two bending examples show the excellent accuracy and high efficiency of the present multilayer composite finite element model.

- The multilayer composite finite element satisfies the continuity condition, natural discontinuity condition and upper/lower surface traction free condition automatically in advance. The stress analysis of straight edge effect problem shows that the results from multilayer composite finite element analysis also satisfy the traction-free-edge condition at free edge.

Following future works are suggested:

- Study the possibility and technique of an-iso-function method for assuming the partial stress field to formulate the multilayer composite element. That is to use less stress parameters to reduce computing time or to use more stress parameters to increase accuracy.

- Develop multilayer composite plate element and multilayer composite shell element for thin laminates.

Bibliography

[1] S. G. Lekhnitskii, *Theory of Elasticity of an Anisotropic Body.* Mir Publishers, English translation from the revised 1977 Russian ed., 1981.

[2] S. W. Tsai and H. T. Hahn, *Introduction to Composite Materials.* Technomic Publishing Co. Inc., 1980.

[3] R. M. Christensen, *Mechanics of Composite Materials.* John Wiley & Sons Inc., 1979.

[4] D. Hull, *An introduction to Composite Materials.* Cambridge University Press, 1981.

[5] S. W. Tsai, *Composite Design.* Thinks Composites, 1988.

[6] O. C. Zienkiewicz, *The Finite Element Method.* McGRAW-HILL Book Company (UK) Limited, 1977.

[7] J. Han and S. V. Hoa, "Three dimensional composite elements for finite element analysis of anisotropic laminated structures," in *Computer Aided Design in Composite Material Technology III* (S. Advani *et al.*, eds.), pp. 255-268, Computational Mechanics Publications, 1992.

[8] N. J. Pagano, "Exact solutions for composite laminates in cylindrical bending," *J. Composite Materials*, vol. 3, p. 398, 1969.

[9] R. B. Pipes and N. J. Pagano, "Interlaminar stresses in composite laminates under uniform axial extension," *J. Compos. Mater.*, vol. 4, pp. 538–548, 1970.

[10] R. B. Pipes, *Solution of certain problems in the theory of elasticity for laminated anisotropic systems.* PhD thesis, Univ. of Texas, Arlington, 1972.

[11] R. B. Pipes and N. J. Pagano, "Interlaminar stresses in composite laminates - an approximate elasticity solution," *J. Appl. Mech. Trans.*, vol. 41, pp. 668–672, 1974.

[12] E. Altus, A. Rotem, and M. Shmueli, "Free edge effect in angle-ply laminates a new three dimensional finite difference solution," *J. Compos. Mater.*, vol. 14, pp. 21–30, 1980.

[13] G. R. Heppler and J. S. Hansen, "High precision singular finite element for fracture analysis of composite structures," *Adv. in Compos. Mater.*, vol. 1, pp. 666–692, 1980

[14] J. J. Engblom and O. O. Ochoa, "Through-the-thickness stress predictions for laminated plate of advanced composite materials," *Int. J. Numer. Meth. Eng.*, vol. 21, pp. 1759–1776, 1980.

[15] B. N. Pandya and T. Kant, "Finite element analysis of laminated composite plates using a high-order displacement model," *Compos. Sci. and Tech.*, vol. 32, no. 2, pp. 137–155, 1988.

[16] J. R. Yeh and I. Tabjbakhsh, "Stress singularity in composite laminates by finite element method," *J. Compos. Mater.*, vol. 20, pp. 347–364, 1986.

[17] R. Natarajan, S. Hoa, and T. Sankar, "Stress analysis of filament wound tanks using three-dimensional finite elements," *Int. J. Numer. Methods Eng.*, vol. 23, pp. 623–633, 1986.

[18] W. Lucking, S. Hoa, and T. Sankar, "Effect of geometry on interlaminar stresses of $[0/90]_s$ composite laminates with circular holes," *J. Compos. Mater.*, vol. 18, pp. 188 198, 1984.

[19] R. Chaudhuri and P. Seide, "Approximate semi-analytical method for perdiction of interlaminar shear stresses in an arbitrarily laminated thick plate," *Comput. and Struct.*, vol. 25, pp. 627 636, 1987.

[20] J. N. Reddy, "A generalization of two-dimensional theories of laminated composite plates," *Communications in Applied Numerical Methods*, vol. 3, pp. 173 180, 1987.

[21] J. N. Reddy, "On the generalization of displacement-based laminate theories," *Applied Mechanics Reviews*, vol. 42, no. 11, pp. S213-S222, 1989. Part 2.

[22] J. Robbins, D. H. and J. N. Reddy, "Modeling of thick composites using a layerwise laminate theory," *Int. J. Numer. Meth. Eng.*, vol. 36, pp. 655 677, 1993.

[23] E. F. Rybicki, "Approximate three-dimensional solutions for symmetric laminates under in-plane loading," *J. Comp. Materials*, vol. 5, pp. 354-360, 1971.

[24] S. T. Mau, P. Tong, and T. H. H. Pian, "Finite element solutions for laminated thick plates," *J. Compos. Mater.*, vol. 6, pp. 304-311, 1972.

[25] T. Nishioka and S. N. Atluri, "Assumed stress finite element analysis of through cracks in angle-ply laminates," *AIAA Journal*, vol. 18, pp. 1125-1132, Sep 1980.

[26] S. S. Wang and F. G. Yuan, "A hybrid finite element approach to composite laminate elasticity problems with singularities," *J. Appl. Mech.*, vol. 50, pp. 835 844, 1983.

[27] S. S. Wang, "Three-dimensional hybrid stress finite element analysis of composite laminates with cracks and cutouts," in *Proceedings of the 5th. Engineer-*

ing Mechanics Division Specialty Conference, Volume 1, (New York), pp. 116 119, ASME, 1984.

[28] S. A. Khalil, C. T. Sun, and W. C. Huang, "Application of a hybrid finite element method to determine stress intensity factors in unidirectional composites," *Int. J. Fract.*, vol. 31, pp. 37 51, 1986.

[29] R. L. Spilker and D. M. Jakobs, "Hybrid stress reduction-mindlin elements for thin multilayer plates," *Int. J. Numer. Methods Eng.*, vol. 23, no. 4, pp. 555 578, 1986.

[30] C. T. Sun and W. J. Liou, "Three dimensional hybrid stress finite element formulation for free vibrations of laminated composite plates," *J. of Sound and Vibr.*, vol. 119, pp. 1 14, Nov 1987.

[31] W. J. Liou and C. T. Sun, "A three dimensional hybrid stress isoparametric element for the analysis of laminated composite plates," *Comput. and Struct.*, vol. 25, pp. 241-249, 1987.

[32] H. Sying and M. L. Liao, "Partial hybrid stress element for the analysis of thick laminated composite plates," *Int. J. Numerical Methods in Engineering*, vol. 28, pp. 2813-2827, 1989.

[33] H. S. Jing and M. L. Liao, "Partial hybrid stress element for transient analysis of thick laminated composite plates," *Int. J. Numerical Methods in Engineering*, vol. 29, pp. 1787 1796, 1990.

[34] M. L. Liao, H. S. Jing, and M. Hwang, "Improvements on the higher order plate element with partial hybrid stress model," *Compu. and Struct.*, vol. 42, no. 1, pp. 45 51, 1992.

[35] K. Moriya, "Laminated plate and shell elements for finite element analysis of advanced fiber reinforced composite structures," *Nippon Kikai Gakkai Ronbunshu a Hen*, vol. 52, pp. 1600 1607, jun 1986.

[36] Y. W. Kwon and J. E. Akin, "Analysis of layered composite plates using a high-order deformation theory," *Comput. and Struct.*, vol. 27, pp. 619-623, 1987.

[37] P. W. Hsu and C. T. Herakovich, "Edge effects in angle-ply composite laminates," *J. Compos. Mater.*, vol. 11, pp. 422-427, 1977.

[38] S. Tang and A. Levy, "Interlaminar stresses of uniformly loaded rectangular composite plates," *J. Compos. Mater.*, vol. 10, pp. 69-78, 1976.

[39] L. Ye and B. X. Yang, "Boundary layer approach to interlaminar stresses in composite laminates with curved edges " *J. of Reinforced Plastics and Composites*, vol. 7, pp. 179 198, mar 1988.

[40] P. Bar-Yoseph and T. H. H. Pian, "Calculation of interlaminar stress concentration in composite laminates," *J. Compos. Mater.*, vol. 15, pp. 225-239, 1981.

[41] P. Bar-Yoseph, "On the accuracy of interlaminar stress calculation in laminated plates," *Compu. Meth in Appl. Mech. and Eng.*, vol. 36, pp. 309-329, 1983.

[42] P. Bar-Yoseph and J. Avrashi, "New variational-asymptotic formulations for interlaminar stress analysis in laminated plates," *ZAMP*, vol. 37, pp. 305-321, May 1986.

[43] N. J. Pagano, "Free-edge stress fields in composite laminates," *Int. J. Solids Structures*, vol. 14, pp. 385 400, 1978.

[44] J. T. S. Wang and J. N. Dickson, "Interlaminar stresses in symmetric composite laminates," *J. Compos. Mater.*, vol. 12, pp. 390-401, 1978.

[45] T. S. Vong, "New variational approach to the delamination problem," *Compos. Struct.*, vol. 5, pp. 245 250, 1986.

[46] S. N. Chatterjee and N. Ramnath, "Modeling laminated composite structures as assemblage of sublaminates," *Int. J. of Solid and Struct.*, vol. 24, pp. 439 458, 1988.

[47] C. Kassapoglou and P. A. Lagace, "Closed form solutions for the interlaminar stress field in angle-ply and cross-ply laminates," *J. Compos. Mater.*, vol. 21, pp. 292-308, 1987.

[48] C. Kassapoglou and P. A. Lagace, "Effecient method for the calculation of interlaminar stresses in composite materials," *J. Appl. Mech.*, vol. 53, pp. 744 750, 1986.

[49] J. M. Whitney and C. E. Browning, "Free-edge delamination of tensile coupons," *J. Compos. Mater.*, vol. 6, pp. 300 303, 1972.

[50] D. G. Berghaus and R. W. Aderholdt, "Photoelastic analysis of interlaminar matrix stresses in fibrous composite models," *Exp. Mech.*, vol. 15, pp. 173 176, 1975.

[51] C. T. Herakovich, D. Post, M. B. Buczek, and R. Czarnek, "Free edge strain concentrations in real composite laminates, experimental theoretical correlation." ASME (paper) Publ. by ASME, (85-WA/APH-10, 7p), New York, 1985.

[52] R. L. Spilker and S. C. Chou, "Edge effects in symmetric composite laminates: importance of satisfying the traction-free-edge condition," *J. Compos. Mater.*, vol. 14, pp. 2–20, 1980.

[53] E. Reissner, "On a certain mixed variational theorem and a proposed application," *Int. J. Num. Meth. Eng.*, pp. 1466 1368, 1984.

[54] E. Reissner, "On a mixed variational theorem and on shear deformable plate theory," *Int. J. Num. Meth. Eng.*, vol. 23, pp. 193 198, 1986.

[55] Q. Huang, "Variational principle of hybrid energy and the fundamentals of 3-d laminate theory a new approach for the analysis of interlaminar stresses in composite materials," in *International Conference of Computation Mechanics*, (Beijing, China), jun 1987.

[56] Q. Huang, *Three Dimensional Composite Finite Element for Stress Analysis of Anisotropic Laminate Structures.* PhD thesis, Mechanical Engineering Dept., Concordia Univ., Montreal, Canada, Feb 1989.

[57] R. L. Spilker, "Hybrid-stress eight-node elements for thin and thick multilayer laminated plates," *Int. J. Numer. Meth. Eng.*, vol. 18, pp. 801–828, 1982.

[58] T. H. H. Pian and P. Tong, "Basis of finite element method for solid continua," *Int. J. Numer. Meth. Eng.*, pp. 3–28, 1969.

[59] R. Rubinstein, E. F. Punch, and S. Atluri, "An analysis of, and remedies for, kinematic modes in hybrid finite elements: selection of stable, invariant stress fields," *Comput. Meth. Appl. Mech. Eng.*, vol. 38, pp. 63–92, 1983.

[60] E. F. Punch and S. N. Atluri, "Application of isoparametric three-dimensional hybrid-stress finite elements with least-order stress fields," *Comput. and Struct.*, vol. 19, pp. 409 -430, 1984.

[61] T. H. H. Pian and M. Li, "Stress analysis of laminated composites by hybrid finite elements, discretization methods in structural mechanics," in *IUTAM/IACM Symposium 1989* (C. Kuhn and H. Mang, eds.), (Vienna, Austria), pp. 361 372, Springer-Verlag, 1990.

[62] T. H. H. Pian, "Derivation of element stiffness matrices by assumed stress distributions," *AIAA J.*, vol. 2, pp. 1333-1336, 1964.

[63] B. Fraeijs de Veubeke, "Bending and stretching of plates, special models for upper and lower bounds," in *Proc. Conf. on Matrix Methods in Struct. Mech.*, AFFEL-TR-66-80, 1966.

[64] S. Ahmad and B. Irons, "An assumed stress approach to refined isoparametric finite elements in three dimensions," in *Finite Element Method in Eng. Proc. Conf. On Fin. Ele. Met. Eng.*, 1974.

[65] R. L. Spilker, S. M. Maskeri, and E. Kania, "Plane isoparametric hybrid-stress elements: invariance and optimal sampling," *Int. J. Numer. Meth. Eng.*, vol. 17, pp. 1469–1496, 1981.

[66] F. Brezzi, "On the existence, uniqueness and approximation of saddle-point problems arising from lagrange multipliers," pp. 129 151, RAIRO 8(R2), 1974.

[67] I. Babuska, J. T. Oden, and J. K. Lee, "Mixed-hybrid finite element approximations of second-order elliptic boundary-value problems, part 1," *Comput. Meth. Appl. Mech. Eng.*, vol. 11, pp. 175 206, 1977.

[68] I. Babuska, J. T. Oden, and J. K. Lee, "Mixed-hybrid finite element approximations of second-order elliptic boundary-value problems, part 2," *Comput. Meth. Appl. Mech. Eng.*, vol. 14, pp. 1 22, 1978.

[69] R. L. Spilker and S. P. Singh, "Three-dimensional hybrid-stress isoparametric quadratic displacement element," *Int. J. Numer. Meth. Eng.*, vol. 18, pp. 445 465, 1982.

[70] T. H. H. Pian and K. Sumihara, "Rational approach for assumed stress finite elements," *Int. J. Numer. Meth. Eng.*, vol. 20, pp. 1685 1695, 1984.

[71] S. V. Hoa, B. Journeaux, and L. DiLalla, "Computer aided design for composite structures," *Composite Structures*, vol. 13, pp. 67 79, 1989.

[72] S. N. Atluri, K. Kathiresan, and A. S. Kobayashi, "Three-dimensional linear fracture mechanics analysis by a displacement-hybrid finite element model," in *Int. Conf. on Struct. Mech. in Reat. Technol.*, 1975.

[73] S. N. Atluri, K. Kathiresan, and A. S. Kobayashi, "Inner surface cracks in an internally pressurized cylinder analyzed by a three dimentional displacement-

hybrid finite element method," in *Int. Conf. on Pressure Vessel Technol. 3rd. PT.2.*

[74] S. N. Atluri and K. Kathiresan, "3d analysies of surface flaws in thick-walled reactor pressure vessels using displacement-hybrid finite element method," *Nuclear Eng. and Design*, vol. 51, pp. 163-176, 1979.

[75] S. N. Atluri, M. Nakagaki, and K. Kathiresan, "Hybrid-finite-element analysis of some nonlinear and three dimensional problems of engineering fracture mechanics," *Comput. and Struct.*, vol. 12, no. 4, 1980.

[76] W. H. Chen and T. F. Huang, "Three-dimensional interlaminar stress analysis at free edges of composite laminate," *Composites and Structures*, vol. 32, pp. 1275 1286, 1989.

[77] P. Conti and A. De Paulis, "Simple model to simulate the interlaminar stresses generated near the free edge of a composite laminate," in *ASTM Special Technical Publication 876*, pp. 35-51, Philadelphia PA, USA: ASTM, 1985.

[78] A. C. Garg, "Delamination - a damage mode in composite structures," *Eng. Fract. Mech.*, vol. 29, pp. 557-584, 1988.

[79] J. Han and S. V. Hoa, "A new finite element approach for interlaminar stress analysis of composite laminates," in *Proceedings of the Second Canadian International Composites Conference* (W. Wallace and Others, eds.), pp. 813-820, Canadian Association for Composite Structures and Materials, Aug 1993.

[80] J. Han and S. V. Hoa, "A three dimensional multilayer composite finite element for stress analysis of composite laminates," *Int. J. Num. Meth. Eng.*, vol. 36 pp. 3903-3914, 1993.

[81] W. C. Hwang and C. T. Sun, "Analysis of interlaminar stresses near curved free-edges of laminated composites using iterative finite element method," *Comput. and Struct.*, vol. 28, pp. 461-467, 1988.

[82] B. M. Irons, "An assumed stress version of the wilson 8-node element." Univ. of Wales, CNME/CR/56, 1972.

[83] D. Karamanlidis and S. N. Atluri, "Mixed finite element model for plate bending analysis," *Compu. Struct.*, vol. 19, pp. 431 445, 1984.

[84] R. Y. Kim and S. R. Soni, "Suppression of free-edge delamination by hybridization," in *Fifth int. conf. on compos. mater.*, (Warrendale WA, USA), pp. 1557–1572, Published by Metallurgical Soc. Inc., Jul 1985.

[85] A. V. Krishna Murty, "Theoretical modelling of laminated composite plates," *Sadhana*, vol. 11, pp. 357 365, dec 1987.

[86] A. V. Krishna Murty and S. Vellaichamy, "On higher order shear deformation theory of laminate panels," *Composte streuturs*, vol. 8, no. 4, pp. 247 270, 1987.

[87] S. W. Lee, "An assumed stress hybrid finite element for three dimentional elastic structural analysis." MIT, ASRL TR170-3, 1974.

[88] K. U. Leuven, "Finite element analysis of interlaminar stress singularities at a free edge in composite laminate," in *Computer Aided Design in Composite Material Technology* (C. A. Brebbia, ed.), pp. 405 414, 1988.

[89] J. Li and E. A. Armanios, "Effect of delaminations on an elastically tailored laminated composite plate," in *Composites Properties and Applications (ICCM/9)* (A. Miravete, ed.), pp. 728 735, 1993.

[90] K. H. Lo, R. M. Christensen, and E. M. Wu, "A high-order theory of deformation - part 2, laminated plates," *J. of Appl. Mech.*, vol. 44, p. 669, 1977.

[91] P. L. N. Murthy and C. C. Chamis, "Composite interlaminar fracture toughness: three-dimensional finite element modeling for mixed mode i, ii and iii fracture." NASA Tech. Memo 88872, 1986.

[92] K. Moriya and T. Ichikawa, "Study on edge protection against delamination for composite laminates (the effects of edge shapes on stress singularities for cross-ply laminates)," *JSME Int. J., series I*, vol. 31, pp. 209–214, 1988.

[93] H. Murakami and G. A. Hegemier, "Mixed model for unidirectional fiber-reinforced composites," *J. Appl. Mech.*, vol. 53, pp. 765–773, Dec 1986.

[94] H. Murakami, "Laminated composite plate theory with improved in-plane responses," *J. of Appl. Mech.*, vol. 53, pp. 661–666, 1986.

[95] T. Nishioka and S. N. Atluri, "Analysis of cracks in adhesively bonded metallic laminates by a 3-dimensional assumed stress hybrid fem," *AIAA (cp811) pap 81-0497*, pp. 66–70, 1981.

[96] K. Peterson, "Derivation of the stiffness matrix for hexahedron element by the assumed stress hybrid method," Master's thesis, MIT, 1972.

[97] T. H. H. Pian and P. Tong, "Finite element method in continuum mechanics," in *Advances in Applied Mechanics* (C. Yih, ed.), (New York), Academic Press, 1972.

[98] T. H. H. Pian, D. P. Chen, and D. Kang, "A new formulation of hybrid/mixed finite element," *Comput. Struct.*, vol. 16, pp. 81–87, 1983.

[99] T. H. H. Pian and D. P. Chen, "On the suppression of zero energy deformation modes," *Int. J. Numer. Meth. Eng.*, vol. 19, pp. 1741–1752, 1983.

[100] R. L. W., E. A. ARmanios, and R. R. Valisetty, "Simplified sublaminate analysis of composites and applications," *Compu. and Struct.*, vol. 20, pp. 401–411, 1985.

[101] E. Reissner, "Reflection on the theory of elastic plates," *Appl. Mech. Rev.*, vol. 38, nov 1985.

[102] E. Reissner, "Note on the effect of transverse shear deformation in laminated anisotropic plates," *Compu. Meth. in Appl. Mech. and Eng.*, vol. 20, pp. 203-209, 1986.

[103] R. L. Spilker, "Finite element models in composite materials," in *Advances in Bioengineering*, pp. 37 38, New York: ASME, 1985.

[104] A. Toledano and H. Murakami, "High-order laminated plate theory with improved in-plane responses," *Int. J. of Solid and Struct.*, vol. 23, pp. 111-131, 1987.

[105] A. Toledano and H. Murakami, "Composite plate theory for arbitrary laminate configurations," *J. of Appl. Mech.*, vol. 54, pp. 181-189, Mar 1987.

[106] C. E. Ueng and K. D. Zhang, "Simplified approach for interlaminar stresses in orthotropic laminated strips," *J. of Reinforced Plastics and Composites*, vol. 4, pp. 273 286, Jul 1985.

[107] R. R. Valisetty and L. W. Rehfield, "Theory for stress analysis of composite laminates," *AIAA Journal*, vol. 23, pp. 1111-1117, 1985.

[108] J. D. Whitcomb and I. S. Raju, "Superposition method for analysis of free-edge stresses," *J. Compos. Mater.*, vol. 17, pp. 492-507, 1983.

[109] J. D. Whitcomb and I. S. Raju, "Analysis of interlaminar stresses in thick composite laminates with and without edge delamination," in *ASTM Special Publication 876*, pp. 69 94, Philadelphia PA, USA: ASTM, 1985.

[110] F. Zhang, "Interlaminar stresses of a laminated composite lap joint," *Scientia sinica, series A*, vol. 31, pp. 69-78, Jan 1988.

[111] N. J. Pagano, "Exact solutions for rectangular bi-directional composites and sandwich plates," *J. Composite Materials*, vol. 4, pp. 22-34, 1970.

[112] J. N. Reddy, "A simple high-order theory for laminated composite plates," *J. of Appl. Mech.*, vol. 51, pp. 745-752, 1984.

[113] A. S. D. Wang and F. W. Crossman, "Some new results on edge effect in symmetric composite laminates," *J. Comp. materials*, vol. 11, pp. 92 106, 1977.

[114] I. S. Raju and J. H. Crews, "Interlaminar stress singularities at a straight free edge in composite laminates," *Compu. and Struct.*, vol. 14, pp. 21 28, 1981.

[115] S. T. Mau, P. Tong, and T. H. H. Pian, "Finite element solutions for laminated thick plates," *J. Comp. Materials*, vol. 6, 1972.

[116] R. L. Spilker and S. C. Chou, "Evaluation of a hybrid stress formulation for thick multilayer laminates," in *Proc. 4th Conf. on Fibrous Comp. in Structural Design*, (San Diego), pp. 13 17, Nov 1978.

[117] R. L. Spilker, "A traction-free-edge hybrid-stress element for the analysis of edge effects in cross-ply laminates," *Comp. Structures*, vol. 12, pp. 167 179, 1980.